Distribution Category:
Energy Conversion
(UC-93)

ANL-80-56

Argonne National Laboratory
9700 South Cass Avenue
Argonne, Illinois 60439

PROCEEDINGS OF THE WORKSHOP ON HYDROCARBON PROCESSING MIXING AND SCALE-UP PROBLEMS

Held at Washington, D. C.
December 13-15, 1978

J. D. Gabor, Editor

Sponsored by the U. S. Department of Energy in cooperation with Argonne National Laboratory and the National Science Foundation.

TABLE OF CONTENTS

---

*Designates Speaker

Preceding page blank

TABLE OF CONTENTS (Contd.)

---

*Designates Speaker

PREFACE

A workshop was convened by the Division of Fossil Fuel Utilization of the U.S. Department of Energy in cooperation with the Particulate and Multiphase Process Program of the National Science Foundation to identify needs for fundamental engineering support for the design of chemical reactors for processing heavy hydrocarbon liquids. The underlying goal of this program is to achieve more effective use of hydrocarbons through more efficient conversion to electrical energy with fuel cells. Petroleum and coal derived liquids are expected to be attractive fuels for dispersed fuel cell power stations, but their application will require a processor to convert these fuels to hydrogen or synthesis gas to be fed to the cell. The problems associated with dispersing liquid hydrocarbons in a reacting gas and mixing within the gas phase are of primary concern. The reactor-design support studies undertaken for this program will also have application to hydrogen generation from heavy feed stacks for coal liquefaction and other processes.

The transactions of the workshop begins with an introduction to the immediate goals of the Department of Energy. Fuel cell systems and current research and development are reviewed. Modeling of combustion and the problems of soot formation and deposits in hydrocarbon fuels are next considered. The fluid mechanics of turbulent mixing and its effect on chemical reactions are then presented. Current experimental work and process development provide an update on the present state-of-the-art.

The editor thanks the authors and the participants in the discussions for their cooperation and help in assembling this report on the transactions of the workshop. Appreciation is expressed to Teenah Chocola, Marlene Bukowski, and Carol Doyle for transcribing the tapes and typing this manuscript.

J. D. Gabor, Editor

PROCEEDINGS OF THE WORKSHOP
ON HYDROCARBON PROCESSING
MIXING AND SCALE-UP PROBLEMS

ABSTRACT

A workshop was convened by the Division of Fossil Fuel Utilization of the U.S. Department of Energy in cooperation with the Particulate and Multiphase Process Program of the National Science Foundation to identify needs for fundamental engineering support for the design of chemical reactors for processing heavy hydrocarbon liquids. The problems associated with dispersing liquid hydrocarbons in a reacting gas and mixing within the gas phase are of primary concern.

The transactions of the workshop begin with an introduction to the immediate goals of the Department of Energy. Fuel cell systems and current research and development are reviewed. Modeling of combustion and the problems of soot formation and deposits in hydrocarbon fuels are next considered. The fluid mechanics of turbulent mixing and its effect on chemical reactions are then presented. Current experimental work and process development provide an update on the present state-of-the-art.

DOE OBJECTIVES - THE IMMEDIATE GOALS

M. Zlotnick, U. S. Department of Energy

The purpose of this workshop is to support the fuel cell activity in the area of fuel processing. We are working on fuel cells; a device that burns hydrogen and oxygen electrochemically to produce electricity. In this case, we are interested in obtaining hydrogen from liquid fuels derived from coal and petroleum. The details of these liquid-fuel conversion processes are the subjects of the following talks.

I am going to talk for about five minutes about the reason for bringing us together in this workshop: We are here primarily to contribute to one technology; autothermal reforming (ATR). The idea of ATR is to mix air, steam and hydrocarbon fuel in proportions such that the net amount of heat required by the endothermic reaction for steam reforming of the hydrocarbon is provided by the partial oxidation of the hydrocarbon in the air. The reason for the workshop is to bring together the people in the engineering and academic communities who have some special knowledge that may be useful to the people in inudstry who are doing the engineering of the ATR devices. Processing of hydrocarbons has been going on for a long time, and the first question that comes up is: What do you need that you haven't already got? There is a well-developed chemical industry. Where are we going relative to where we are?

It turns out that substantial development is required before state-of-the-art processes can be practical with fuel cell power plants. If you are going to produce electricity efficiently, you can't afford to be wasteful in processing the fuel. Beyond that, for the fuel cell to be useful in many of the applications that are being discussed later, they have to operate unattended, respond quickly to load changes and, of course, be economical to produce. Generally, the state-of-the-art fuel processing in the petrochemical industry is reasonably far away from meeting our requirements at this time without engaging in further development.

To give you a feel for the kind of technology development that is needed, we're fortunate to have an example. The devices in the lower right-hand corner of the photograph in Figure 1 are two steam reformers having a capacity of 3 million cubic feet of hydrogen. These are steam reformers of the type being used in the United Technology Corporation 4.8 megawatt fuel cell power plant that is scheduled for testing at a Consolidated Edison site in New York next year. In the background is a conventional steam reformer of the same capacity. That contrast is a more dramatic way of showing the kind of development that had to be carried out then. A list of the specifications is shown in Figure 2. This development consisted only of sophisticated and careful engineering. No new laws of nature were invented in producing this new device. That's the kind of hard work we are talking about. It's engineering work.

Figure 1.

COMPARISON OF UTC AND CONVENTIONAL REFORMERS

CHARACTERISTIC	UTC REFORMER	CONVENTIONAL REFORMER
FAST LOAD RESPONSE	15 SECONDS	5 MIN - 1 HOUR
RAPID START-STOP CAPABILITY	START - 4 HOURS STOP - INSTANTANEOUS	START 8 - 24 HOURS STOP 1 - 6 HOURS
REFORMER FUEL	PROCESS OFF-GAS	RAW FEEDSTOCK, #2 FUEL OIL ETC.
PROCESS PRESSURE	35 - 60 PSIG	150 - 600 PSIG
FURNACE PRESSURE	35 PSIG	0.1 - 1 INC. H_2O VAC.
PRESSURE DROP AT RATED THROUGHPUT:		
PROCESS SIDE	15 PSI	35 - 65 PSI
BURNER SIDE	15 IN H_2O	2 - 15 PSI
TURNDOWN RATIO	10:1	3:4 - 4:1
OPERATION	UNATTENDED (REMOTE CONTROL CAPABILITY)	OPERATOR CONTROLLED
MAXIMUM DIMENSIONS	11½'H 10'W	NONE
MAXIMUM WEIGHT	70000 POUNDS	NONE
TOLERANCE TO SHIPPING LOADS	3.5 G'S VERTICAL 4.0 G'S HORIZONTAL	NONE

FC9076
R782302

Figure 2.

We are not interested in inventing new scientific techniques, nor are we interested much in improving the technology beyond what's needed to do the job that we are setting out to do. It is fairly well defined, well constrained approach. The purpose of the applied research we want to plan with the aid of this workshop is to build the engineering tools and information needed to engineer the ATR more effectively.

At this point, as we begin the workshop, it seems that we need to know many things. We may need to understand the reaction path — unfolded from the flow -- as sort of basic tool relevant to the solution of the problem. Kinetics and thermodynamics data for the species that are initially there and that are formed in the process would seem to be an element of the problem. We may, also, need to do better in semiempirical predictions for the fluid mechanics. One approach might be to improve techniques for working with cold flow experiments -- experiments and measurements where the chemical reactions are not involved -- and try to integrate these data with the kinetics and thermodynamics information obtained separately.

Generally, we want to make use of experiment and theory. In cases where it's harder to produce the theory than the experiment, we want to use the experiment. In cases where it's harder to produce the experiment than theory, we want to use the theory. Pragmatism is the order of the day.

Comment and Reply on

"DOE Objectives"

by M. Zlotnick

I. T. Osgerby: What are the cold flow experiments you are talking about?

M. Zlotnick: Cold flow experiments, to me, mean to try to test a manageable segment of a reactor at a large enough scale (perhaps full size) so that you know how to scale it to full size. If you know the physical properties of the gases that you are dealing with in a nonreacting flow, and are in a position to make measurements of the velocities and the state of the gas, then you may be able to take the results from the cold flow measurements and, by folding in your knowledge of the chemistry, be able to make inferences about what will happen in a practical device. One objective of this workshop might be to improve the tools for doing this.

An alternative, of course, is to start from the Navier-Stokes equations, put in all sorts of details about turbulent flow, and turn the crank. Maybe that's the way we go ahead, but I am skeptical. We don't necessarily have to come out with a single approach here. But, as I said before, we want to be pragmetic. The problems are here, now, and we think in terms of getting some useful answers in a two-year time scale. Of course, the problem is not going to be solved in two years, and I think that there will be people worried about the same problems twenty years from now. So, there are no rigid constraints.

We want to get ideas and not impose ideas on the group we called together, because we need ideas.

FUEL CELL SYSTEMS

R. D. Pierce
Argonne National Laboratory

My objective today is to give a cursory overview of fuel cell systems, for the benefit of those members in our audience who are not familiar with the fuel cell program. I realize that many in the audience have been working with fuel cells for years and they know a lot more about them than I do. I hope they will help me if we get questions. As Marty showed in one of his slides, there are several features of fuel cells that make them attractive for power generation. The first of these is their potential for high efficiency. Because they produce electricity electrochemically, they are not limited by Carnot efficiency. They maintain their very high efficiency over wide ranges of load, down to perhaps 25% of the design load. This makes them attractive as load following devices. They are quiet and non-polluting. Some of this credit for non-pollution comes because the system itself is not very tolerant to sulfur and requires a low sulfur feed. Fuel cell power plants can operate with low water requirements by using dry cooling. These features give them greater site flexibility than other power systems. They are attractive for installation in urban areas where other types of plants would be unacceptable and where it is extremely expensive to run transmission lines, or for the rural applications where the load centers are widely disbursed. As Marty mentioned, modular construction works out well for fuel cells, giving them a potential for factory fabrication with the economy in time and money that can come from that type of production. The modular-type construction also gives a plant the option of relatively simple scaleup at a later date and of doing maintenance on a portion of the system while the plant remains in operation. With the current state of the art, all the near term fuel cell concepts involve oxidation of hydrogen. They differ in the particular electrolyte used and the electrochemical reactions involved. Alkaline fuel cells using potassium hydroxide electrolyte and pure hydrogen and pure oxygen reactants were used successfully on space craft. The main reason they have not been developed in the U.S. for land based application is that the electrolyte is intolerant of carbon dioxide. The two types of fuel cells receiving the major support at the present time are the phosphoric acid fuel cell, which is known as the first generation fuel cell, and the molten carbonate fuel cell, or second generation cell. These each can use impure hydrogen as fuel, but the molten carbonate system has the additional advantage that it can use carbon monoxide-hydrogen mixtures. Therefore, synthesis gas coming from a gasifier is compatible with that system.

Figure 1 is a schematic of the phosphoric acid fuel cell. The electrolyte for the cell is in a thin porous matrix containing concentrated phosphoric acid, and the electrodes are thin porous carbon containing a small amount of platinum catalyst. At the anode, hydrogen reacts to form hydrogen ions and liberate electrons to the external circuit. The hydrogen ions diffuse through the electrolyte to the cathode where they react with oxygen and accept electrons from the external circuit to form water. Typical operating parameters are given on the figure.

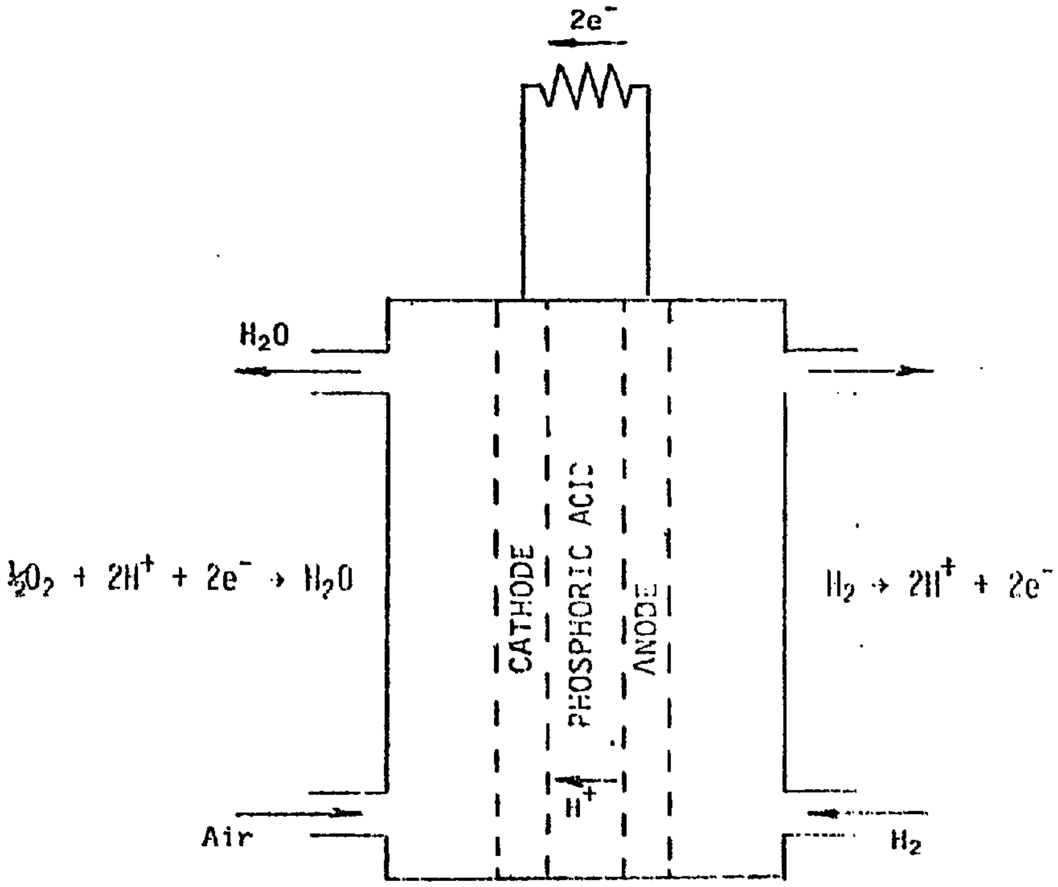

Temp	165-190°C
Power	100-200 W/ft^2
Voltage	0.64 v
Current	0.15-0.35 A/cm^2

Fig. 1. Phosphoric Acid Fuel Cell

The molten-carbonate fuel cell which is shown schematically in Fig. 2, has a paste-type electrolyte that is a dispersion of lithium aluminate particles, which are inert to the system, and a molten carbonate salt (generally lithium carbonate-potassium carbonate). This paste electrolyte forms a clay-like structure which is referred to as a tile. The anode is a porous nickel alloy, and the cathode is nickel-oxide. At the cathode, oxygen, carbon-dioxide, and electrons from the external circuit react electrochemically to form carbonate ions. These ions migrate through the electrolyte to the anode and react with hydrogen to form water and carbon dioxide and liberate electrons to the external circuit. In a practical system the carbon dioxide from the anode will be recycled to the cathode. I mentioned earlier that carbon monoxide also can be utilized by these fuel cells. It is generally agreed that this occurs principally by the two step path involving first the gas shift reaction (shown in Fig. 2) to produce hydrogen followed by the electrochemical oxidation of hydrogen, but there could also be some direct electrochemical oxidation of carbon monoxide. As hydrogen is depleted and water is produced in the anode gas, the gas shift equilibrium favors carbon monoxide consumption. For a phosphoric acid plant, the gas shift can be performed in a reactor ahead of the fuel cell.

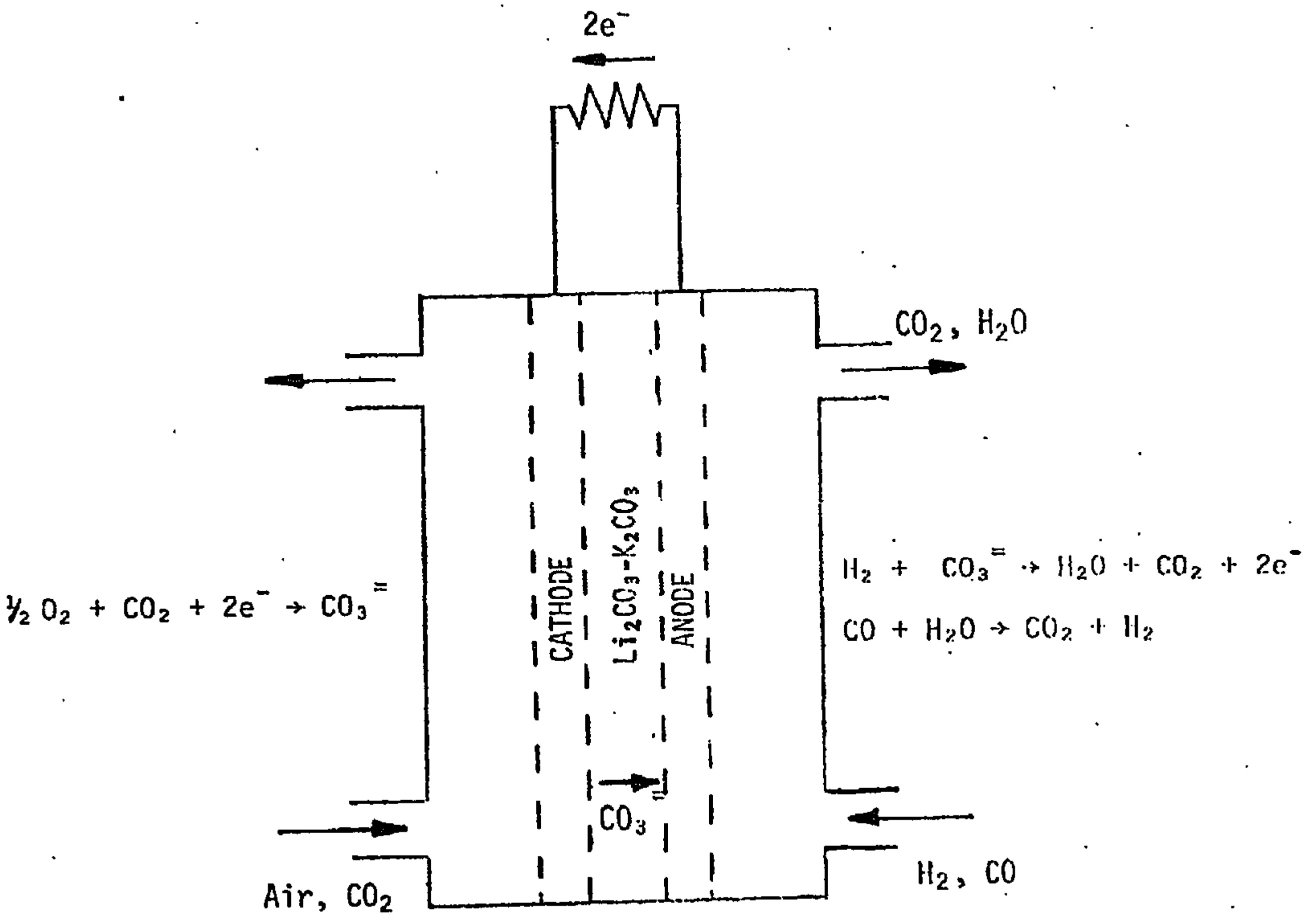

Temp	650°C
Power	125 W/ft^2
Voltage	0.85 v
Current	0.16 A/cm^2

Fig. 2. Molten Carbonate Fuel Cell

A fuel cell's performance varies with the concentration of the reactants, and as the reaction proceeds the performance of the cell is going to be diminished. Diluents such as nitrogen, which may be introduced in a fuel handling, also will affect the performance of the cell. There is some practical limit on what utilization can be obtained in a flow through these cells. A carbonate cell ideally might have a fuel that is 50% hydrogen and 25% carbon monoxide; more likely the fuel will be about 30% hydrogen and 10% carbon monoxide. A good system might consume 85% of that hydrogen-carbon monoxide mixture. The cathode feed might be 70% air and 30% carbon dioxide, and utilization is likely to be about 50% for the oxygen and 25% for the carbon dioxide.

There is a sulfur tolerance problem with the molten carbonate fuel cells. The nickel anode will react with hydrogen sulfide in the fuel gas if the hydrogen to H_2S ratio is low enough. Once nickel sulfide forms, the high surface area of the anode can be destroyed through the formation of a eutectic between nickel and nickel sulfide that melts slightly below the cell operating temperature of 650°C. But if the sulfur in the fuel does not react with the nickel, it will be oxidized outside the cell along with any carbon not yet converted to CO_2, and if not removed, the sulfur will be introduced to the cathode along with the carbon dioxide. At the cathode, SO_2 will react with the carbonate salt to form sulfate ions. Although initially the sulfate ions will reduce back to sulfide at the anode, the reaction is wasteful of fuel and sulfur may recirculate and accumulate in the system until an unacceptable level is reached. The best approach in handling sulfur and the acceptable levels are still to be determined. One approach that has been mentioned is to set a specification on sulfur that the anode can accept, and process the recycle stream from the anode to prevent sulfur dioxide from reaching the cathode.

With either type of fuel cell, it is necessary to assemble a number of cells in a series in order to get useful voltages for a power generator. In most engineering concepts the cells are assembled like a filter press to form what is referred to as a stack. Of course there are various ancillaries that must go with the fuel cell to make up a power generator. The phosphoric acid system is nearing commercialization, and there have been phosphoric acid power generators operated. The carbonate program, on the other hand, has been in a stage of cell development. This second system is worth pursuing because it has potential for higher efficiencies, because its higher operating temperature provides more useful waste heat, and because it is compatible with synthesis gas. Right now, DOE is about to issue a request for proposal (RFP) for engineering development of the molten carbonate system. This RFP is to cover the development of the readiness to build and test full-scale stacks and will involve system studies of fuel-cell power plants.

Figure 3 indicates the three major subsystems that comprise a fuel cell plant. These are the basic fuel cell stack, the power conditioner to convert the DC power to AC power that can be tied into an electric grid, and a fuel processor that can convert available fuel to a form compatible with the fuel cell. The fuel processor is our concern at this meeting. I have included the definition for heat rate on this figure. Heat rate is frequently used to describe the performance of generating equipment; clearly, the lower its value, the better the performance. A good combined cycle generator at design capacity would have a heat rate of perhaps 8500 Btu/kW. With that type of

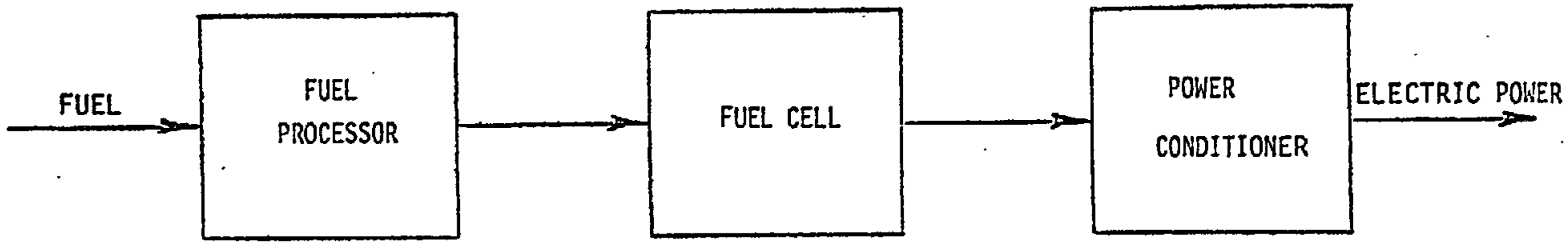

$$\text{Heat Rate} = \frac{\text{Btu in fuel feed}}{\text{kW electricity out}}$$

Fig. 3. Fuel Cell Power Plant

system (a steam turbine and a gas turbine), the heat rate would increase to greater than 11,000 Btu/kW at 40% load. For a fuel-cell plant we are hoping large plants will have heat rates of only 6800 Btu/kW, and the goal for small plants is 7500 Btu/kW. In order to reach these goals, the heat requirements and available heat in the fuel processor and fuel cell subsystems must be carefully integrated to conserve heat.

The fuel and fuel processor that is practical will depend on the scale of operation of the fuel cell plant. Table 1 lists four major categories of fuel cell application.

TABLE 1

POSSIBLE APPLICATIONS FOR
FUEL CELL POWER PLANTS

Application	Fuel	Size
Commercial, Residential	CH_4	50 kW
Industrial Cogeneration	Liquid	5-50 kW
Dispersed Utility	Liquid	5-50 kW
Central Station	Coal	600 MW

The first is a relatively small-scale fuel cell that might be used for a shopping center, or hospital, or a residential application. The most attractive fuel for this type of unit is methane, which is easily steam reformed. The proponents of these systems believe that a well-designed system could provide all of the heating and electrical requirements of an apartment complex or a commercial building using no more fuel than currently is used for heating requirements. This part of the fuel cell program has been pursued under the TARGET project (that's an acronym for Team to Advance Research for Gas Energy Transformation). That was a project organized by United Technologies and a group of the gas utilities. About five or six years ago, they field tested some sixty 12.5 kW generators using pipeline gas as fuel, and a few years ago, they ran a 40 kW pilot plant. About a year ago, the Gas Research Institute (GRI) assumed the responsibilities for developing these small fuel cells from the TARGET project. GRI is currently trying to upgrade the 40 kW pilot plant to a prototype for some fifty units that would be field tested. They are hoping to have DOE cooperation in supporting the field testing.

At the other end of the size spectrum is the central station. Most people believe that the large plants should employ a coal gasifier producing synthesis gas for the fuel cell stacks. However, for the intermediate-size dispersed plants, coal gasification almost certainly will be uneconomical and unacceptable to the plant's neighbors. For these industrial cogeneration and dispersed utility plants, liquid fuels will be employed. Aspects of the processing of these fuels will be the subject of the following talks.

The phosphoric acid system has made inroads into the technology for dispersed generating plants. There is under construction a 4.8 MW unit to be located in lower Manhattan Island and to provide power to the Consolidated Edison grid. That unit is a product of the FCG-1 Project (Fuel Cell Generator-1) organized by the electric utilities. That project built and operated using naphtha with steam reforming, and was hooked into the utility grid. Martin Zlotnick mentioned the impressive steam reformer design incorporated in the FCG-1 plants. That entire plant including the fuel processor is to be assembled from skid-mounted modules.

Both DOE and EPRI currently are sponsoring research to assure the capability of using fuels heavier than naphtha for fuel cell applications. Consideration of these fuels, which clearly will require more severe processing, lead to the work on autothermal reforming that Marty mentioned. John Young, in the next talk, will discuss technology related to the more severe processing. Figure 4 is a very conceptual fuel processor and fuel cell integrated system. The flowsheet is not optimized, but indicates features that I want to point out. The reactor gasifies liquid fuel for the fuel cell. There will have to be some gas clean up, but it is unlikely that much gas cleanup can be done economically at dispersed generating stations. Many heat exchangers will be employed to conserve heat throughout the system. The compatibility of the available and required heat around the plant could be an important variable in selecting the processing approach and the reactor design. The impact of the auxiliary components on the rapid load following capability that is desirable for these smaller plants must be assessed. One stated goal is that the plant be able to drop to 25% load in a minute. It may be necessary to provide gas storage if the reactor cannot follow the load.

In current stack designs for molten carbonate fuel cells, the cells we cooled with the anode and cathode gas streams. The anode gas stream leaving the stack will still have about 15% of the heating value remaining. Figure 4 indicates that this fuel would be burned (probably catalytically) and this heat recovered. If a turbine were employed to recover more electricity from the waste heat, the overall system would likely lose much of its load response capability. After water is condensed and removed, the oxidized anode gas is recycled to the cathode as a source of carbon dioxide. The condensed water is returned to the reactor. I have indicated in several places available heat (waste heat?). I hope that the engineers will find effective ways of using that heat to increase the overall efficiency of the system.

The bulk of the content of our workshop now will be concentrated in the reactor; more specifically, the front end of the reactor, which is much like a rich combustor.

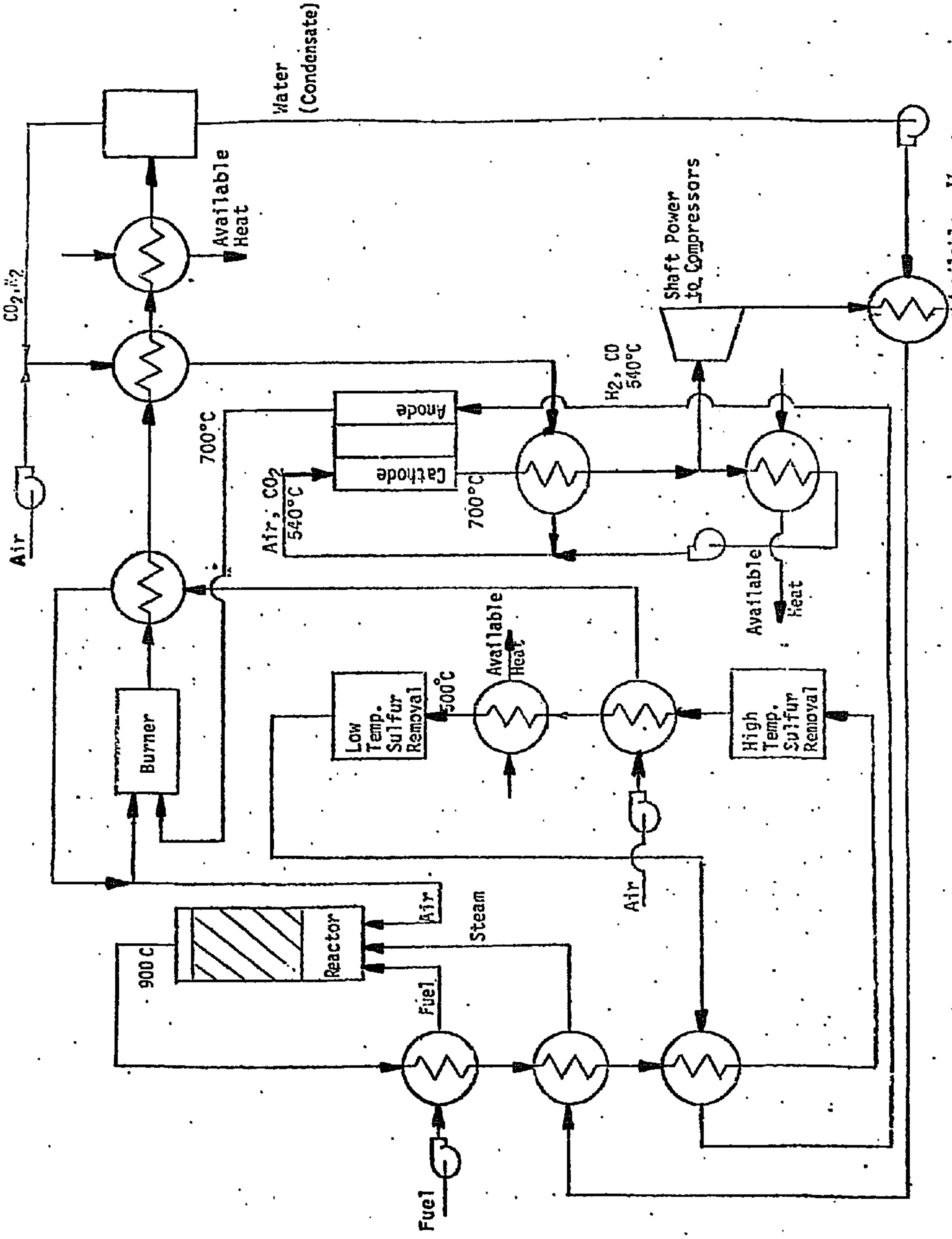

Fig. 4. Fuel Processor and Fuel Cell Integrated System

CURRENT STATUS OF FUEL CELL-FUELS PROCESSING R&D

by

John E. Young
Argonne National Laboratory

The first paper of this workshop presented a summary of general fuel cell requirements and goals. Several of the points that I will make in this paper may seem repetitious, but they need to be stressed and elaborated upon, as they relate to fuels processing needs for fuel cell power plants.

The type of fuel processor and, in fact, the type of fuel used in the processor will be strongly affected by the use for which the fuel cell power plant is designed. Centralized baseload generating stations - 40 megawatts or larger - can use low-cost fuels. These may include very heavy oils (residua) but would most likely be coal-derived synfuels. These large-scale plants permit the use of dirtier fuels because the extensive gas cleanup requirements associated with the use of these fuels can be handled economically. Baseload stations will have very high load factors which remain relatively constant over extended periods of time. This permits the use of gasifiers and other high capital cost components at constant optimum throughput.

In contrast to the baseload station, dispersed generating plants will be small in scale, with a capacity of 1 to 50 megawatts. Dispersed fuel cell generators could be installed in remote areas - where minimum capacity is needed, but transmission costs from baseload stations would be high. Dispersed plants could also be used for peak or intermediate load service. Hence, both the fuel cells and the fuel processor must have high turn-down ratios--from 100 to roughly 20 percent capacity. Subsequently, unless hydrogen storage capacity is built into the generating station (which increases capital costs and introduces additional safety related problems), the fuel processor must be capable of handling wide variations in throughput. These changes in throughput must be accomplished in a few seconds, depending upon the load requirements in the electric power grid system. Likewise, processors used in dispersed power plants must be able to tolerate occasional complete shut-down and start-up of operation, all within relatively short times.

Because of their size, these units will probably be built most economically as modules, which could be assembled on-site in the appropriate combinations to achieve the desired total capacity. These modularized units should be compact and easy to interconnect with a minimum of on-site labor involved. Dispersed units must have very simple operation and maintenance procedures, and preferably permit unattended operation. Gas cleanup and associated by-product handling must be minimized. Even a small fuel processor would require facilities for sulfur disposal--in the form of solid sulfur or some sulfur-laden sorbant, however, any dispersed fuel processor that would produce heavy tars, solid carbon or carbon sludges would most likely be unacceptable. The fuel throughput for these relatively small fuel processors would be 100-1000 barrels/day, if the system operates at high load factors. If the dispersed power plant is cycling for load leveling purposes, the total fuel throughputs would be significantly less.

Representative fuels for these processors encompass a wide range of properties. The fuel processors used in current fuel cell demonstration units use low boiling fuels--specifically naphtha or natural gas. Naphtha is the fuel used in the FCG-1 4.8 MW demonstrator presently being installed in downtown Manhattan. Methanol is another possibility for use as a light fuel, if large methanol plants for production from coal come into operation in the future.

The range of fuels of primary interest for use in dispersed fuel cell plants is middle and heavy distillates. Processing of these fuels for fuel cell use is currently being investigated under sponsorship from both DOE and the electric utilities (through EPRI), with the major emphasis being placed on No. 2 fuel oil. The ultimate goal is to have the capability of using heavy distillates and a wide range of liquids derived from coal. Coal liquids can vary in boiling point from very light (naphtha range) to that of a No. 6 or residual fuel. The high aromatics content of the coal derived liquids--hence the greater tendency to form soot in the fuel processor--is a very serious problem.

The processes that are currently applicable to the generation of fuel cell syngas run the gamut from conventional steam reforming to gasification. Gaseous fuels and very light liquids, *i.e.*, methane, methanol, or naphtha, can very efficiently be converted to fuel cell feeds by conventional steam reforming. There are constraints with these fuels however, on the sulfur content and also on the aromatics content in the case of naphtha. Conventional steam reformers such as those used in the FCG-1 demonstrator unit will handle paraffinic naphtha, where the aromatics content is kept very low.

Conventional steam reformers operate in the temperature range of 480-850°C. If complete hydrocarbon conversion ($\sim$99%) is required, the exit temperature must be in the 820-850°C range. However, conventional reformers are extremely sensitive to catalyst poisoning by any sulfur present in the fuel. The heavy fuels would generally have a much higher sulfur content than would be tolerated in a conventional steam reformer. Much higher operating temperatures are required in order to use a nickel-containing reforming catalyst with high sulfur feedstocks. This is accomplished in high severity steam reformers where the exit temperature can range up to 1050°C. At these higher temperatures, even nickel catalysts maintain some steam reforming activity. In fact, above approximately 950°C, nickel sulfide is thermodynamically unstable, although the extent of chemisorption of H_2S by nickel at these temperatures is not well defined. In addition, at these higher temperatures, the reaction rate for carbon gasification (by steam) is significant, which would aid in the prevention of carbon buildup in the reactor while using heavy, high aromatic fuels.

Number 2 fuel oil can be converted to fuel cell feeds by means of high severity steam reforming, but this has not been reduced to commercial practice yet.

High temperature steam reformers are heated by external firing of the reformer catalyst tubes. However, the process heat can be supplied by adiabatic combustion of a portion of the fuel inside the reformer tube, by injection of a small amount of air with the fuel and steam at the inlet of the reformer, resulting in a combination of partial oxidation and steam reforming reactions. This latter process is known as autothermal steam reforming.

Simple catalytic partial oxidation (without the reforming reaction), has been demonstrated on a bench scale by Siemens of Germany (Henkel, 1972) using gas oils as feed, but this process is not commercially available. Also, at the bench scale, catalytic partial oxidation has been investigated at JPL, and in fact, a paper describing this work will be presented later in this workshop. Differentiation between autothermal reforming (ATR) and catalytic partial oxidation is difficult - if you add steam to a catalytic partial oxidation system in order to control carbon formation, you are approaching conditions characteristic of an autothermal reformer. For fuel cell use, addition of steam to the catalytic partial oxidation reactor is necessary - otherwise the oxygen (or air) requirement is too high, too much of the fuel is converted to CO_2 rather than CO and H_2 and the conversion of fuel is incomplete. In addition, too much diluent nitrogen is introduced into the product gas, which degrades the performance of the fuel cells power plant.

Thermal partial oxidation, such as the Texaco heavy oil gasification process is presently commercially available for use with heavy distillates or even residua. However, these processors are quite large, and they have not been scaled down to the point where they can be efficiently used in dispersed fuel cell power plants. In addition, these gasification processes generally result in the formation of a significant amount of solid carbon, which complicates gas cleanup and would result in the need for handling an additional undesirable by-product in dispersed fuel processors.

An important point must be made regarding processes such as the Texaco gasification process. These processes have very high reactor exit temperature typically 1450-1500°C. The fraction of the fuel heating value that is converted to the sensible heat of the product gas is 30% or better, so very efficient heat recovery systems must be included in the gasifier system, which would then require a steam turbine bottoming cycle in the power plant - a factor that would most likely be unacceptable for power generating stations.

There are no commercial processes yet available utilizing autothermal reforming (ATR) with distillate fuels. ATR was developed for use with naphtha and lighter fuels by European engineering companies for production of hydrogen, primarily for use in fertilizer manufacture. I will describe two of these European concepts, primarily to point out a critical difference in their reactor inlet designs. Figure 1 shows schematically the Topsøe SBA autothermal reforming process. Steam is preheated, mixed with fuel, and then heated further to 656°C. This mixture is blended with pre-heated air or oxygen-enriched air immediately prior to introduction to the reactor. In the Topsøe reformer, the combustion is carried out non-catalytically in the upper stage of the reactor. The partially combusted mixture and steam then pass through the nickel-containing reforming catalyst bed. The product gas is quenched, passed through a heat recovery unit, shift converted, and then passed to the downstream process. It would not be a simple matter to adapt this process for operation with distillate fuels. The mixing in the header region of this reactor is relatively inefficient, hence with heavy feedstocks, regions of inhomogenity can occur. This increases the tendency to produce soot because of regions of severely fuel-rich combustion and can increase the danger of the formation of explosive mixtures (Catalytica, 1977).

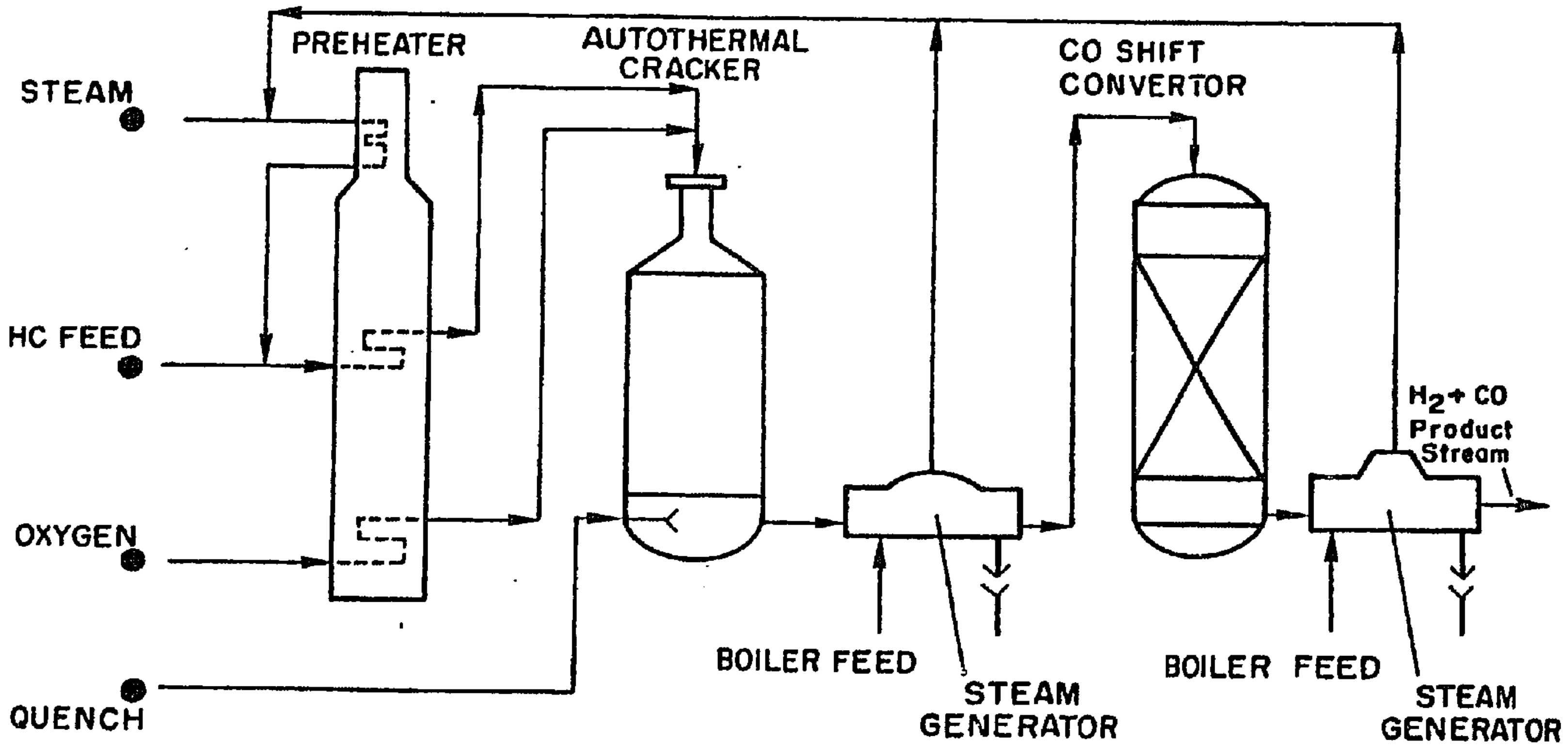

Figure 1. Schematic Diagram of the Topsøe SBA Autothermal Reforming Process. (Nitrogen, 1962)

The BASF autothermal reforming process (Fig. 2) has been demonstrated with fuels such as gasoline or aromatic naphthas with sulfur contents up to 3000 wppm. At the reactor inlet, however, is included a platinum light-off catalyst, which permits introduction of the reactants at much lower temperatures. The very rapid temperature rise resulting from the use of this partial oxidation catalyst serves to minimize carbon formation both in the fuel preheaters which can now be operated at lower temperatures and in the downstream catalyst beds.

Two high-severity process schemes are currently under investigation with DOE and/or EPRI funding. With high sulfur and high aromatic oils, externally fired high-temperature steam reformers (HTSR) do not have a high enough thermal efficiency to meet the current goals for dispersed power plants. However, if these reformers are operated at slightly lower temperatures, the thermal efficiency improves greatly, but the hydrocarbon content of the product gas is unacceptably high. If this HTSR operated at reduced temperatures is followed by an autothermal secondary reformer, the hydrocarbon slip from the HTSR is converted to syngas at higher thermal efficiency, while a minimum of diluent nitrogen is added to the product gas via the combustion air. EPRI is supporting development of this hybrid process utilizing the Toyo Engineering Total Hydrocarbon Reforming process as the HTSR step followed by an autothermal secondary reformer such as the Topsøe SBA reformer described earlier or UTC's autothermal reformer currently under development.

Autothermal reforming of middle distillates and coal liquids is being investigated by UTC, Engelhard Industries, and Jet Propulsion Laboratory. More information on the UTC and JPL efforts will be presented in subsequent talks at this workshop. As had been indicated for the Topsøe and BASF processes, the fact is quite apparent that the formation of carbon in ATR reformers is a very serious problem when highly aromatic fuels are used.

Because addition of oxygen consumes part of the heating value of the input fuel, the overall goal of this development effort is to reduce the oxygen-to-fuel-carbon ratio to a minimum level possible to prevent carbon formation. However, in order to maintain the necessary high reaction temperatures in the reformer, low oxygen-to-carbon ratios mean high reactant preheat temperatures, which also can contribute to carbon formation in the preheaters and mixers.

It is the purpose of this workshop to identify areas of research that would be applicable to facilitate better definition and subsequent solution of this carbon formation problem, not only in autothermal reformers but also in other high severity reformers.

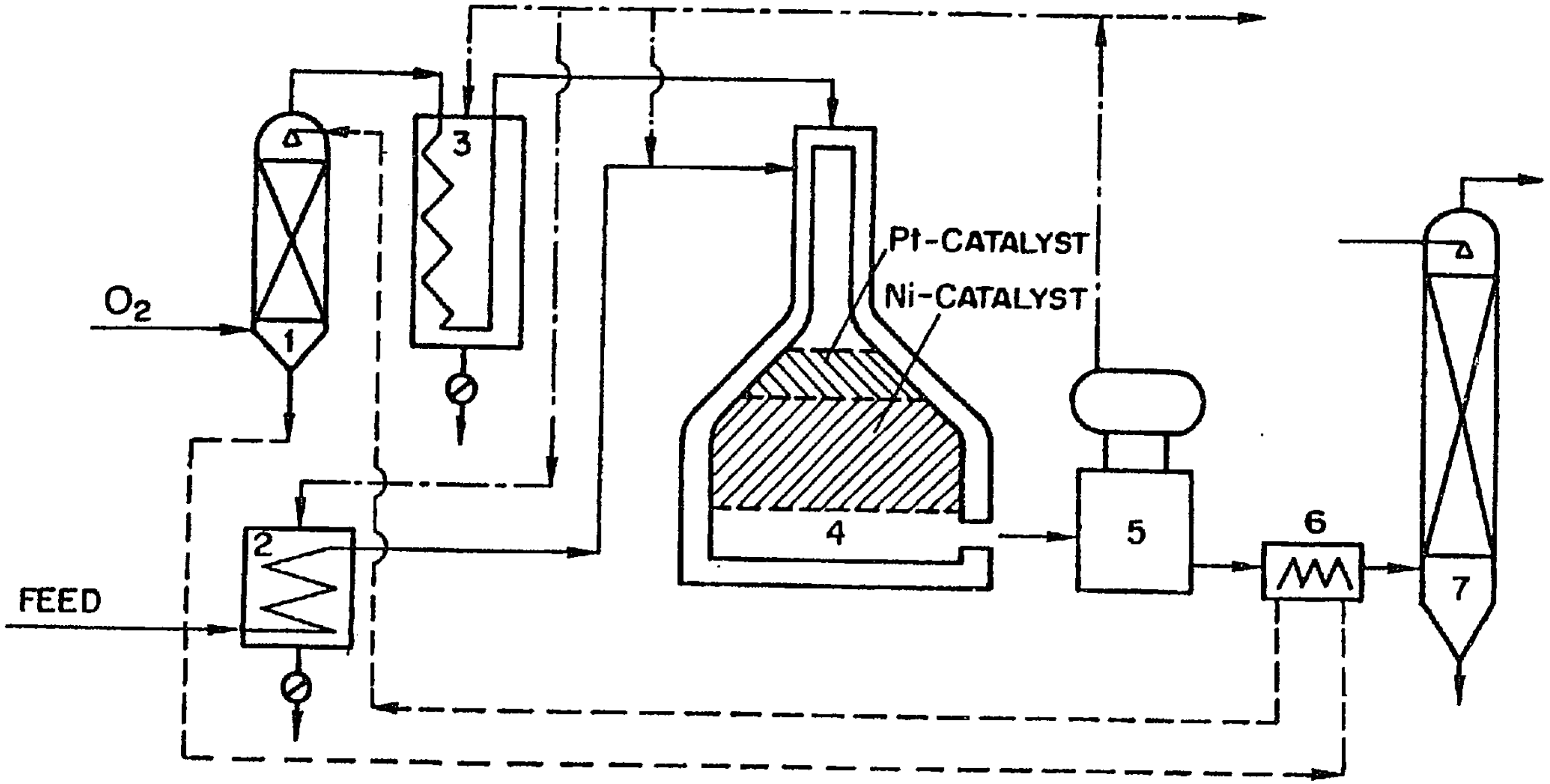

Fig. 2. Schematic Diagram of BASF Autothermal Reforming Process (Schmulder, 1965)

References

1. Henkel, H. J., Kostka, H., and Michel, A., "Autothermal Gasification of Liquid Hydrocarbons by Partial Oxidation," presented at the Fuel Processing Meeting in Palo Alto, CA, April, 1977.

2. Nitrogen, 35 (May, 1962).

3. Schmulder, Van P., Brennstoff-Chemie 46, 23(1965).

4. Catalytica Associates, "Assessment of Fuel Processing Alternatives for Fuel Cell Power Generation," Final Report, EPRI-RP919-1, September, 1977.

CHEMISTRY IN DEPOSIT FORMATION IN HYDROCARBON FUELS

J. W. Frankenfeld and W. F. Taylor, Exxon Research and Engineering Company

Presented by John W. Frankenfeld

In this presentation, I plan to give you an overview of our work at Exxon on the stability of hydrocarbon-based fuels.

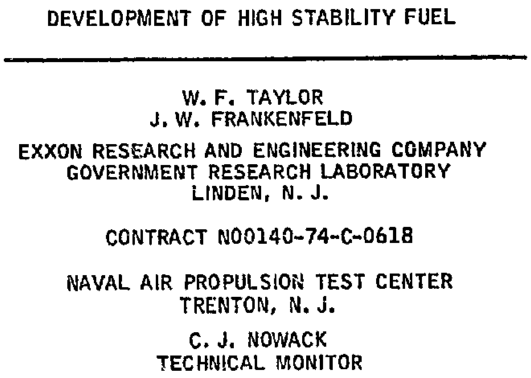

DEVELOPMENT OF HIGH STABILITY FUEL

W. F. TAYLOR
J. W. FRANKENFELD

EXXON RESEARCH AND ENGINEERING COMPANY
GOVERNMENT RESEARCH LABORATORY
LINDEN, N. J.

CONTRACT N00140-74-C-0618

NAVAL AIR PROPULSION TEST CENTER
TRENTON, N. J.

C. J. NOWACK
TECHNICAL MONITOR

Fig. 1.

This program, which is largely under the sponsorship of the U.S. Navy, has as its major objectives the elucidation of the chemistry of deposit formation and a search for clues and how to prevent it. Although we have concentrated on jet fuels and diesels in this work, most of the generalization formed will be applicable to other types of fuel as well. My talk will be divided into two basic topics:

Development of thermally stable JP-5 fuel

The effect of nitrogen compounds on deposit formation under ambient conditions

I. DEVELOPMENT OF HIGH STABILITY JP-5

The reasons for undertaking this program are outlined here.

At one time, the Navy was interested in very high speed aircraft. Such aircraft generated extremely high temperatures which exert thermal stress on the fuel. It was essential to develop a fuel which could withstand such conditions. We decided to try to modify ordinary JP-5 to improve its thermal stability rather than to develop a new exotic fuel whose cost would preclude its general use. Our approach was to study the chemistry of fuel breakdown and subsequent deposit formation and to search for clues as to how to render the original fuel more stable to thermal stress. We were particularly interested in the effects of fuel composition, trace impurities and dissolved oxygen content. I will discuss today those aspects of the problem which are of greatest interest to this group. In so doing, I will try to point out how our results may impact on processing and handling of future hydrocarbon fuels, particularly those which may be somewhat different from fuels in general use today.

DEVELOPMENT OF A HIGH STABILITY JP-5 FUEL

GENERAL BACKGROUND

- WITH A MACH 4.5 AIRPLANE, RAM AIR TEMPERATURES ARE IN THE RANGE OF 1400°F.
- FUEL IS THE ONLY HEAT SINK AVAILABLE ON THE AIRCRAFT FOR COOLING.
- IF FUEL FAILS UNDER THERMAL STRESS, AIRCRAFT COULD BE RENDERED INOPERABLE.

Fig. 2.

Before we go any further, a word about methodology is appropriate. Our approach to studies such as this has always been to start with model systems and work our way back to "real world" fuels. The bewildering array of chemical species in actual JP-5, we feel, renders the opposite approach difficult, if not impossible, to pursue. Our apparatus for measuring thermal stability is a unique one.

ADVANCED FUEL STABILITY UNIT

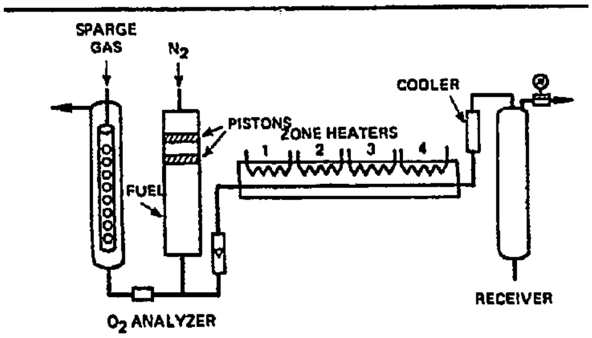

Fig. 3.

It is especially designed to enable us to measure the rate of deposit formation at four different temperatures in a single run. The deposits formed are determined by a combustion technique using a modified carbon analyzer (see Fig. 4).

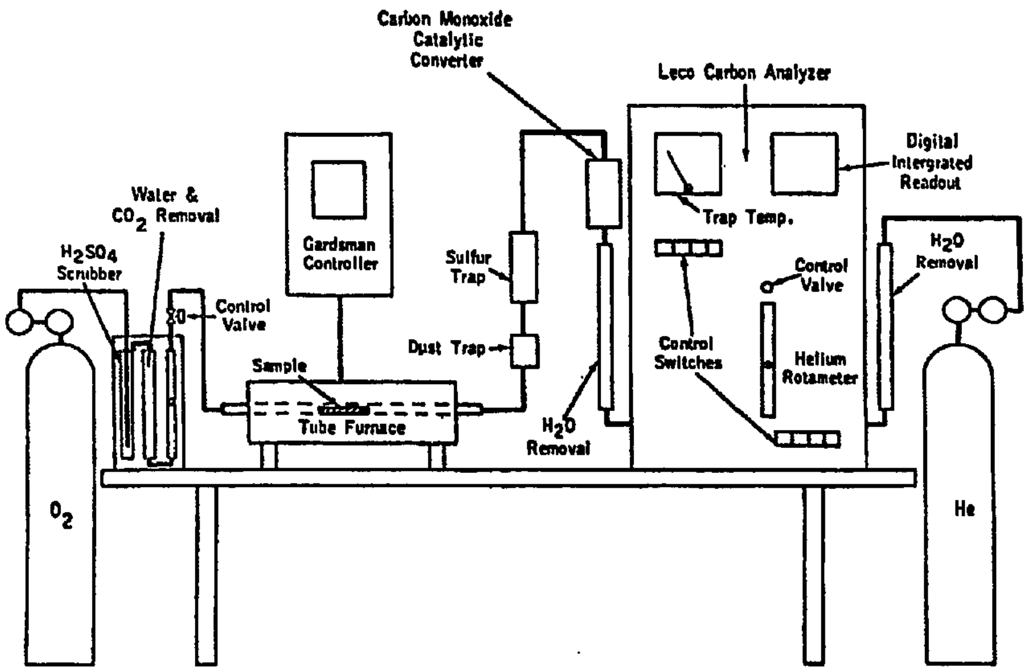

ANALYTICAL SYSTEM FOR MEASUREMENT OF CARBONACEOUS DEPOSITS

Fig. 4.

Deposits such as we obtain are generally thought to arise from free radical autoxidative polymerization of hydrocarbons as shown in Fig. 5.

MECHANISM OF AUTOXIDATIVE
DEPOSIT FORMATION

$$\mathrm{R{-}H + initiator \longrightarrow R\cdot + product} \qquad (1)$$

$$\mathrm{R\cdot + O_2 \longrightarrow R{-}O{-}O\cdot} \qquad (2)$$

$$\mathrm{R{-}O{-}O\cdot + R - H \longrightarrow R\cdot + R{-}O{-}O{-}H} \qquad (3)$$

$$\left.\begin{array}{ll} \mathrm{R\cdot + R\cdot} & \longrightarrow \\ \mathrm{ROO\cdot + R\cdot} & \longrightarrow \\ \mathrm{2\ ROO\cdot} & \longrightarrow \end{array}\right\} \text{STABLE PRODUCTS} \qquad \begin{array}{l} (4) \\ (5) \\ (6) \end{array}$$

Fig. 5.

EFFECTS OF HYDROCARBON TYPE
ON DEPOSIT FORMATION

HYDROCARBON TYPE	DEPOSITS RELATIVE TO n-DODECANE = 1.0
$\underline{n}$-C_{12}	1.0
$\underline{n}$-C_{10}	0.8
$\underline{n}$-C_{16}	1.5
$\underline{i}$-C_{12}	2.3
AROMATICS (PURE)	1-5
AROMATICS (10% BLEND)	0.1-0.8
OLEFINS	3-50
NAPHTHENES	0.5-0.8

Fig. 6.

In general, as I will attempt to demonstrate, our results are explanable on this basis. Let me turn now to a brief summary of the major parameters affecting deposit formation in air saturate fuels. First, the effects of hydrocarbon types.

In the range of C_{10}-C_{16}, the higher molecular weight paraffins produce fewer deposits at a given temperature. Branching increases the rate of deposit formation. Aromatics afford more deposits than paraffins in pure form, but actually seem to inhibit deposit formation when blended with paraffins. Napthenes behaved much as did aromatics in these studies.

Olefins, in general, are quite deleterious to fuel stability. However, their influence varies with type as shown in Fig. 7.

SUMMARY OF DEPOSIT FORMATION TENDENCIES
OF OLEFIN-n-DECANE BINARY BLENDS

10% Olefin Added To Binary Blend	Structure of Olefin	Rate of Deposit Formation of Blend at 275°F, $g/cm^2/4$ hours x 10^6
Vinylcyclohexane	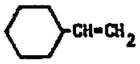	29.4
4-Vinylcyclohexene	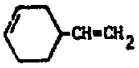	198.
Allybenzene	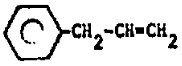	91.2
4-Phenyl-1-butene	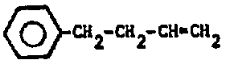	86.9
1-Phenyl-2-butene	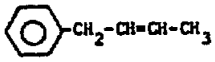	26.5
7-Methyl-3-methylene 1,6 octadiene	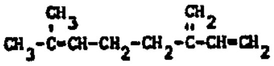 $CH_3-\overset{CH_3}{\overset{\vert}{C}}=CH-CH_2-CH_2-\overset{CH_2}{\overset{\Vert}{C}}-CH=CH_2$	190.
1-Decene	$CH_2=CH-(CH_2)_7-CH_3$	35.6
Indene	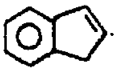	354.
n-Decane alone		10.0

Fig. 7.

The most reactive species are diolefins with non-conjugated terminal double bonds.

Among the most deleterious impurities are sulfur compounds. Arrhenius plots of deposit formation rates for some representative sulfur compounds are compared with pure hydrocarbons in Fig. 8.

THE EFFECT OF THE ADDITION OF 1000 PPM S

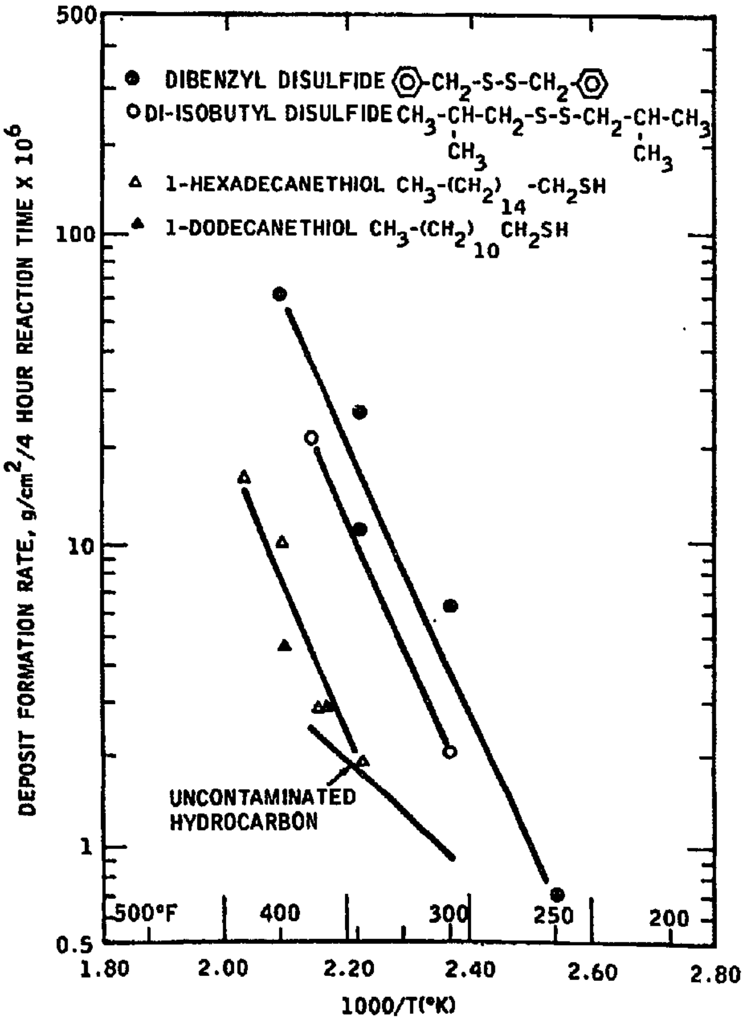

Fig. 8.

Sulfur compounds, no doubt, serve as initiators for the free radical autoxidative polymerization. Thus, the order of reactivity of various sulfur compounds parallels either the ease of formation of radicals or the relative reactivities of the radical species formed. This is illustrated in Fig. 9.

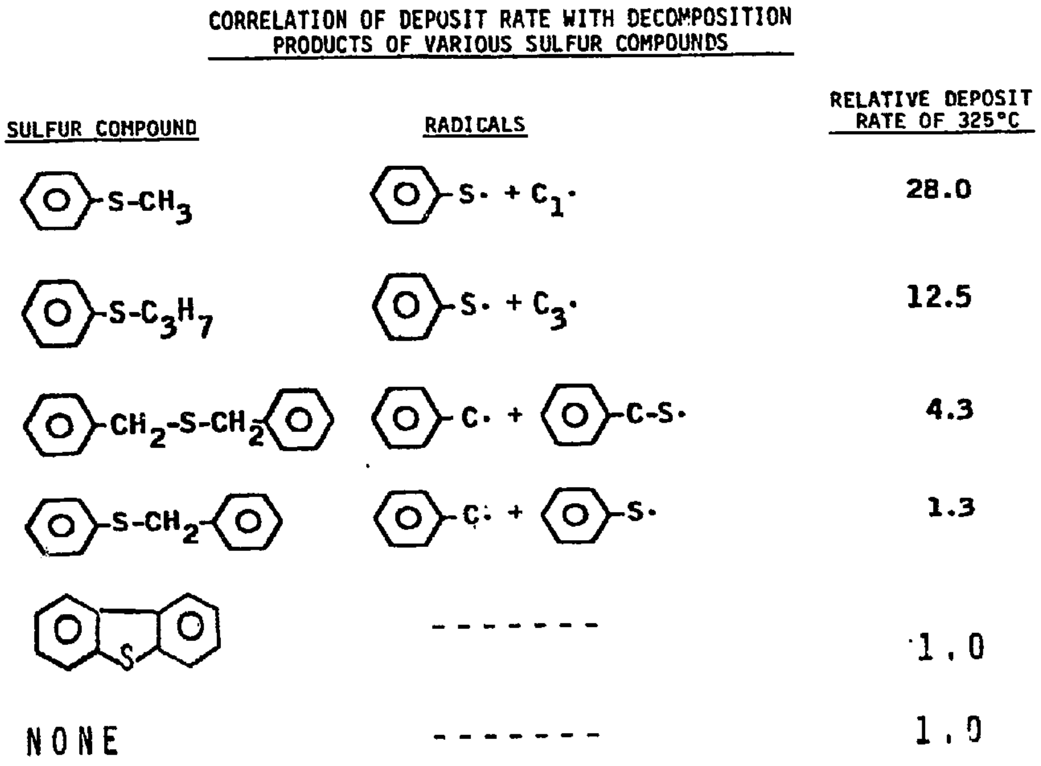

Fig. 9.

The very stable benzyl radicals afford lower rates than the reactive alkyl radicals. Among the latter, methyl radicals have been shown to be about 2.5 times as reactive as propyl radicals. In these studies, sulfides affording methyl radicals produced deposits 2.2 times as rapidly as their propyl radical counterparts. Sulfur compounds, such as thiophene, which produce no radicals on pyrolysis (or do so with great difficulty) show no tendency to promote deposit formation.

Nitrogen compounds are also deleterious to fuel stability as shown in Fig. 10.

Once again, reactivity varies with structure with pyrrolic types being the most deleterious. I'll have more to say about this later.

One of the more interesting aspects of the stability problem involves the effects of metals. We have studied both metal surfaces, that is, the tubes in the advanced fuel unit (Fig. 3) were constructed with different metals, and dissolved metals (e.g., metal "soaps" such as acetonylacetates). Metals can participate in free radical oxidations in a variety of ways.

It would appear from this that metals can either promote or inhibit such reactions. Work described by others indicates this is, indeed, true.

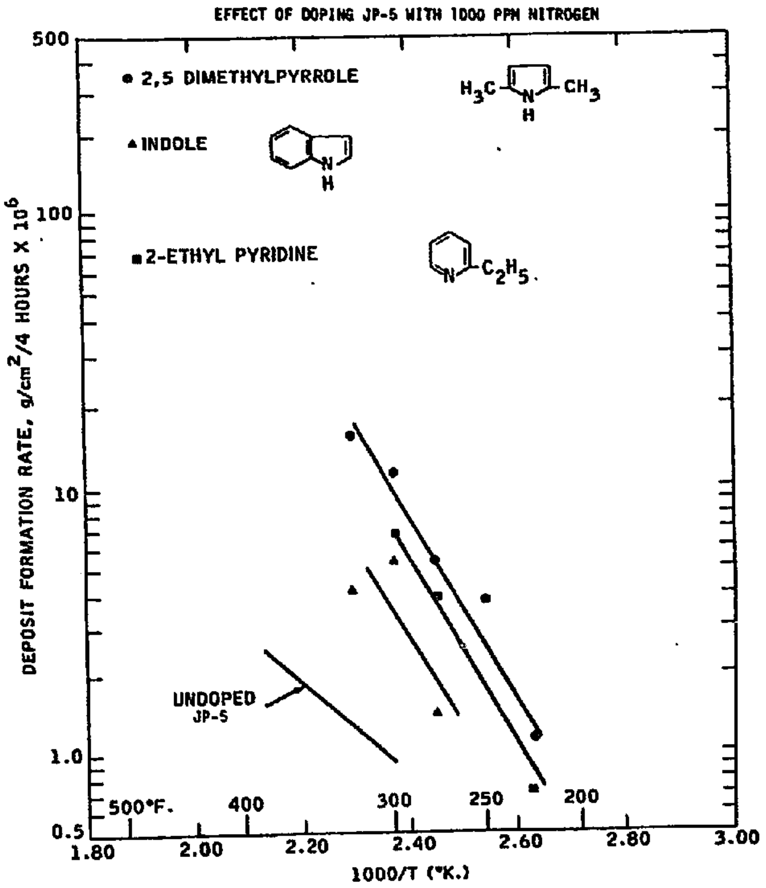

Fig. 10.

EFFECTS OF TRACE METALS
ON FREE RADICAL OXIDATIONS

INITIATION

$M^2 + RH \longrightarrow R\cdot + M^+ + H^+$

$(MO_2)^{2+} + RH \longrightarrow M^{2+} + R\cdot + HO_2\cdot$

PROPAGATION

$M^{3+} + ROOH \longrightarrow M^{2+} + RO\cdot + OH^-$

TERMINATION

$M^{2+} + R\cdot \longrightarrow$ INERT PRODUCTS $+ M^+$

$M^{2+} + ROO\cdot \longrightarrow$ INERT PRODUCTS $+ M^{3+}$

Fig. 11.

METAL CATALYZED OXIDATION OF TETRALIN AT 65°C
(KAMIYA AND INGOLD, 1969)

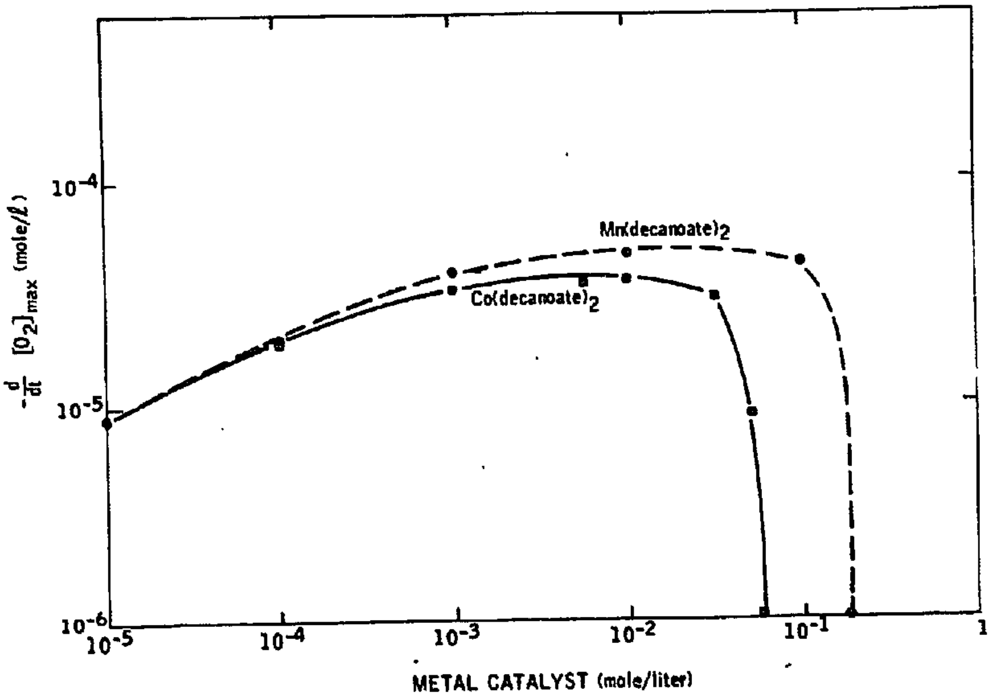

Fig. 12.

At low concentrations, the metals studied accelerated oxidation; while at higher concentrations, they strongly retarded the reaction. Some results of wor work on the effects of both metal surfaces and dissolved metals in air saturated JP-5 are shown in Fig. 13.

EFFECTS OF METALS ON
DEPOSIT FORMATION IN JP-5 FUEL

	RELATIVE DEPOSIT RATE		
METAL	SURFACE (400°F)	DISSOLVED 200°F	DISSOLVED 350°F
NONE	---	1.0	1.0
SS-304	1.0	---	---
PURE Ti	1.0	---	---
Ti-AL-V	4.0	---	---
Ti-AL-Mo	2.6	---	---
Al	1.0	---	---
Cu	5.7	10	200
Fe	---	1.5	50
Co, Ni	---	6.0	60

Fig. 13.

Both types showed significant effects with copper being the most reactive metal studies. Later on, I'll contrast these results with those obtained in deoxygenated systems. In general, then, we find that in air saturated fuels, the hydrocarbon profile, sulfur compounds, nitrogen compounds and metals can all have adverse effects on fuel stability.

What about oxygen-poor systems? If we are correct in our assumption that deposits are formed due to oxidative polymerization, removal of the dissolved O_2 should confer stability on JP-5 fuel. The effects of deoxygenating a high quality, additive-free fuel are illustrated in Fig. 14.

DEOXYGENATION CAN MARKEDLY DECREASE DEPOSIT FORMATION

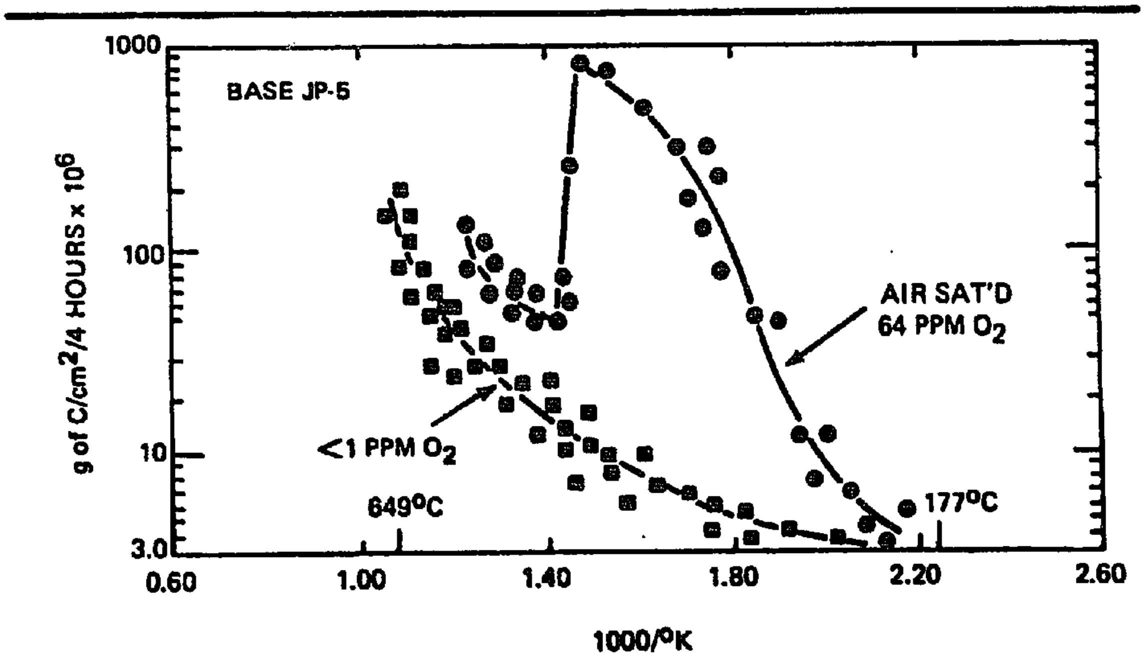

Fig. 14.

It is clear that deoxygenation can make a very significant improvement in fuel stability. We find, for example, that the "break point" temperature for high quality JP-5 can be increased from 550°F to over 1100°F this way. Unfortunately, all fuels do not respond equally well to this sort of treatment.

The jet A shown in Fig. 15 was known to be a poor quality fuel. One of the main differences between it and "thermally stable" fuels was the presence of trace impurities, particularly sulfides. These observations stimulated further work on the effects of fuel composition on deposit formation in deoxygenated systems; the results of which I plan to summarize here.

The first compounds we investigated were sulfur-containing. These were studied at 3,000 - 4,000 ppm S levels, consistent with present day sulfur specifications. A summary of results is shown in Fig. 16.

DEOXYGENATION IS NOT A "MAGIC CURE-ALL"

FUEL	QUALITY	RELATIVE TOTAL DEPOSITS AIR SAT'D	RELATIVE TOTAL DEPOSITS DEOXYGENATED
JP-7	EXCELLENT	0.16	0.10
BASE JP-5	↓	BASE=1.00	0.13
30% JP-5/70% THERMALLY STABLE		1.22	0.25
ASHLAND JP-5		1.66	0.27
ASHLAND JET A		1.87	0.35
AMERICAN OIL JET A	POOR	3.40	15.4

CONDITIONS: 6.9 MPa, 150 TO 315°C.

Fig. 15.

THE MAJORITY OF SULFUR COMPOUNDS ARE DELETERIOUS

SULFUR COMPOUND CLASS (a)	TOTAL DEPOSITS RELATIVE TO AS IS FUEL (b)
SULFIDE	1.87 TO 8.25
THIOL	2.62
DISULFIDE	4.48 TO 4.89
POLYSULFIDE	5.01
CONDENSED THIOPHENE	0.66 TO 0.91

(a) INDIVIDUAL COMPOUNDS ADDED (3,000 PPM S) TO BASE JP-5
(b) CONDITIONS: 6.9 MPa, 350 TO 538°C, <1 PPM O_2

Fig. 16.

It is clear that most sulfur compounds can have a strong influence even on deoxygenated fuels. Particularly deleterious are sulfides, disulfides and polysulfides, which readily produce free radicals on pyrolysis. Thiophenes are actually stabilizing to deoxygenated fuels.

The effects of various nitrogen compounds were studied at the 100 ppm N level. Results are given in Fig. 17.

NITROGEN COMPOUNDS ARE NOT DELETERIOUS BY THEMSELVES

NITROGEN COMPOUND CLASS (a)	TOTAL DEPOSITS RELATIVE TO BASE FUEL (b)	AIR SATURATED
PYRROLES	0.70 TO 0.88	8.0 - 15
PYRIDINES	0.89 TO 1.32	6.0 - 10
AMINES	0.82 TO 0.97	---
OTHERS	0.70 TO 0.93	---

(a) INDIVIDUAL COMPOUNDS ADDED (100 PPM N) TO BASE JP-5
(b) CONDITIONS: 6.9 MPa, 350 TO 538°C, <1 PPM O_2

Fig. 17.

These compounds, by themselves, did not promote deposit formation under high temperature stress. This is in sharp contrast to their highly deleterious nature in air saturated systems. We are not sure why this is true. Perhaps the decomposition products are either fuel-soluable or do not deposit out on tube walls.

The influence of various oxygen compounds was also investigated:

THE EFFECT OF ORGANIC OXYGEN COMPOUNDS VARIES

ORGANIC OXYGEN COMPOUND CLASS (a)	TOTAL DEPOSITS RELATIVE TO AS IS FUEL (b)
PEROXIDE	1.94 TO 6.00
CARBOXYLIC ACID	0.87 TO 2.00
PHENOL	0.97 TO 1.38
FURAN	0.95 TO 1.01
ALCOHOL	0.91 TO 1.38
KETONE	0.83 TO 1.64
ESTER	0.88 TO 1.68

(a) INDIVIDUAL COMPOUNDS ADDED (100 PPM O) TO BASE JP-5
(b) CONDITIONS: 6.9 MPa, 350 TO 538°C, <1 PPM O_2

Fig. 18.

These varied from very deleterious (peroxides) to virtually non-deleterious (alcohols) depending upon type and level added. Peroxides are especially important and are worth another look:

PEROXIDES ARE HIGHLY DELETERIOUS

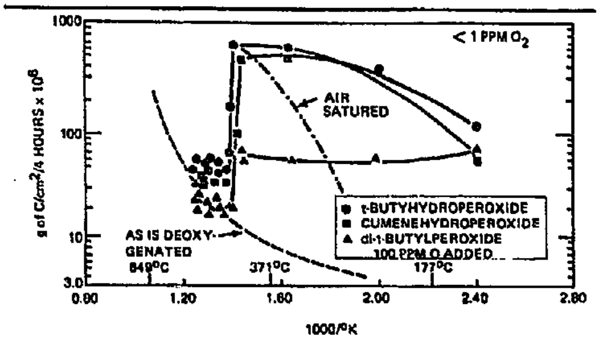

Fig. 19.

Peroxides were found to be more deleterious than sulfur compounds, even when present at much lower concentrations. The shapes of the peroxide Arrhenius plots are similar to those from an air saturated fuel in the absence of any additives. This implicates peroxides as major cause of deposits in air saturated fuels.

Under deoxygenated conditions, nearly all types of hydrocarbons are stable to temperatures up to 1000°F. Exceptions are certain olefins:

EFFECT OF OLEFIN TYPES

- SOME OLEFINS WERE DELETERIOUS
  - ACETYLENES
  - DI-OLEFINS WITH TERMINAL BONDS
  - MONO-OLEFIN AROMATICS WITH CONJUGATED SIDE CHAINS
- OTHER MONO AND DI-OLEFINS DID NOT INCREASE DEPOSIT FORMATION

Fig. 20.

These structure-activity relationships roughly parallel those found in the air saturated fuels. Acetylenes were extremely deleterious. Fortunately, they are seldom found in large quantities in petroleum based fuels.

A study of interactions between trace impurities was carried out. In some instances, two innocuous compounds interacted to give deposits, while neither of the two species were deleterious when tested alone. In other cases, compounds interacted to retard deposition formation. A summary of the major interactions uncovered is shown in Fig. 21.

INTERACTIONS INVOLVING TRACE IMPURITIES WERE FOUND

- PYRROLES INTERACTED WITH ACIDS, OLEFINS AND CONDENSED THIOPHENES TO INCREASE DEPOSIT FORMATION
- ORGANIC OXYGEN COMPOUNDS, E.G., ALCOHOLS, ESTERS AND KETONES, INTERACTED TO INHIBIT DEPOSIT FORMATION

Fig. 21.

An example of how interactions work is given in Fig. 22.

The effects of metal surfaces on deposit formation rates in deoxygenated fuel is presented in Fig. 23, and contrasted with results obtained in air saturated systems. A quite different order of reactivity was encountered.

Dissolved metals had only a minor effect in deoxygenated fuels. Copper, an especially deleterious metal in air saturated fuels, was much less reactive in oxygen poor systems.

I have delayed until now any discussion of the characteristics of the deposits, because I want to compare those obtained in air saturated and oxygen poor fuels. Both types are appropriately described as varnish-like.

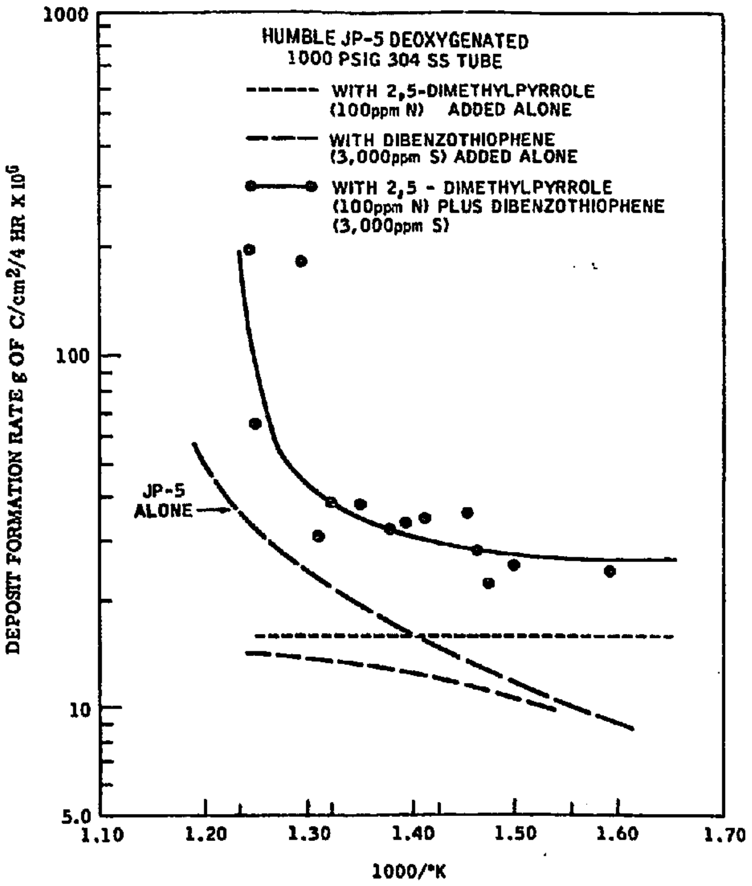

Fig. 22.

EFFECTS OF METAL SURFACES ON DEPOSIT FORMATION
AIR SATURATED VS. DEOXYGENATED JP-5

METAL SURFACES	RELATIVE DEPOSITS AIR SATURATED (400°F)	DEOXYGENATED (300-1000°F)
SS-304	1.0	1.0
COPPER	5.7	---
Cu-Ni	---	1.5
PURE TITANIUM	1.0	3.5
Ti-AL-V	4.0	0.9
ALUMINUM	1.0	5.5*

*TO 600°F

Fig. 23.

EFFECTS OF DISSOLVED METALS ON
DEPOSIT FORMATION IN DEOXYGENATED JP-5

METAL	RELATIVE DEPOSITS (300-1000°F)
NONE	1.0
Cu (100 PPB) (200 PPB)	1.2 2.0
Fe (10 PPB) (100 PPB)	1.7 2.9
V (100 PPB)	0.5

Fig. 24.

CHARACTERISTICS OF DEPOSITS

- VARNISH LIKE-INTRACTABLE
- MUCH ENRICHED IN OXYGEN
- ENRICHED IN
    - NITROGEN
    - SULFUR

Fig. 25.

They tend to adhere very strongly to metal surfaces and can be extremely difficult to remove. Samples which have been analyzed appear much enriched in oxygen and significantly higher in sulfur and/or nitrogen when these elements are present in the fuel, although the oxygen content is lower in deposits from deoxygenated fuels.

The two types differ in morphological characteristics.

In the air saturated fuel, it appears that deposits form as microspheres in the bulk fuel and collect on the surfaces after impingement from moving fluid. This results in many spherical particles adhering to the surface. Where O_2 is largely absent, those deposits which form seem to do so directly on the surface and have a more plate-like appearance. This is further evidence for a different mechanism of deposit formation in the two cases.

As a result of these studies, we have compiled some recommended processing and handling techniques for maximizing fuel stability. These are outlined in Figs. 27 and 28.

II. EFFECTS OF NITROGEN COMPOUNDS ON DEPOSIT FORMATION DURING FUEL STORAGE

With the rapid depletion of both U.S. and world-wide petroleum, reserves alternate; that is, non-petroleum fuels are becoming of greater and greater interest. It is generally agreed that the synthetics most likely to be

EFFECTS OF DISSOLVED O_2 ON DEPOSIT MORPHOLOGY

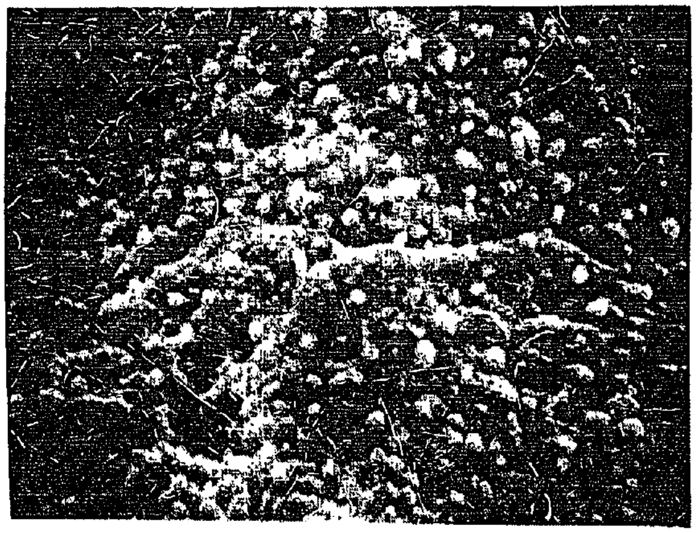

77 PPM O_2

0.3 PPM O_2

Fig. 26.

PROCESSING CONSIDERATIONS FOR
PETROLEUM-BASED FUELS

- MINIMIZE
  - PEROXIDES - ORGANIC ACIDS
  - SULFIDES - THIOLS-di-POLYSULFIDES
  - NITROGEN COMPOUNDS
  - OLEFINS
- AVOID
  - "DOCTOR" SWEETENING
  - EXCESS ACID OR CAUSTIC
- RECOMMENDED
  - HYDROTREATING
  - ABSORBENTS

Fig. 27

STORAGE OF "HIGH STABILITY FUELS"

- LIMIT
  - DISSOLVED O_2
  - LIGHT EXPOSURE
  - TEMPERATURE
  - DELETERIOUS METALS
- DEDICATED FACILITIES MAY BE NECESSARY

Fig. 28.

important in the relatively near term, 1980 to perhaps the year 2000, will be shale liquids, coal liquids, tar sand crude oils and methanol derived from coal. Processes are currently available for the production of liquid fuels from all these sources. However, the investment costs are high and the fuels they will afford are likely to be quite different from conventional products derived from petroleum. This latter point is illustrated by Fig. 29.

CHARACTERISTICS OF CRUDE OILS DERIVED FROM VARIOUS SOURCES

	PETROLEUM	SHALE	COAL
% N	.1-.5	1-3	.6-1
% O	0.5-5.0	6	7-15
% S	.6-6	.6-3	.3-2
SATURATES %	70-90	10-40	5-20
AROMATICS %	10-20	25-50	10-50
POLARS %	<1	1-3	50-80
OLEFINS	1-2	25-50	1-5

Fig. 29.

Although syncrudes vary considerably, depending on source and production methods, some generalizations seem clear:

Shale liquids will be higher in nitrogen, slightly higher in oxygen, more olefinic and have more polar compounds than crude petroleum. Coal liquids, on the other hand, will have less nitrogen than shale, but will be much higher in oxygen, aromatics and polar compounds than either petroleum or shale-derived crudes.

Nitrogen compounds are among the most difficult of these non-hydrocarbons to remove or convert. In addition, they are deleterious to fuel stability. This has been known in a general way for some time, and is illustrated by the plot shown in Fig. 30, which shows three jet fuels, prepared by hydrotreating

Variation of JFTOT Breakpoint Temperature With Nitrogen Level After Hydrotreatment

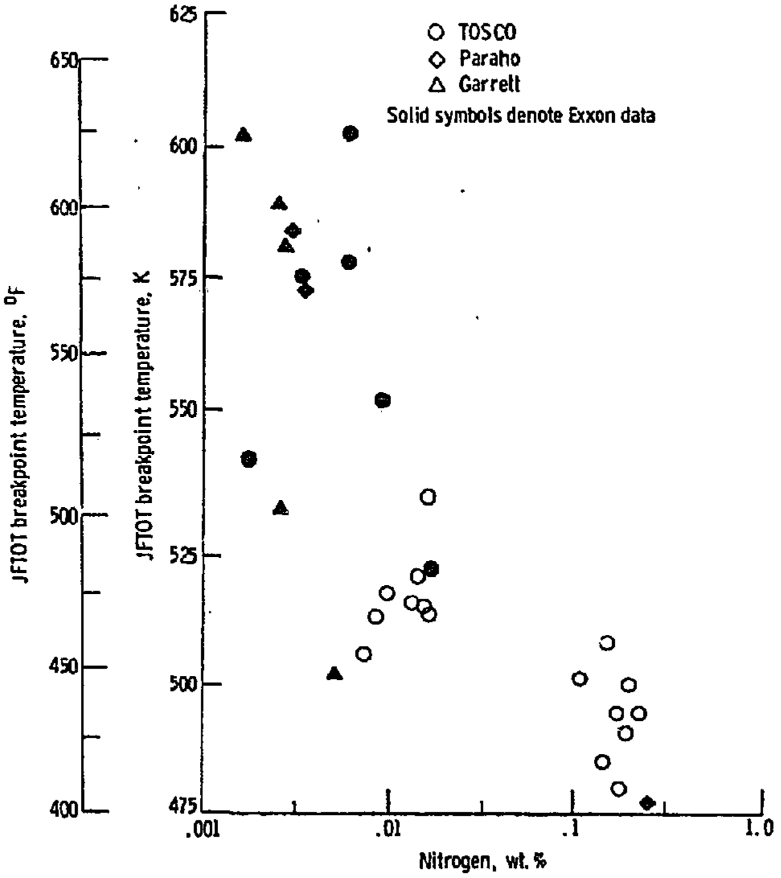

Fig. 30.

shale, subjected to the standard JFTOT thermal stability test. Shown here are plots of breakpoint temperature vs. nitrogen content for samples of varying degrees of hydrotreating. Clearly, the higher the nitrogen content, the poorer the thermal stability. Many of these samples were severely hydrotreated and, yet, still retained sufficient nitrogen to affect stability.

In addition, we had observed during a previous fuel stability program that trace amounts of certain nitrogen compounds promoted sludge or sediment formation in otherwise stable JP-5, even when stored under ambient conditions.

This is illustrated by Figs. 31 and 32.

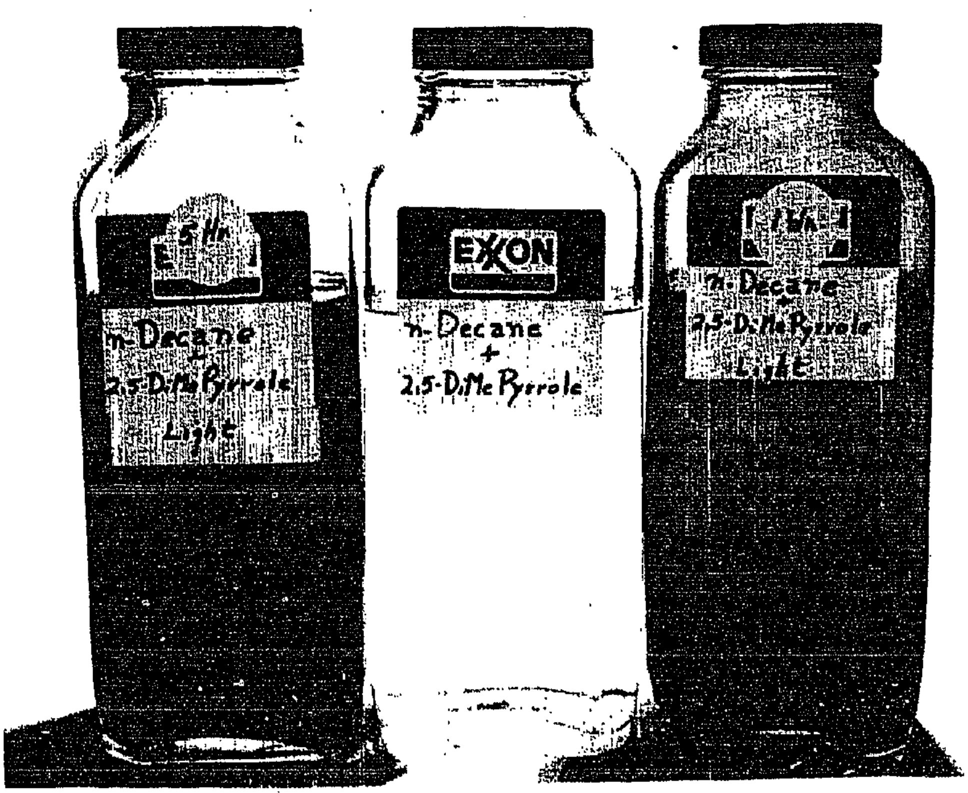

Fig. 31.

Figure 31 shows the effects of .2% of nitrogen in the form of 2,5-dimethylpyrrole (DMP) added to decane and stored at room temperature in light for a few hours and one week. An immediate darkening of the fuel is observed followed by heavy sludge formation. These experiments were conducted in decane, but exactly the same phenomena were observed in JP-5.

Figure 32 is actual shale liquid, produced with considerable effort, to meet all jet fuel specifications, yet it still affords considerable sludge on storage. Additive-free petroleum derived JP-5, on the other hand, was

Fig. 32

relatively clear after eight years. The major difference between these samples and those in Fig. 31 is nitrogen content.

Intrigued by these observations, we performed an experiment in which we measured the sediment formed in JP-5 under various conditions. Plots of sediment formation vs. time are shown in Fig. 33.

The reactions to form sediment proved to be influenced by acids, light, and oxygen present in the fuel. Thus, the most rapid rate of sediment formation was observed in cases where air saturated fuels containing both 2,5-dimethylpyrrole and a typical organic acid, n-decanoic, were stored in the presence of light. Neither the base fuel nor the fuel with acid added alone afforded any detectable sediment. Nor was the color of the fuel altered in any way in the absence of the nitrogen compound. As a result of these preliminary observations, the present study was undertaken to investigate this phenomenon further.

In the experiments I'll describe today, high quality n-decane was employed as the diluent or "model fuel". This was further purified by percolation through columns of activated alumina to remove traces of reactive polar materials. The nitrogen compounds were tested at the 2000 ppm level (nitrogen basis) which is within the limits expected from fuels derived from shale or coal. Samples were stored either in total darkness or under uv radiation at

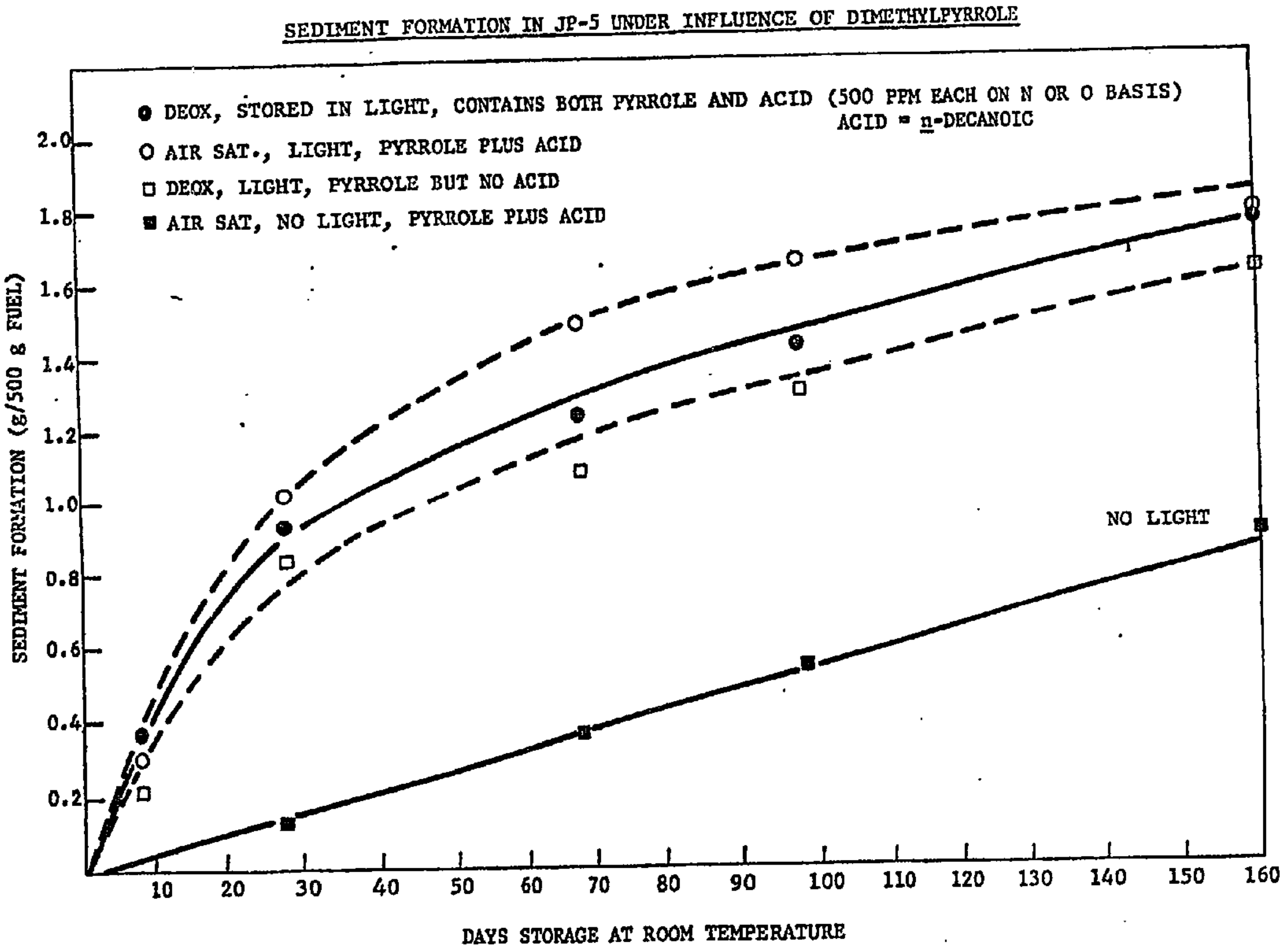
SEDIMENT FORMATION IN JP-5 UNDER INFLUENCE OF DIMETHYLPYRROLE
● DEOX, STORED IN LIGHT, CONTAINS BOTH PYRROLE AND ACID (500 PPM EACH ON N OR O BASIS)
ACID = n-DECANOIC
○ AIR SAT., LIGHT, PYRROLE PLUS ACID
□ DEOX, LIGHT, PYRROLE BUT NO ACID
■ AIR SAT, NO LIGHT, PYRROLE PLUS ACID
NO LIGHT
SEDIMENT FORMATION (g/500 g FUEL)
2.0
1.8
1.6
1.4
1.2
1.0
0.8
0.6
0.4
0.2
10
20
30
40
50
60
70
80
90
100
110
120
130
140
150
160
DAYS STORAGE AT ROOM TEMPERATURE

Fig. 33.

a wavelength of 336 nm, with an intensity of 1100 w/CM^2. Other samples were exposed to normal sunlight to serve as controls.

The predominant nitrogen-containing species found in light distillates from shale are shown in Fig. 34.

NITROGEN COMPOUNDS FOUND IN SHALE OIL LIGHT DISTILLATE

TYPE	WT. % OF TOTAL N
ALKYLPYRIDINES	42
ALKYLQUINOLINES	21
ALKYLPYRROLES AND INDOLES	19
CYCLIC AMIDES	3
ANILIDES	2
WEAK AND NON-BASIC N	11

Fig. 34.

Representative compounds of these types were chosen for this study. The effects of various nitrogen compounds on sediment formation are given in Fig. 35.

EFFECTS OF 2,000 PPM OF N COMPOUNDS ON SEDIMENT FORMATION IN n-DECANE (STORED IN LIGHT)

COMPOUND TYPE	SEDIMENT (g/500 g DECANE) IN 60 DAYS
PYRROLE	0.4
ALKYL PYRROLES	0.2-2
INDOLE	0.05
ALKYL INDOLES	0.05-2
CARBAZOLE	.005
ARYL AMINES	0-.005
ALKYL AMINES AND AMIDES	0

Fig. 35.

It is clear from this data that sediment formation is not unique to 2,5-dimenthylpyrrole (DMP), although, of those compounds tested, DMP produced the greatest amount. In fact, the compounds giving the most sediment were all of the pyrrole type. None of the amines or amides studied produced sediment, although considerable darkening of the fuel was observed. It appears, from what we have seen so far, that the most deleterious compounds fall in the non-basic classification. Basic nitrogen compounds are much less important with respect to sediment formation.

The substitution pattern of alkyl groups on the pyrrole and indole nucleus also play a role.

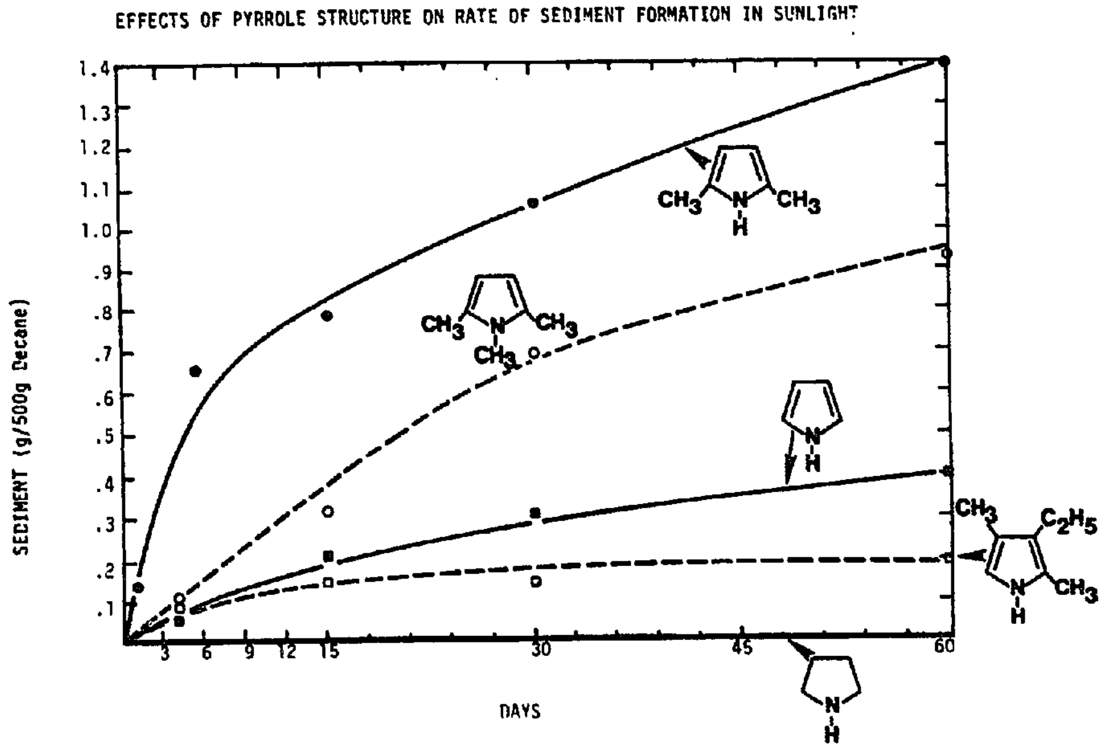

Fig. 36.

The important elements, for greatest reactivity, are:

At least one double bond

An alkyl group at position 2 or 5

An unsubstituted carbon at position 3 or 4

Very similar results are obtained with the indole series.

III. EFFECTS OF DILUENT

The hydrocarbon content of the fuel appears to have only minor effects on the sedimentation reactions. This is illustrated by the curves in Fig. 37.

In these experiments, two typical aromatic hydrocarbons were added, in amounts expected in shale liquids, to the decane diluent, along with DMP. As you see, the plot of sediment formation vs. time is virtually superimposable with that obtained with DMP in decane alone.

EFFECTS OF AROMATICS

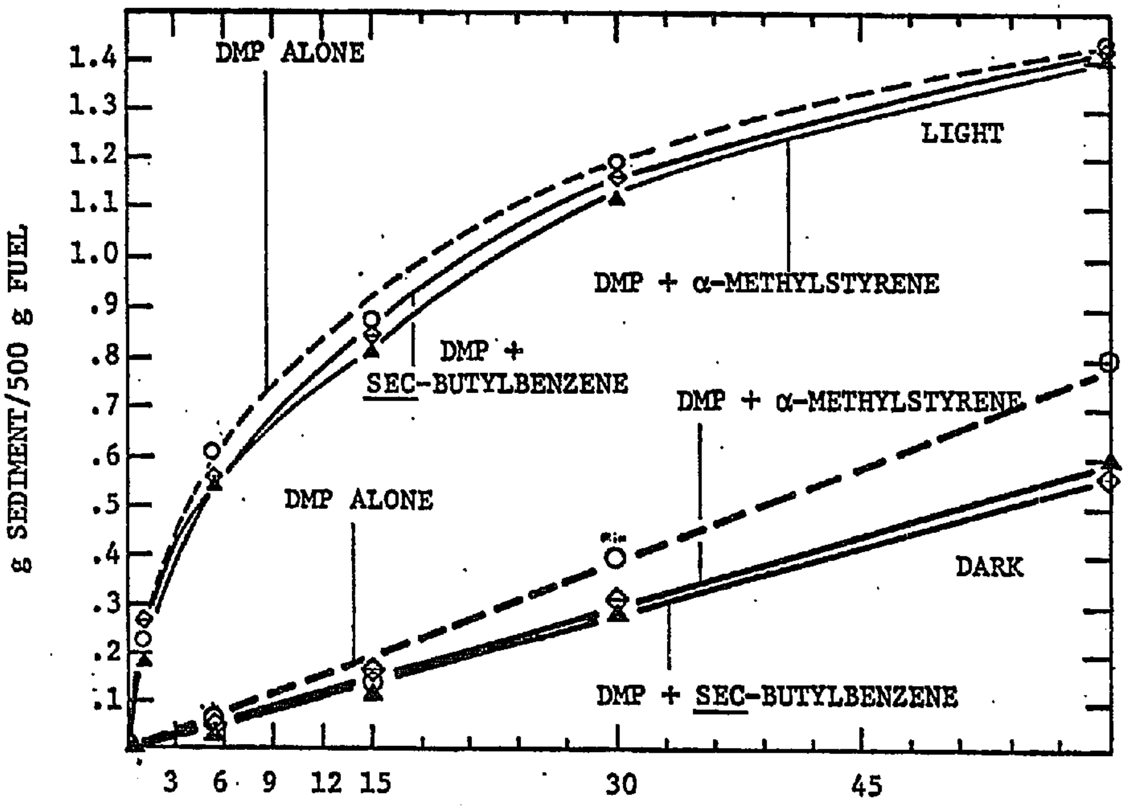

STORAGE TIME (DAYS)

Fig. 37.

IV. EFFECTS OF STORAGE CONDITIONS

On the other hand, storage conditions have a considerable effect on sediment formation. For example, light promotes sludge formation to a great extent. This is apparent from Fig. 38.

The difference between the irradiated and dark-stored samples is quite large early in the period and tends to get much smaller later. With DMP, sediment in the irradiated sample exceeded that for the dark sample by a factor of ten after one day, but was only about 38% greater after 60 days. This suggests that exclusion of light will retard, but not prevent sediment formation.

Samples stored in sunlight formed sediment slightly more rapidly than the UV irradiated material. This effect is not of practical significance, but may have a bearing on the mechanism of sediment formation.

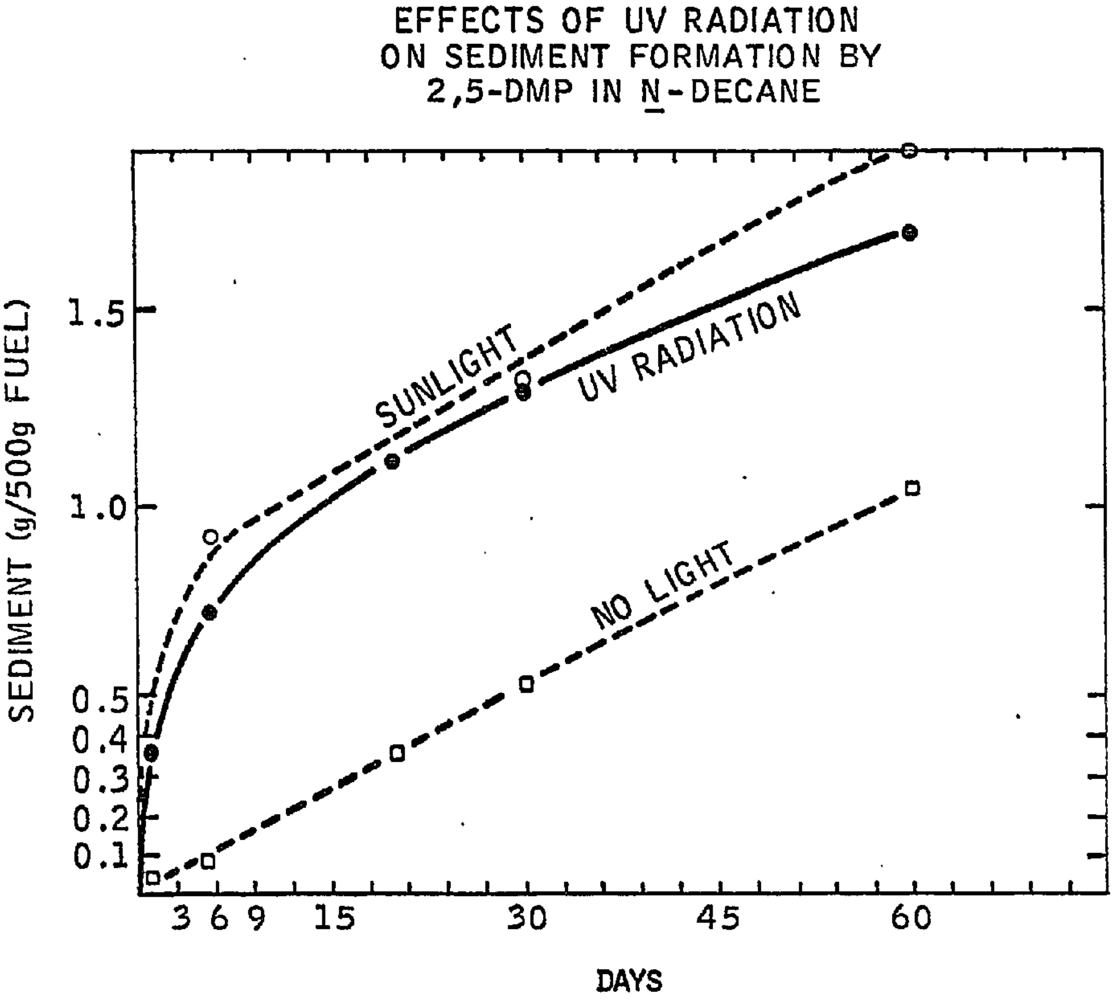

Fig. 38.

It should be noted that the build up of sediment in the dark follows a straight time relationship, while the light catalyzed reaction does not. The dark reaction appears to be at least "pseudo" zero order, while the catalyzed reaction is of a higher order. It should, also, be emphasized that the shape and general magnitude of the curves obtained in n-decane is in excellent agreement with those from actual JP-5 fuel.

It was clear from the outset that sediment formation is an oxidative reaction and that the dissolved oxygen content of the fuel influences the reaction. For example, the formation of color is considerably retarded in solution which has been sparged with nitrogen to remove dissolved oxygen.

Shown in Fig. 39 are two solutions of DMP in decane air saturated and deoxygenated after five hours' storage in light. The difference is quite significant, especially at this relatively short storage time. More quantitative results are shown in Fig. 40.

Fig. 39.

EFFECTS OF DISSOLVED OXYGEN
ON SEDIMENT FORMATION WITH DMP

ppm O_2	Stored	Sediment 15 Day	(g/500 g) 60 Day
<1	Sun	.15	
70	Sun	.68	
<1	UV	.21	.92
	Dark	.02	.23
70	UV	1.05	1.71
	Dark	.21	.89

Fig. 40.

The deoxygenated samples afforded about 1/5 the amount of sediment after 15 days in the light, and 1/10 under dark storage. This ratio fell to 1/2 and 1/4, respectively, after 60 days. A combination of exclusion of light and deoxygenation reduced sediment by 87% over 60 days and by over 95% over 15 or 30 days.

V. EFFECTS OF TRACE IMPURITIES

We have started a study on the effects on non-hydrocarbon impurities on sludge formation. Among the most important types of such impurities are organic acids, which are known to promote oxidative polymerization of pyrroles. Some data on the influences of representative organic acids are given in Fig. 41.

SEDIMENT FORMATION WITH DMP
UNDER THE INFLUENCE OF ORGANIC ACIDS

ACID	STORAGE CONDITIONS	CUMULATIVE SEDIMENT (G/500 G DECANE)	
		15 DAYS	60 DAYS
NONE	LIGHT	.869	1.52
	DARK	.197	.840
N-DECANOIC	LIGHT	1.25	1.84
	DARK	.497	1.50
CYCLOHEXANE CARBOXYLIC	LIGHT	1.26	1.83
	DARK	.621	1.84
BENZOIC	LIGHT	.858	1.96
	DARK	.414	1.12

Fig. 41.

All types studied promote sediment formation. The effects were particularly noteworthy in samples stored in darkness, where the acids doubled the rate of sediment formation. More rigid specifications for acid content may be necessary for future shale-derived fuels.

Phenols have the opposite effect. That is, they tend to inhibit or retard sediment formation. For example, Fig. 42 shows the effect of added di-t-butylphenol on sedimentation with DMP.

A 58% reduction in sediment formation was obtained under light storage at 60 days and 80% reduction after 15 days, as compared to controls. Under dark storage conditions, the corresponding reductions were 40% and 80%. It is noteworthy that the samples containing the phenol gave less sediment under light storage than did DMP alone in the dark. Thus, this material appears effective in combatting both the "light" and "dark" reaction. Other phenols are also effective. However, di-t-butylphenol is the best inhibitor we have yet studied.

EFFECT OF DI-t-BUTYLPHENOL ON SEDIMENT FORMATION WITH 2,5-DIMETHYLPYRROLE IN DECANE

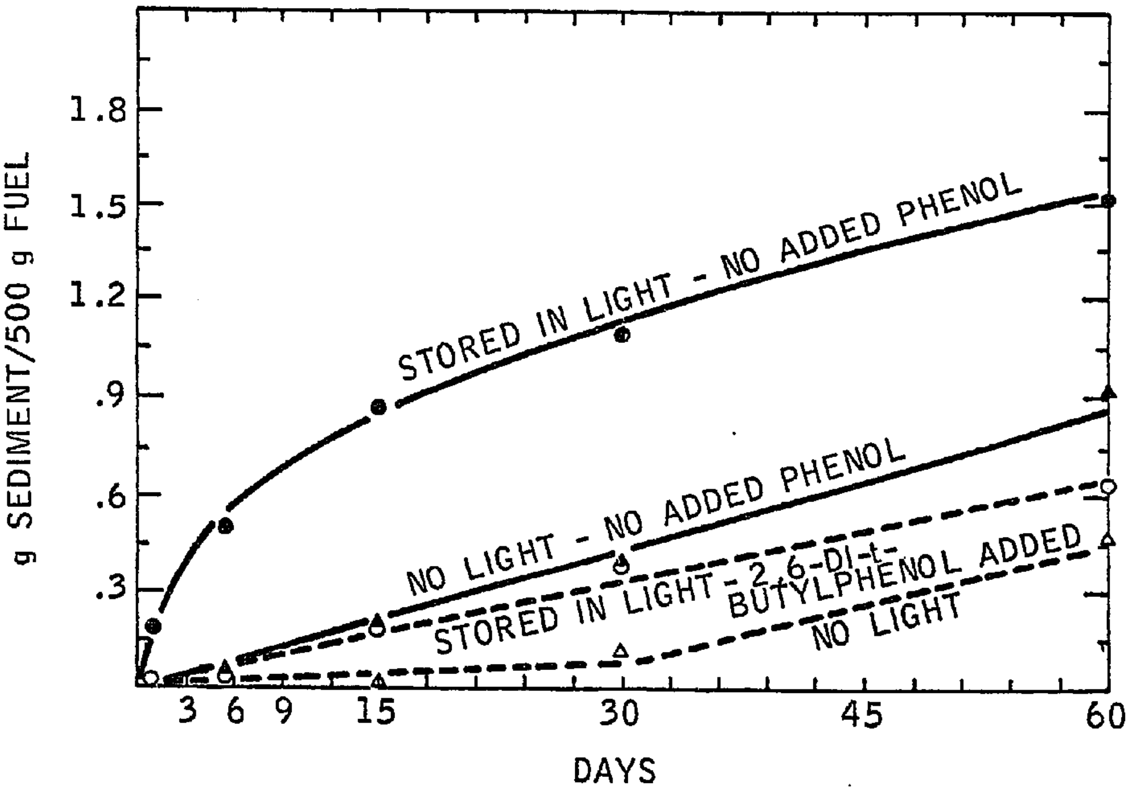

Fig. 42.

VI. CHEMICAL STRUCTURE OF THE SEDIMENTS

We are also interested in determining the structure and mechanism of formation of these sediments in hopes of finding ways of avoiding the problem. The elemental analyses for various sediment samples are given in Fig. 43. Note that all were stored under similar conditions and all were air saturated.

ELEMENTAL ANALYSIS OF SEDIMENTS FROM 2,5-DIMETHYLPYRROLE

Source	% C	% H	% N	% O
JP-5 (80 DAYS)	59.71	5.54	11.29	23.28
DECANE (5 DAYS)	62.28	5.33	11.86	20.53
JP-5 + C_{10} ACID	62.30	5.88	10.95	20.07
AVE. 11 SAMPLES	61.30	5.67	11.29	21.51

CALC. FOR $C_6H_7NO_{1.5}$:

C = 61.54 H = 5.98 N = 11.97 O = 20.51

Fig. 43.

Significantly, samples from a variety of sources have nearly the same compositions, so long as the oxygen contents are similar. Neither components of the diluent nor the acid catalyst seem to be incorporated in the sludge.

The data suggests that the deposits are made up largely of repeating units of the dimethylpyrrole. This is clear since the average C/N ratio in the sediments (6.3/1) is very close to the C/N ratio of dimethylpyrrole (6/1). Thus, no other carbon-containing species have been introduced. On the other hand, considerable oxygen (about 1.5 atoms per N) has been incorporated at the expense of 2 hydrogen atoms.

The approximate average molecular composition normalizes to $C_{6.3}H_{7.0}N\,O_{1.7}$. Possible structures for the sediment obtained with DMP are shown here.

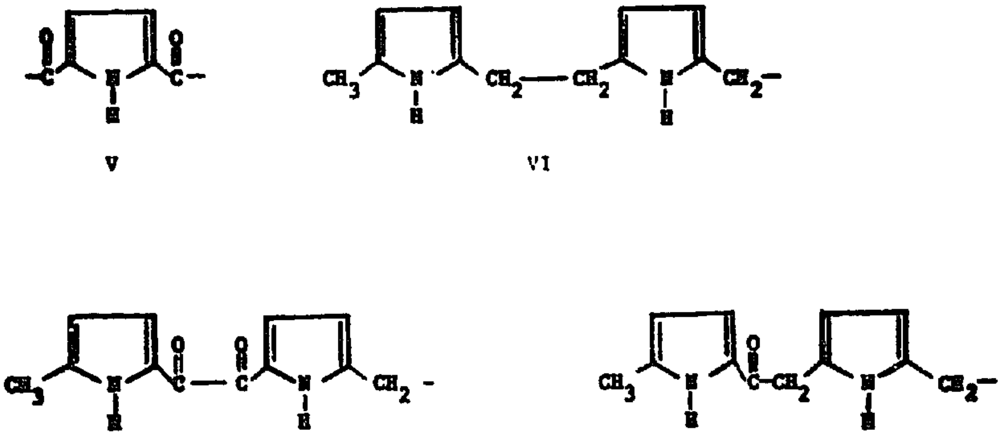

V

VI

VII

VIII

Fig. 44.

The infrared and mass spectra of the sediments suggest that a mixture of these structures is present. The methylpyrrole moiety appears intact and both carbonyl and ether type atoms may be present. The largest parent peaks observed lie about 380-420 mass units. This represents only 3-4 repeating pyrrole units. However, the problem may not be quite so simple. Other structures are also possible.

We are continuing work in this area. Based on the somewhat preliminary results presented today, we can tenatively conclude:

Nitrogen compounds can be seriously deleterious to the storage stability of synfuels (Fig. 46).

(A) Non-basic, especially pyrrolic types, are deleterious: many other nitrogen-containing compounds are not.

(B) The pyrrolic compounds themselves vary in the magnitude of their influence on sediment formation. The rate is

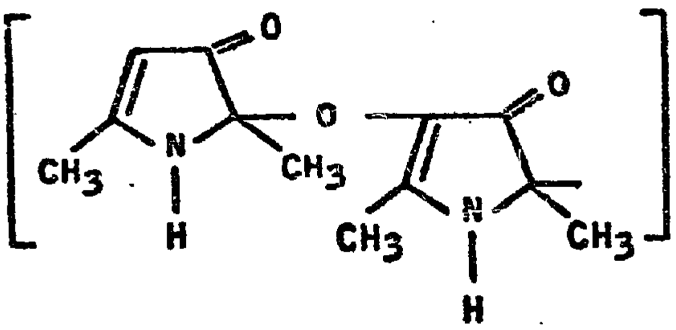

II

$C_6H_7NO_{1.5}$

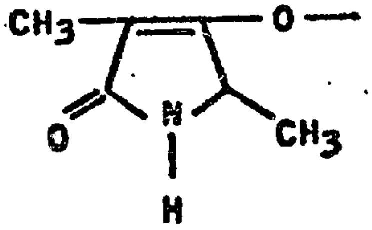

III

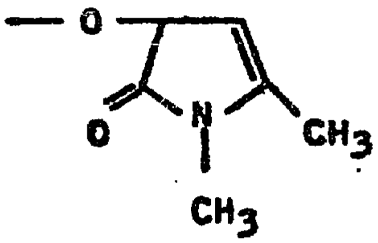

IV

Fig. 45.

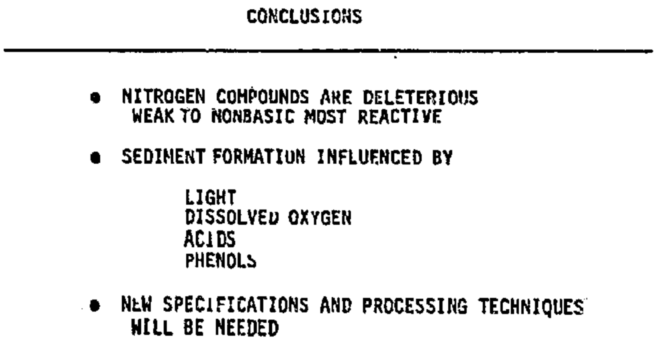

CONCLUSIONS

- NITROGEN COMPOUNDS ARE DELETERIOUS
  WEAK TO NONBASIC MOST REACTIVE
- SEDIMENT FORMATION INFLUENCED BY
  - LIGHT
  - DISSOLVED OXYGEN
  - ACIDS
  - PHENOLS
- NEW SPECIFICATIONS AND PROCESSING TECHNIQUES
  WILL BE NEEDED

Fig. 46.

especially high with 2,5-dimethylpyrrole.

Storage conditions may play an important role; the effect of light and oxygen content are particularly noteworthy.

Certain trace impurities are also important in their effects on promoting sediment formation.

(A) Carboxylic acids accelerate the formation rate: the effect is most pronounced in the dark.

(B) Some phenols inhibit sediment formation: structural effects are important.

The sediments appear to have a definitive structure which may be amenable to analysis. With DMP, this appears to be low to medium molecular weight oligomers, consisting of partially oxidized repeating units of the nitrogen compound.

Comments and Replies on

"Chemistry of Deposit Formation in Hydrocarbon Fuels"

by J. Frankenfeld

K. Wray: The units given on the deposit rates, the square centimeters...

J. Frankenfeld: That's the tubing surface.

K. Wray: That starts out as a clean well-defined area.

Slide 8

J. Frankenfeld: We, we're very careful that the tubing is consistent.

K. Wray: What's the oxidation in the absence of catalyst?

J. Frankenfeld: It won't go to zero. There is always going to be some oxygen uptake in the absence of catalyst. There is a fair amount of controversy on the mechanism of metal catalyzed autoxidation. The effect of metals is still a little bit up in the air. We know there is one; but exactly the chemistry involved is not perfectly clear. We have looked at both metal surfaces and dissolved metals. In studying the metal surfaces, we simply take the tubing that I showed you on the third slide, which, in our standard case, is 304 stainless steel, fabricate it with various other metals, and we get some unusual results. We find, for example, that pure titanium doesn't seem to have much of an effect, nor does pure aluminum.

I. Osgerby: What is the surface condition of this tubing? Is the surface characterized?

Slide 12

J. Frankenfeld: It's quite smooth. That "quite" is in quotes. We have not carefully controlled that.

K. Wray: A sealed tube is not expected to have a large surface area.

J. Frankenfeld: You're right. Actually, when this program got under way, we were talking about the one thing; the Boeing SST. They were considering air frame manufacture. The aircraft people were considering different tubing they might use for fuel delivery systems. These were the sort of things they recommended, and we used tubing provided, in some instances, by them. I don't think their tolerances were expected to be very close with respect to smooth surface inside tubing.

I. Osgerby: I don't understand what your figures are on the catalyst surface.

J. Frankenfeld: Those are relative deposits to stainless steel 304. The total deposits are much higher than this, it is just that relative to the stainless steel standard tubing, we find these sort of results. If I were to give you all of the raw data of ten year's work, we'd be here until next week so I'm trying to summarize and I didn't make that clear. I'm sorry.

B. Gerhold: What's the . . . 350 at?

J. Frankenfeld: Those are temperature regimes.

B. Gerhold: Is that tube or fuel temperature?

Slide 13

J. Frankenfeld: Tube. People have continually asked me "what is the bulk fuel temperature within?" We are now struggling with the way to measure it. People in the combustion area are vitally interested in that. The important thing to keep in mind is these are comparisons rather than raw numbers.

I. Osgerby: Are these steam heated tubes?

J. Frankenfeld: Oh, no. It is a furnace.

G. Kamm: Did you go to temperatures any higher than 400, and did you observe the same type of relationship?

J. Frankenfeld: Yes. The order is the same at higher temperatures, the total activity increases.

G. Kamm: Would you care to say how high you did go?

Slide 13

J. Frankenfeld: We have gone as high as 1100°-1200°F in this unit. Mostly, in the case of deoxygenated fuels. You see, again, in the case of air saturated fuels, we get what we would consider fuel breakdown at temperatures in the 500°F range. In some of this early work, we didn't pursue them above that point, but as you start plotting, you see that the Arrhenius plots go up sharply above 500°F. I'll show you some later with deoxygenated cases, where the breakdown is at a much higher temperature. But this early work didn't go much above 500°F. Actually, pure aluminum couldn't stand more than 500°F, anyway.

J. Bett: Is there a relationship between these numbers and residence time in the tube?

J. Frankenfeld: These are relative numbers. The residence time is less important than you would think. But it does have an effect.

G. Kamm: Does that 10cc per minute imply a laminar flow through the tube?

J. Frankenfeld: Yes. There are certainly some theoretical problems in what's going on inside that tubing. I was going to show you some of these in a while, but we really haven't characterized that very well. We're going to try to devise a new unit. People in NASA are quite interested in this, and they have asked us, "what's the temperature in there? Where does it go from wall to wall?" We don't know. Apparently, the same people are very interested in this. It would be very useful to find some way to measure that. We're going to continue with this work, for a while, and we're going to try to get at that problem. We simply just don't know, right now.

Slide 13

I. Osgerby: What are the metals involved?

J. Frankenfeld: These are acetonylacetonates. They are, what you might call, a metal soap. We've also looked at suspending parts per billion of pure metals. You get what's essentially an engineering definition of a solution in that you can't filter it through the finest kind of milipore. It wouldn't be a true solution, as a chemist would look at it.

R. Edelman: What pressure was this done at?

J. Frankenfeld: Generally, about 7 megapascals. Pressure has a minor effect on what we've studied.

R. Edelman: I'm talking about vaporization of the fuel.

J. Frankenfeld: No, we're not vaporizing the fuel. This is flow in the liquid phase.

R. Edelman: Also, with liquid-phase reactions, wouldn't the pressures affect the reaction with the oxygen present?

Slide 13

J. Frankenfeld: Certainly, in the air-saturated case, ... I didn't want to get into this particularly, but no doubt, pressure in the air-saturated fuel has quite an effect. When we take the oxygen out, we see no effect of pressure.

I. Osgerby: The mechanisms involved in that are interesting, too. Has anyone looked at that? It starts out at a higher level than in the air saturated case, but with essentially the same sort of case.

J. Frankenfeld: That's an area we haven't explored thoroughly. I'll show you later on curves we get when we add peroxide that are almost exactly the same. This represents a build up of those reactive species. If you add a peroxide to the fuel, you <u>start</u> almost at the top of the curve. I'll show you the curves later on. Those (peroxides) would seem to be the reactive species when you have an air saturated fuel.

I. Osgerby: Then wouldn't residence time be a factor in this?

J. Frankenfeld: Yes, of course. You see, undoubtedly, residence time is going to have an effect. There's no question about it.

R. Edelman: Is the fuel continuously recirculated?

J. Frankenfeld: Oh, no. It is not continuously circulated. We store it after it comes out.

R. Edelman: It would be useful to know what the nature of the suspended material is.

J. Frankenfeld: Yes, it would be interesting to see what it is. We are only measuring deposits that are the wall because that was our original mission. We see some anomalous effects in the effluent fuel. We know that some fuels are breaking down, the color up, for example, but they don't give us deposits. Either gaseous deposits or fuel soluble deposits are formed or there are suspended deposits we don't see.

Slide 14

R. Edelman: The origin of these particulates may have an important effect in the subsequent combustion process.

J. Frankenfeld: Absolutely. This study was designed mainly to show what would happen to fuel lines and fuel nozzles. Later on, of course, you may be concerned about recycled deposits, but you're absolutely correct. Some of these materials we know are breaking down, yet they are not giving us deposits. That is, again, a separate study. It's very interesting, and something should be done about that. When we've got the time, we'll do it.

K. Wray: Is the implication that you've done tests that show that the phenomena does, in fact, occur on the walls?

J. Frankenfeld: I'm going to show you some electron micrograph pictures later on. We get different morphologies when it seems like deposits are forming in the bulk fuel as opposed to on a wall. We think that in air saturated cases, at least, the deposits are formed in the bulk fuel. The evidence for this is very, very sketchy. I really am not going to stick my neck out to say, "absolutely proven", but we think that is the case. On the other hand, if you don't have air or oxygen in the fuel, the morphology is quite different and it would look, to me at least, more likely that the deposits are actually formed on the surface.

K. Wray: The spurt coming out at the exit; has that got deposits in there?

J. Frankenfeld: Generally not. Some color some times, typical of the nitrogen compound, but not actual deposits. One thing to do is to blow the darn stuff (*i.e.*, effluent fuel) down and see what's in it. We ought to do that; no question about it.

R. Edelman: Isn't 7 megapascals greater than the critical pressure of the fuel?

Slide 26

J. Frankenfeld: You don't think there is any vapor phase at that point?

R. Edelman: That's what I'm asking.

J. Frankenfeld: That's true. At something like 400 or 500°C, I'm not sure. I don't know how else to explain that sudden drop off. We measure the gas from the outlet. There is often considerable amount of gaseous pressure from the outlet.

G. Patterson: Is there a difference between the makeup of the varnish which is formed above and below this layer?

J. Frankenfeld: We don't know yet. There's a difference in the varnish between air saturated and deoxygenated systems and I'll show you that in a minute.

G. Patterson: It looks to me like the transition here might really involve the kind of deposit which is being formed.

J. Frankenfeld: That's an interesting point. I really don't know except that the data is reproducible. We have much data that shows these types of of curves. I certainly belive the curves. I'm not sure I believe the official explanations. I throw that out to you, chew it up, and throw it back to me later.

J. Young: Over the four hour duration that you're talking about, how thick would the deposit be on the surface?

J. Frankenfeld: Very, very thin. We have a hard time getting it out.

J. Young: Could they completely cover the metal surface?

J. Frankenfeld: They appear to completely cover the metal surface. Oh, yes. Even in four hours.

J. Young: So, after a very short period of time, you're now looking at a continuous film of "varnish"- not a metal?

J. Frankenfeld: That's right, and the people who design combusters were very interested in this, because of what is the heat transfer rate. In fact, experts have told me exactly opposite (tales). "Oh, it's going to improve it" (heat transfer) one said. "It's going to inhibit it", another said. I'm not an expert in this area; I don't know. But yes, they cover the surface.

Slide 26

J. Young: But also, it tends to reduce the effects of your tube material?

J. Frankenfeld: Yes, possibly. But we, and others, have shown that metal effects operate even through the coating. (This may indicate some discontinuity.)

J. Houseman: Is the tube almost warmer than a liquid in this case?

J. Frankenfeld: Yes. Unquestionably.

J. Houseman: Is that why deposits are on the tube?

J. Frankenfeld: Well, as I say, I think that is open to question. Now, I have nothing more than the testimonies of experts and some of the morphology from the scanning micrograph I have shown you. They (the deposits) are spherical. I can't see why they'd be spherical if they were formed on the surface. Spherical deposits are being formed in the bulk fuel.

G. Patterson: Are the ones toward the stainless steel core different from the saturated or the deoxygenated? (Slide 23)

J. Frankenfeld Oh, certainly. You can only compare things vertically here (Slide 23) not horizontally. Of course, that's a single temperature (400°F) there. The other results were over the range of 300 to 1000°F. Normally, you have a magnitude of about 100 times greater with the (air saturated fuel) stainless steel under the same conditions. From 400°F up particularly, the difference becomes quite apparent. But you don't have to compare these things vertically. I could not give you all the raw data; we are trying to summarize it.

I. Osgerby: What are we actually looking at?

J. Frankenfeld: Actually, you're looking at the tube itself. We sent small segments of tube down to Scan Atlanta. Scan Atlanta operated the scanning electron microscope. Shermer has discussed this in some detail in a paper years ago. He reaches some of the same conclusions about the formation of spherical particles in the bulk fuel, which is the most likely place for spherical particles to form. We get much less of that in the case of the deoxygenated system this at least suggests the deposit is forming on the walls. Slide 26

J. Houseman: In that bottom picture, we are still looking at a deposit where we don't see bulk after the deposit?

J. Frankenfeld: The experiments were run the same way, the tubes were cut up and he managed to get a picture of the inside of a tube.

J. Houseman: But the dark gray material at the bottom ...

J. Frankenfeld: That's deposit. That's not the tube surface. That's the deposit. I'm speculating, but I think that in the air saturated cases you are getting spherical particles of deposits formed in the bulk fuel. As they pass by, they tend to impinge on the surface and stick.

X. Reed: What's held constant here? Is there a constant total amount of deposit in the two slides or are they both of the same four hour run? What's held constant?

J. Frankenfeld: Luckily in these particular cases, the total deposits were not far off being the same.

X. Reed: Otherwise it would be a serious problem.

J. Frankenfeld: It turned out that, in these particular cases, the total deposits were about the same, otherwise we couldn't draw a thing from these pictures. The deposit formation rate was about the same and it just turned out that we were lucky in this case, but we certainly expected the air saturated deposits to be much higher. In this case, they were not.

G. Patterson: Was any effort made to try to estimate the relative weight or amount of spherical deposit here and the continuity? The amount of spherical may be insignificant.

J. Frankenfeld: Right. I'm sure that, if it had impinged on the surface, eventually it is going to agglomerate. We did not measure it but I feel sure the differences are real.

I. Osgerby: In this paper you conclude that the deposit rate is greater with an oxygenated system than with a deoxygenated system. I'm not quite sure how to interpret that.

Slide 26

J. Frankenfeld: The rate of flow, in this special case (Slide 26) was slower. We didn't really intend to do this, but, luckily, we measured about the same deposit rate in this particular tube. Ordinarily, you are right; they would not be the same. It would be off by quite a magnitude depending on oxygen contents.

I. Osgergy: Does it matter whether it's spherical or whatever? Is the process occurring? I mean, in practice, maybe you might not know anything in four hours.

J. Frankenfeld: Oh, no. Of course not. These airplanes are going to be flying for thousands of hours perhaps. That's the problem. If we're limited to four hours, we don't have to worry about it. You certainly are not clogging any tubing. If it builds up over a thousand hours, then you are running into a problem. The morphology is only a clue aimed at understanding the phenomena.

R. Edelman: But you don't know what the instantaneous rate of build up is.

J. Frankenfeld: Yes, we do know the rate in terms of the carbon. We don't know the thickness of the film by any means.

K. Wray: How do you know it's linear that far out?

J. Frankenfeld: We don't.

K. Wray: When the results depend on the metals, you expect it's not linear?

J. Frankenfeld: I suspect it's not linear.

G. Kamm: There is a fair amount of information that said it's not linear.

J. Frankenfeld: Yes, I don't think it's linear either.

J. Young: Would it be appropriate to interpret that top photograph as saying you also have the continuous phase in addition to granular material?

J. Frankenfeld: I think so. You're not looking at an absolute difference in kind here. A difference in magnitude of spherical particles. It's shakey, but other people have interpreted similar data. I'm throwing it out to you as a possibility. It looks like the mechanism of formation in the two cases is different. Not only from this data, but from one I have shown you on the effects of the impurities.

R. Edelman: What is the composition?

J. Frankenfeld: Of the what--the fuel?

R. Edelman: No, of the deposit. You have indicated in general that the deposits are rich in oxygen and sulfur. What about the differences between these two?

J. Frankenfeld: Not very much. We haven't explored it to a great detail. It's very hard to capture deposits. It looks like the deposits are similar in these cases. There is enough oxygen for the low level of deposits we are seeing. Deoxygenation mainly affects the total amounts. The fuel itself is identical except for the oxygen content.

PART II OF TALK

J. Bett: Did you intend to say that the raw liquid costs are reasonable?

J. Frankenfeld: Oh, no, no. Even the raw liquid costs are high. Retorting of shale, for example, is going to cost money (as does mining of shale)--but the costs of processing from that point on are also very high. I don't want to make a point of that. That's not the purpose of my talk. I just sort of threw that in. But they are going to be high. Not only are these fuels going to be expensive, but they are not going to look like petroleum based fuels. That's the gist of this paper.

J. Bett: Are they going to be blends?

J. Frankenfeld: Oh, I think they will be blended, so I think the outlook for them is in blending in refineries. I don't think that you are going to burn shale as it is, but that's an opinion of mine and by no means an accepted one.

J. Bett: Does it happen in both light and darkness?

J. Frankenfeld: It happens in darkness much slower. We'll show that. It's strongly light catalyzed, but it can by no means be prevented in the dark; only retarded.

Slides 3 and 4

K. Wray: What's the point at which you can begin measurements?

J. Frankenfeld: First day.

K. Wray: In application, how is this going to apply through storage and transit and delivery?

J. Frankenfeld: That's a good question. This problem has just been identified. What to do about it is very much up in the air. But in the proper magnitude of the problem, (and I'm telling you, this is not minor) the amount of sludge formed is tremendous. Something is going to have to be done about it, I think, this continued build up.

I. Osgerby: How much phenol did you say you added?

J. Frankenfeld: 500 ppm oxygen level. By the way, thiophenols are even better for a while, but then they quickly stop being retardants and actually tend to increase sediments; perhaps because of oxidation to sulphonic acids; sulphonic acids are known to be catalysts. We're looking into that now. Phenols do seem to work. Although, after you get around sixty days, the effects begin to fall off some.

<u>END OF TALK</u>

Slide 42

J. Bett: I think the interesting aspect of your results to mixer design really is the residence time-temperature relationship.

J. Frankenfeld: That's the one thing we didn't study.

J. Bett: If that area were expanded, one could get some feeling for how close to a hot mixing zone one could introduce a fuel before getting into trouble. I think that would be a generic problem in all mixers. Another interesting point is that in your table showing the relative rates of deposits on different surfaces, the value for stainless steel is unity, while for everything else the values are greater.

J. Frankenfeld: Greater or about equal, with the exception of some of the titanium tubes.

J. Bett: An interesting question would then be: "What component is it of the steel that is inhibiting the formation of deposit?"

J. Frankenfeld: Whether it is actually inhibiting or not, I don't know. I think that we have to look at what's the component in the others that catalyzing it. One has to look and see what the surface characteristics of those tubes are. Copper is a bad actor whether it is dissolved or whether it is on the surface. That's a correlation that we can draw, which, I think, may indicate that it's something to do with copper.

K. Wray: For a more catalyzed reaction, you are going to want to know the temperatures at the wall. General conductivity you see at the walls might predominate.

J. Frankenfeld: Can you tell me how I can measure the temperature?

R. Edelman: You don't know how to measure the bulk fuel temperatures?

J. Frankenfeld: Not in our unit. We'll have to design a new unit with larger tubing and somehow get a thermocouple in there.

Questions: What tube diameter do you use now?

J. Frankenfeld: About .038 in OD. It's small. We need a different type of unit.

R. Edelman: You might also want to look at the surface-to-volume ratio while keeping the flow velocity the same. People have looked at this problem for aircraft engines.

J. Frankenfeld: It is very different. That's this thermal stability, and they find the same kind of metal effect that we find. That would be some kind of indirect evidence that it isn't a surface phenomenon. Our tube was very small, and you can't get at those.

A. Varma: I'm still trying to understand where this fits in the fuel processor. Are we worrying about deposits on the catalyst surfaces? I don't see these deposits taking place in the mixer region in the gas phase reaction.

J. Frankenfeld: If you are going to worry about soot, it seems to me that this is going to be a problem in the mixer.

A. Varma: Yes, soot will be a problem in the mixing region. I was asking about deposits due to fuel stability problems.

J. Frankenfeld: Petroleum derived fuel is a different story. We don't get this from petroleum.

M. Zlotnick: Is there trouble in the course of producing the fuel?

J. Frankenfeld: Maybe. The Navy received the fuel from I won't say where. It was supposedly hydroprocessed, carefully processed shale. It was just like tar. They really didn't know what to do with it.

M. Zlotnick: To learn more about how this works, how to avoid deposits, wouldn't it help you in the process of producing your own shale?

J. Frankenfeld: I've heard very optimistic reports lately about how one can acid treat and hydroprocess and get a really low nitrogen shale. However, to our way of thinking, the low nitrogen wasn't so low, and the costs associated with that process are very large. But they are getting fairly good results if cost is ignored.

G. Kamm: We looked at your approach to measuring deposits for heater designs and we never could rationalize the surface to volume ratio. This test is great for a comparative purpose, but we couldn't develop a commercial heater design. Do you have any guidance along those lines?

J. Frankenfeld: No. I agree with you. That's why I say most of this was in comparison. We were looking at how we could make improvements by deoxygenating the fuel. That's all this is designed to do. I couldn't help you on that.

M. Zlotnick: What about coal liquids?

J. Frankenfeld: Most of the work I showed you is in a model system, essentially purified dealing with nitrogen compounds that have been added. One slide I showed you was on shale liquid. Coal is another problem. We do not try to simulate coal, because the Navy is not particularly interested in coal. They don't want an aromatic fuel for jet applications--certainly not diesel applications. Still, some of this may occur in coal as well.

SPRAY COMBUSTION MODELS: A REVIEW*

G. M. Faeth, The Pennsylvania State University

ABSTRACT

Due to recent theoretical and experimental advances, modeling spray combustion can be contemplated as a means of supplementing traditional cut and try combustor development methods. This review describes spray models that are currently being developed and their validation. The review is limited to steady, turbulent two- and three-dimensional systems typified by furnaces and gas turbine combustors. Both locally homogeneous flow models, where the phases are assumed to be in kinematic and thermodynamic equilibrium at each point in the flow, and more complete two-phase flow models, which allow for finite rate processes between the phases, are considered.

NOMENCLATURE

a	acceleration of gravity
B_O	oxidation transfer number, Eq. (25)
B_Y	mass transfer number, Eq. (24)
C_D	drag coefficient
C_i	parameters in turbulence model, $i=\mu$, $\varepsilon 1$, $\varepsilon 2$, g1, and g2
C_p	specific heat at constant pressure
d	nozzle or injector diameter
D	drop diameter
$f, \bar{f}$	instantaneous and time averaged mixture fraction
g	square of mixture fraction fluctuations
h	heat transfer coefficient, Eq. (16)
h_{fg}	heat of vaporization
k	kinetic energy of turbulence
m	drop mass
m_i	mass of species i in drop
m_t	total evaporation rate of drop
p(f)	probability density function
Pr	Prandtl number
Q_i	heat of reaction per unit mass of fuel i
Q_r	heat of reaction, Eq. (28)
r	radial distance
Re	Reynolds number, Eq. (20)
t	time
T	temperature
$u, \vec{u}$	mean velocity in x direction, velocity vector
$\vec{u}_p$	particle velocity vector
v	mean velocity in r direction
v^o	weighted mean velocity in r direction, Eq. (7)
x	axial distance
$\vec{x}_p$	particle position vector
Y_i	mass fraction of i
α	void fraction
ϵ	dissipation rate of turbulence kinetic energy
ε_i	mass flux fraction of i
θ	spray angle
λ	thermal conductivity
λ_g	transverse turbulent microscale
μ	laminar viscosity

---

* The author's research on spray combustion is supported by NASA Contract NGR 39-009-077 under the technical management of R. J. Priem of the Lewis Research Center.

μ_t	turbulent viscosity
ν_i^o	stoichiometric coefficient, Eq. (21)
ρ	density
σ_i	turbulent Prandtl/Schmidt number, $i=k, \varepsilon, f$, and g
τ_p	particle relaxation time, Eq. (31)
ϕ	generic property

subscripts

a	nonfuel gas
c	centerline property
f	liquid fuel
F	flame
o	injector exit conditions
O	oxidant
s	drop
∞	ambient conditions

INTRODUCTION

Recent theoretical and experimental progress has led to renewed interest in the detailed modeling of spray combustion processes in practical devices. This includes intensive development of turbulence models of flow and combustion processes, as well as the availability of general-purpose computer codes capable of solving the model equations. The rapid development of new experimental methods (e.g., laser Doppler anemometry, laser diffraction sizing of particles, holography, etc.), has also enhanced capabilities for evaluating such predictive methods.

In these circumstances, the development and validation of numerical models of spray combustion processes can be contemplated. The availability of such models reduces the need for cut and try methods during combustion chamber development. The problems posed by alternative fuels and new pollution and performance objectives have provided new incentive for model development since traditional design methods are uncertain and costly when faced with a multiplicity of goals.

Significant progress has already been made toward the development of spray combustion models. In some cases, the models are being employed during the development of practical combustors.[1,2] Much remains to be done, however, before comprehensive spray models become reliable design tools capable of accurately predicting the performance, heat transfer characteristics, and pollutant production of combustion chambers.

The objective of this review is to describe spray combustion models that have been developed, and their validation. Critical areas where more research is needed in order to improve model effectiveness will also be suggested. A number of recent reviews consider the evaporation and combustion of individual drops, and the qualitative description of sprays.[3-12] The present review supplements this information by concentrating on spray models and their comparison with experiments.

The review is largely limited to steady, turbulent two- and three-dimensional spray processes, typified by furnaces and gas turbine combustors. Emphasis is placed on finite difference solutions. Lumped parameter models, (e.g., modular models or stirred reactor models), have been described by Mellor[13,14] in recent reviews.

Within the finite difference group of solutions, two major classes can be distinguished:

(1) Locally homogeneous flow (LHF) models, where the phases are assumed to be in kinematic and thermodynamic equilibrium at each point in the flow.

(2) Two-phase flow (TPF) models, where finite rates of transport between the phases are considered.

The development of TPF models is of greatest practical importance, since LHF models are generally valid only when the drops in a spray are small. However, both approaches will be considered since LHF models have distinct advantages in some cases, and have also been subjected to more complete evaluation than TPF models, to date.

The review begins with a discussion of LHF models and their comparison with experiment. Current methods of treating drop transport characteristics and the interaction between phases are then considered. The review concludes with a description of current TPF models and their validation.

LOCALLY HOMOGENEOUS FLOW MODELS

Description of Model

The basic premise of LHF models is that transport between the phases is fast in comparison to the development of the flow field as a whole. This implies that at each point in the flow, all phases have the same velocity and are in thermodynamic equilibrium. This requirement is most easily met when the dispersed phase is a gas and the continuous phase is a liquid, due to the relatively low inertia and thermal capacity of bubbles. Therefore, LHF models are reasonably successful for bubbly flows and for processes of condensation and reaction when gas jets are injected into liquids (if buoyancy effects are small).[15-17]

The application of the LHF approximation is more questionable for sprays. However, some workers have noticed striking similarities between the structure of flames fueled with gases and with well-atomized sprays (peak drop number densities in the range 10-20 μm), when the two flows have the same stoichiometry and momentum.[18,19]

For sprays, the LHF approximation is appropriate when drop sizes are small, when the densities of the phases are nearly the same, and when the rate of development of the process as a whole is slow. This implies that the validity of the LHF approximation can be assessed if characteristic response times (length) of the drops and the process as a whole are compared.[12,19,20] Practical application of these criteria, however, often presents real difficulties. A priori predictions of process lengths are frequently not available until some model has been applied. Drop characteristics (stopping times, evaporation times, heat-up times, etc.) strongly depend on the environment of the drop within a spray, which is also not known in the absence of some model.

The major advantage of LHF models is that they require minimum information concerning injector characteristics, since drop size distributions, etc., play no role in the calculations. Calculation procedures are essentially identical to those employed for gas fueled flames, which are widely available and require shorter computation times than the more complex TPF procedures. Finally, the results of LHF calculations can provide a useful first approximation of the flow, allowing characteristic response times to be assessed, a posteriori.

Equation of State

The major difference between calculations for gas fueled and LHF liquid fueled combustion concerns the equation of state of the system. Common assumptions for turbulent single-phase flow are that the exchange coefficients of all species and heat are the same; the combustion process is adiabatic; radiation, viscous dissipation and kinetic energy are negligible; and that molecular rates of reaction are infinitely fast so that local thermodynamic equilibrium is maintained.[21-24] If the same principles are extended to the LHF model, a particularly simple form for the equation of state is obtained.

The assumption that species exchange coefficients are the same implies equality of both the laminar and turbulent components of the diffusivities. This is a reasonable approximation for gases,[21-24] but is more questionable for gas-liquid mixtures. Even at the LHF limit, the laminar diffusivity of small drops is much smaller than gas molecules, although turbulent diffusion rates are approximately the same.[25] The effect of laminar diffusion in turbulent flow is not thought to be large with respect to mean properties, however, and the approximation appears reasonable.[24] With this assumption, the mixture fraction (the fraction of mass at a given point which originated from the injector) is a passive scalar or conserved property of the flow.

Adding the assumption of local thermodynamic equilibrium requires that reaction rates and phase equilibration between the gas and liquid phases are infinitely fast. When combined with the equal species exchange coefficient assumption, this assumption implies that the local state of the mixture is completely specified by the pressure, the velocity, the mixture fraction and the temperature or total enthalpy.

A further simplification is obtained when the assumption of equal exchange coefficients is applied to energy transport, as well, and radiation, wall heat losses, viscous dissipation and kinetic energy effects can be neglected. At this limit, the local state of the mixture is completely specified by the pressure and mixture fraction, alone. The properties at each point in the flow correspond to the thermodynamic state attained when an amount (f) of injector fluid and (1-f) of ambient fluid, at their initial states, are adiabatically mixed.

With this procedure, the effect of dissociation in high temperature regions of the flow can be handled using conventional chemical equilibrium programs.[26] In fuel-rich regions of the flow, the presence of liquid fuel and other condensibles must be considered. The output of the calculation provides the density, enthalpy, temperature, composition, etc., of the flow as a function of mixture fraction.

Figure 1 is an example of an equation of state as a function of (f) under the previous assumptions. The properties correspond to the combustion of pressure atomized liquid n-pentane, burning in air at atmospheric pressure. Both the liquid fuel and the air are initially at 298 K. The effect of dissociation at high temperatures and the presence of liquids at mixture fractions near unity make the relationship between properties and mixture fraction decidedly nonlinear. Other plots of this type for single-and two-phase systems may be found in the literature.[17,21,24,27]

Conservation Equations

The formulation will be continued under the assumptions listed for the equation of state. This yields a relatively simple probability approach for modeling the reacting LHF, which minimizes the number of equations to be solved and concurrently the number of empirical parameters that must be specified in order to obtain a solution.

With the equation of state defined for the two-phase mixture, the subsequent formulation is identical to single-phase flow models. Early applications of the LHF models for sprays employed integral models to represent the turbulent flow.[28-30] However, current models employ two-equation models of turbulence which have been recently developed for single-phase flows.[27,31,33] This approach is also being used in current TPF models and will be considered in the following.

In order to fix ideas, the case of a spray directed vertically in an infinite stagnant media is considered, following Ref. 27. The flow is assumed to be axisymmetric and the boundary layer approximations are applied. A turbulent viscosity is employed, which is obtained from a k-ε turbulence model, and the effect of unmixedness is handled by writing an equation for mixture fraction fluctuations.[33] Variable density effects are treated by Reynolds averaging, following the work of Lockwood and coworkers.[21,22] In this case, the Boussinesq approximation is used to represent velocity density correlations, although a number of terms introduced by density fluctuations are ignored for lack of better information.

With these assumptions, the conservation equations become

$$\frac{\partial \rho u}{\partial x} + \frac{1}{r}\frac{\partial}{\partial r}(r\rho v^{o}) = 0 \tag{1}$$

$$D(u) = a(\rho_{\infty} - \rho) \tag{2}$$

$$D(\overline{f}) = 0 \tag{3}$$

$$D(k) = \mu_t \left(\frac{\partial u}{\partial r}\right)^2 - \rho\varepsilon \tag{4}$$

$$D(\varepsilon) = C_{\varepsilon 1}\frac{\varepsilon}{k}\mu_t \left(\frac{\partial u}{\partial r}\right)^2 - C_{\varepsilon 2}\,\rho\,\frac{\varepsilon^2}{k} \tag{5}$$

$$D(g) = C_{g1}\mu_t \left(\frac{\partial \overline{f}}{\partial r}\right)^2 - C_{g2}\,\rho\,\frac{\varepsilon g}{k} \tag{6}$$

where

$$\rho v^{o} = \rho v + \overline{\rho' v'} \tag{7}$$

and for $\phi = \overline{f}$, u, k, ε or g,

$$D(\phi) = \rho u \frac{\partial \phi}{\partial x} + \rho v^{o}\frac{\partial \phi}{\partial r} - \frac{1}{r}\frac{\partial}{\partial r}\left(r\frac{\mu_t}{\sigma_{\phi}}\frac{\partial \phi}{\partial r}\right) \tag{8}$$

The turbulent viscosity is obtained from ε and k as follows:

$$\mu_t = C_{\mu}\rho k^2/\varepsilon \tag{9}$$

The boundary conditions for Eqs. (1) - (8) are

$$r = 0,\ \frac{\partial \phi}{\partial r} = 0;\quad r = \infty,\ \phi = 0 \tag{10}$$

The initial conditions are given by the mass flow rate, thermodynamic state and thrust of the injector, along with specification of k and ε at the injector.[27]

An alternate formulation, developed by Bilger and coworkers,[34,35] considers density fluctuations through the use of Favre averages. This approach provides a somewhat improved treatment of variable density planar shear layers than the Reynolds averaging procedure outlined here,[36] and might usefully be applied to LHF models where large density variations are the norm. When the Favre averaging is applied to the present problem, the equations to be solved are identical to Eqs. (1) - (10). The differences in the methods appear in the evaluation of properties such as time averaged density, concentrations, etc.

Continuing with the Reynolds averaging method, the mean value of any scalar quantity (other than $\overline{f}$, g, k and ε) can be determined from its variation with f (for example, as illustrated in Fig. 1), if the probability density function p(f) for f is known as a function of position. Then, the mean values are given by

$$\phi = \int_0^1 \phi(f)p(f)df \tag{11}$$

The probability density function p(f) has been measured in some flows.[34,35,37]

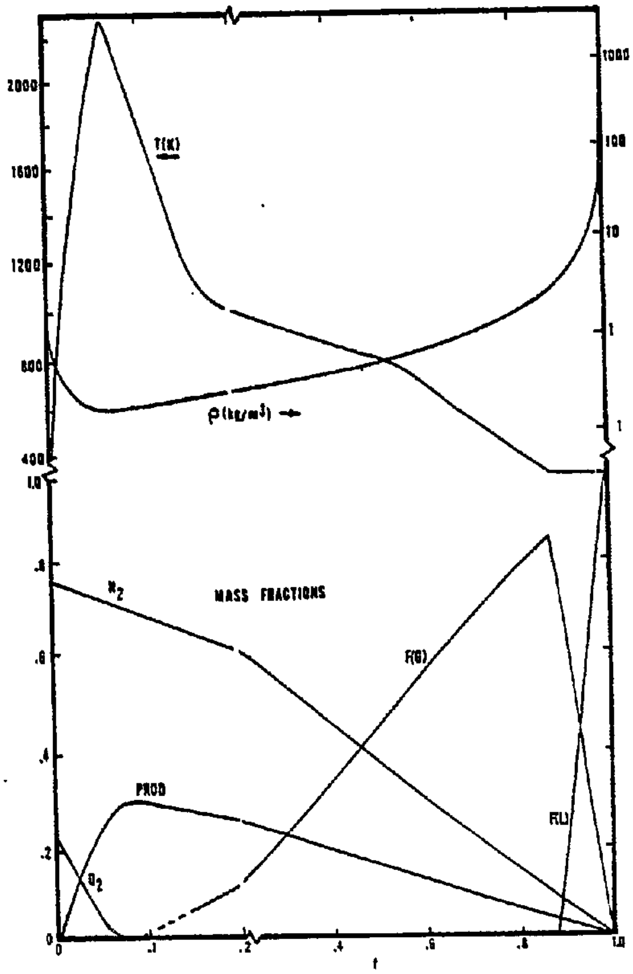

Fig. 1. Flow properties as a function of mixture fraction for the combustion of liquid n-petane in air, reactions at 298 K, 0.1 MPa.

Various distribution functions have been used to correlate the results, clipped Gaussian distribution, incomplete beta functions, rectangular waves, etc.[21,24,34] Distributions of this type are characterized by their most probable value and variance. These parameters can be determined by noting that

$$\bar{f} = \int_0^1 f p(f) df \; ; \; g = \int_0^1 (f - \bar{f})^2 p(f) df \tag{12}$$

where both $\bar{f}$ and g are known from the integration of Eqs. (1) - (10). Therefore, Eq. (12) provides two implicit equations which can be solved to find the most probable value and variance of the distribution. With these quantities known, Eq. (11) yields the property values, ρ, T, etc.

Aside from the selection of a functional form for the probability density function, values for the empirical constants must be assigned. Since the purpose of a LHF model is to provide a means of extending existing single-phase flow models to treat a two-phase flow, the values of the constants are generally selected to match experimental results for single-phase flows.[27]

Finite Rate Processes

A desirable feature of the probability density function procedure is that it does not employ any empirism beyond that of a nonreacting flow, aside from the specification of a functional form or the probability distribution function. There are many instances, however, where modifications are necessary. The method is no longer valid when radiation or heat losses from the system are present, or when kinetic energy effects and viscous dissipation are significant. When an air atomizing injector is used, a portion of the combustion process is premixed, and the chemical equilibrium assumption is less effective, particularly near the injector where fuel and oxidant can coexist at relatively low temperatures. Naturally, it would also be desirable to consider some of the finite rate aspects of the reaction and drop gasification processes, within the LHF model framework.

In cases of this type, the state of the mixture is no longer solely fixed by f, and additional scalar conservation equations must be solved, stagnation enthalpy, fuel conservation, concentration of inert species, etc. Joint probability density functions must be considered as well, having dimensions equal to the number of properties required to fix the state of the system. Pope[38] and Lockwood[39] present some suggestions along these lines; however, these methods have not been applied to sprays, as yet.

An approach that has been applied to sprays, for both LHF and TPF models, involves application of Spalding's eddy break-up model of turbulent combustion.[23,24,40,41] The method is used to describe the reaction rate of fuel (or fuel vapor for a TPF model). For a TPF model, the rate often is taken to be the smaller of either a global Arhennius expression (based on mean properties) or the eddy break-up expression[23,24]

$$R_{fu,EBU} = -C_R \rho g_{fu}^{1/2} \varepsilon / k \tag{13}$$

where C_R is a constant having a value on the order of unity, and g_{fu} is the square of the fuel concentration fluctuation, which satisfies an equation similar to Eq. (6).[38,41-43] Equation (13) provides the needed source term in the fuel vapor mass conservation equation, and can be coupled by stoichiometry to other species in the system, assuming a one-step reaction. With this approach, properties such as density are normally based on mean values. In the case of LHF flow, two limiting rates are also used, but they include heterogeneous effects and validation of the approach is limited.[32]

Methods of treating rate processes in turbulent flows are rapidly developing, and there are conceptual problems with the eddy break-up model and the treatment of flow properties by these methods.[24,38,39,43] However, the EBU model has achieved some success in the past for gas fueled combustion and is encountered in a number of the current spray combustion models.

Solution

General purpose computer codes are available for solving Eqs. (1) - (11).[44] The formulation and computer codes for treating elliptic and three-dimensional flows are also available from past work.[45-47]

Model Validation

Table 1 is a summary of some LHF models that have been reported for sprays. The list is not exhaustive, but represents typical cases where reasonably well-defined measurements were available to test the predictions. In particular, phenomenalogical models that embody LHF approximations have also been developed to simulate spray combustion in diesel engines.[48-52] Due to the transient three-dimensional nature of diesel combustion, however, convincing validation of the components of such models has not been achieved.

In general, the LHF approximation overestimates the rate of flow development. An exception to this involves the experiments of Newman and Bruzostowski,[29] where a liquid near its thermodynamic critical point was injected into a gas at high pressure. At this condition, the reduced surface tension of the liquid favors the production of small drops and the density of the liquid approaches that of the gas. Both effects favor the application of a LHF model.

Figure 2 is an illustration of the comparison between measurements and predictions obtained by an integral model.[30] The experimental results include the vapor penetration length of vapors injected into subcooled liquids,[16,53] the length of reacting gas jets (yielding condensed reaction products) in molten metals,[17] flame lengths of gaseous fuel jets in stagnant air, the data of Newman and Brzustowski,[29] and liquid fuel spray and flame lengths in stagnant air (pressure atomized injection of room temperature liquid, SMD = 30 μm, pressures in the range 0.1-9MPa).[30]

The empirical parameters of the flow model were selected to match the characteristics of single-phase jets. The effect of turbulent unmixedness on transport rates was represented by an unmixedness parameter, based on condensing jet data where the LHF model is most accurate. The remaining

Table 1

Summary of LHF Models of Spray Evaporation and Combustion

Reference	Model[a]	Experiment[b]	Assessment
Thring and Newby (1953)[28]	Integral, EQ	Combustion of air and steam atomized spray, 0.1 MPa	Qualitative agreement
Newman and Brzustowski (1971)[29]	Integral, EQ	Evaporation of pressure atomized liquid near its critical point, 6-9 MPa	Good agreement for spray boundary
Shearer and Faeth (1977)[30]	Integral, EQ	Combustion of a pressure atomized spray, SMD = 30 μm, liquid injection temp. 298 K, 0.1-9 MPa	Theory overestimates spray and flame boundary by 30 - 50%, poor estimation of flow width
Shearer, et al. (1978)[27]	k-ε, EQP	Evaporation of an air atomized spray, SMD = 29 μm, 0.1 MPa	Theory overestimates rates of development of process
Khalil and Whitelaw (1976)[31]	k-ε, EQP	Combustion of a pressure atomized spray, swirl, SMD = 45, 100 μm, 0.1 MPa	Theory overestimates rate of development of process, error decreases as SMD decreases
Khalil (1978)[32]	k-ε, MEBU	Same as Ref. 31	Improved prediction in some cases

[a] EQ implies local thermodynamic equilibrium, EQP implies equilibrium with probability distribution function for properties, MEBU implies modified eddy break-up model.

[b] Pressures are those of spray environment, all flows are steady.

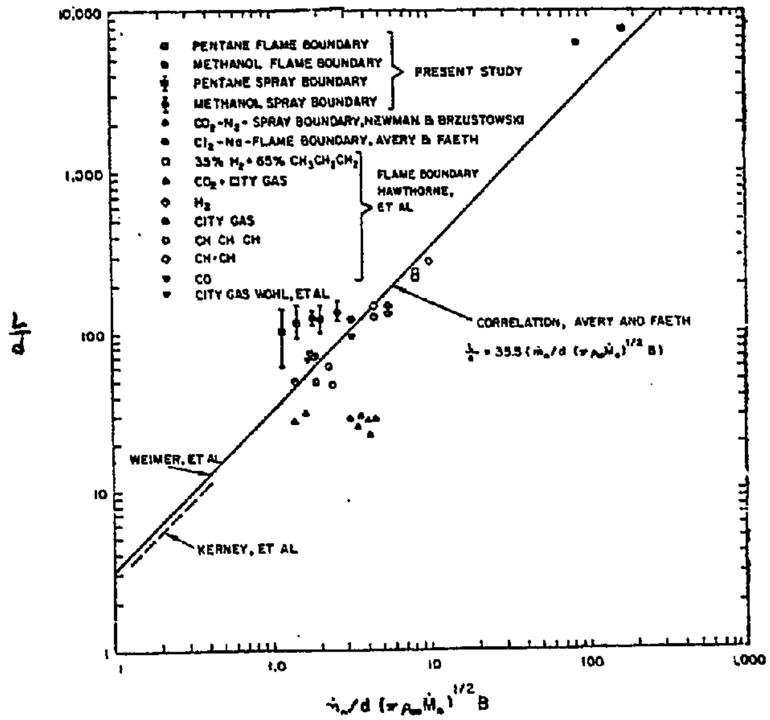

Fig. 2. Correlation of penetration length data for jets with LHF integral model; m_o and M_o are mass and momentum excess flow rates at injector, B is the appropriate driving potential.[30]

results are predictions based on these parameters. The estimation of the length of gas flames is reasonably good. The spray measurements of Newman and Brzustowski,[29] where conditions favor the LHF approximation, are overestimated. (The model of Ref. 29 provides better agreement with this data. The computational problems are associated with the difficulties in selecting properties near the critical point.)[30] However, the model underestimates the remaining spray measurements by 30-50%, with the errors actually being largest at the highest test pressures (9MPa).[30] In this case, although the density difference between the phases is smaller at high pressures, slip near the injector is still important since the process as a whole is shorter.

The integral models are relatively crude, and a more convincing examination of the LHF approximation can be obtained by considering the k-ε models described earlier. Shearer and coworkers[27,56] provide a systematic evaluation which considers a variety of turbulent axisymmetric jets and sprays, flowing in a stagnant environment. This includes an isothermal air jet in air,[27,56-59] heated air jet in air,[60] an air jet in water,[61] and an evaporating Freon 11 spray in air (injector diameter 1.19 mm, air atomizing, SMD =

29 μm, air mass fraction in injector flow 0.127).[27,56]

Similar to Lockwood and Naguib,[21] optimizing the agreement between predictions and measurements for single-phase constant and variable density jets yielded the model constants.[56] The optimization yielded values identical to those found by Lockwood and Naguib,[21] which are summarized in Table 2.

Table 2

Constants in the Turbulence Model[56]

Constant	Value	Constant	Value
C_μ	0.09	σ_k	1.0
$C_{\varepsilon 1}$	1.44	σ_ε	1.3
$C_{\varepsilon 2} = C_{g2}$	1.89, 1.84, 1.82[a]	σ_f	0.7
C_{g1}	2.8	σ_g	0.7

[a] Constant density flows, variable density flows, and potential core region for all flows, respectively.

Undesirable features of this model are that slightly different values of $C_{\varepsilon 2} = C_{g2}$ are appropriate for constant and variable density flows. Different constants are also needed for the shear layer, near the exit of the jet, and the fully-developed portions of the flow. Other assessments of the model constants yield similar results.[21-24,33-35,45] A clipped Gaussian probability density function was employed in the results to be illustrated. The effect of using other distribution functions is not large.[21]

Figures 3 and 4 are illustrations of the radial variation of mean velocity and mixture fraction for the various jets, in the fully-developed region of the flow. The radial similarity coordinate, r/x, is used on the figures in order to indicate the degree to which the model predicts the width of the flow. The agreement between theory and experiment is reasonably good for all the flows, in spite of significant density variations in some cases. The turbulence quantities $\overline{u'v'}$ and k are also predicted quite well for the same cases.[27,56]

A somewhat more stringent test of the model is provided by examining the axial variation of velocity and mixture fraction in the jets. These results are illustrated in Figs. 5 and 6. It is seen that the axial variation of velocity and mixture fraction is strongly influenced by the density ratio of the flow (ρ_o/ρ_∞ varies in the range 10^{-3}-10). The velocities are predicted reasonably well, except for the spray where the rate of velocity decay is somewhat overestimated. The mixture fraction decay for the air jet in liquid is underestimated; however, this could be due to sampling errors since

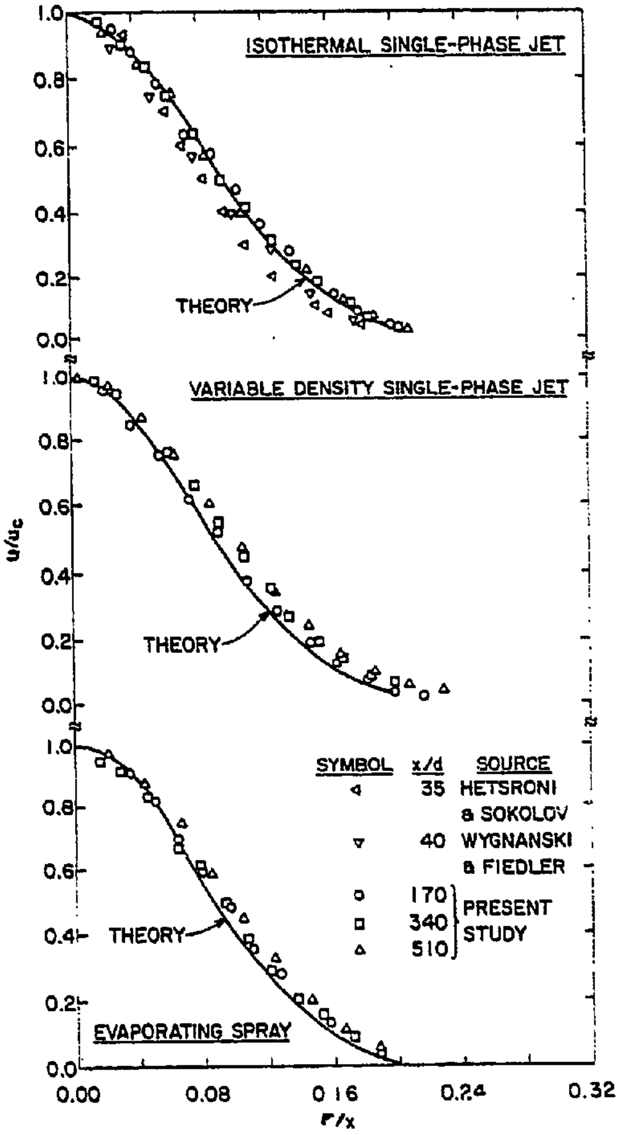

Fig. 3. LHF predictions and measurements of radial mean velocity profiles for constant and variable density gas jets and an evaporating spray.

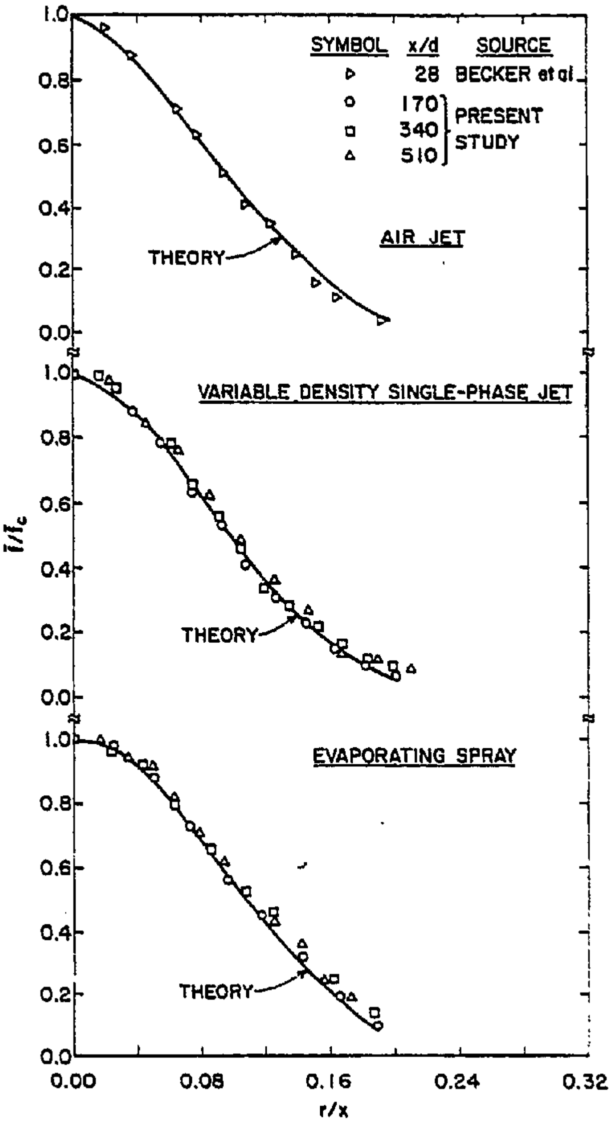

Fig. 4. LHF predictions and measurements of radial mean mixture fraction profiles for constant and variable density gas jet and an evaporating spray.

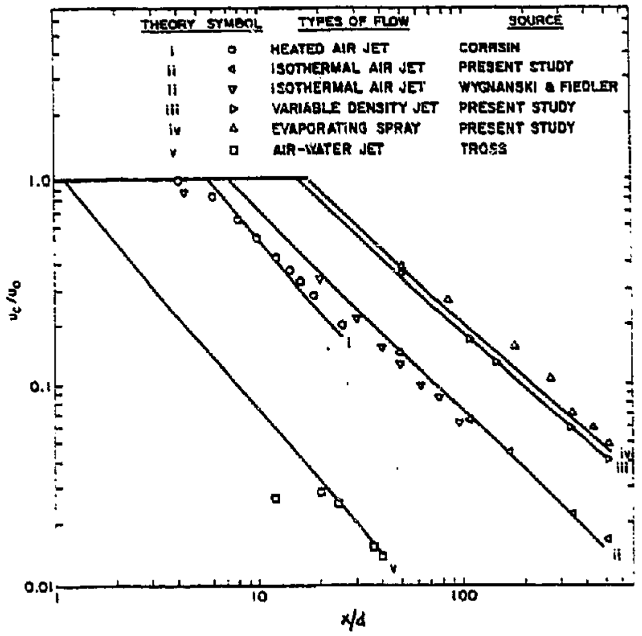

Fig. 5. LHF predictions and measurements of axial mean velocity variation for constant and variable density gas jets, gas jets in liquids and an evaporating spray.

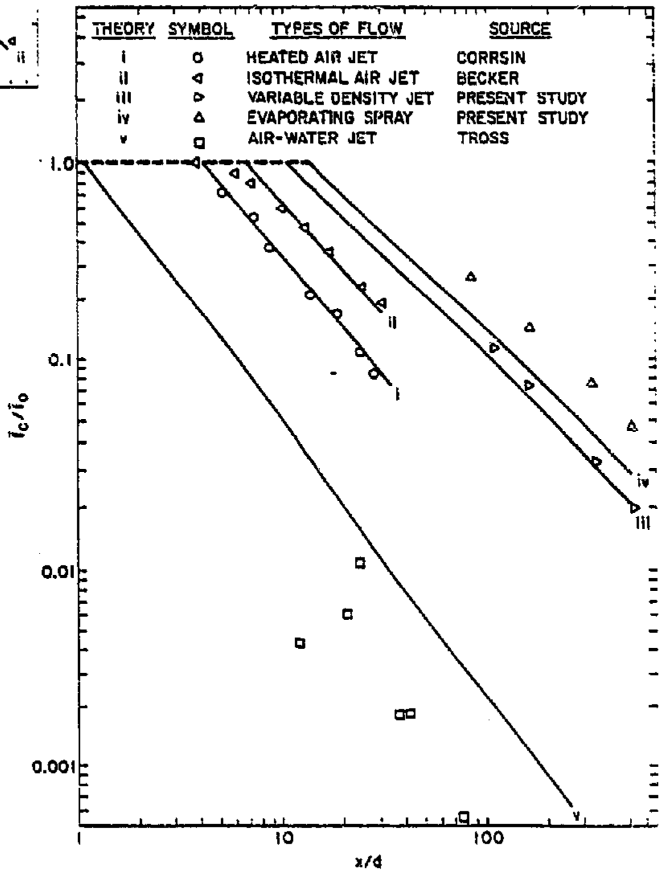

Fig. 6. LHF predictions and measurements of axial mean mixture fraction variation for constant and variable density gas jets, gas jets in liquids and an evaporating spray.

the probe technique used to measure concentration generally underestimates the concentration of gas.[61] For the spray, the rate of decay of mixture fraction is clearly overestimated. The examination of temperature and liquid flux data for the spray provides further evidence that the theory overestimates the rate of flow development.[27,56]

The problem with predicting the spray, using the LHF model, can be directly attributed to slip and loss of thermodynamic equilibrium between the phases, rather than the choice of empirical constants in the model. This was determined by computing drop life histories for drops moving down the axis of the spray, employing the predictions of the LHF model to estimate local gas velocity, composition and temperature. The details of the calculations are discussed in the next section. Since uncertainties in properties and the method of selecting proper average properties for transport quantities can significantly influence the predictions, the lifetime calculations were calibrated using single drop experiments. The results of the computations are illustrated in Fig. 7.

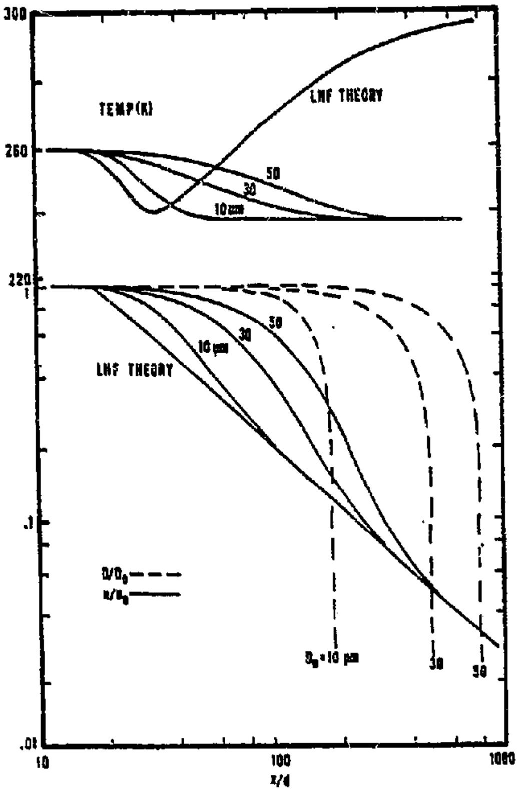

Fig. 7. Drop life history predictions in an evaporating Freon 11 spray.

It is seen that the drop velocities decay more slowly than the gas velocity, even for drops as small as 10 μm. Drop temperatures also respond too slowly to the gas temperature variation. In the downstream region, the drops tend to approach a wet-bulb temperature, which is significantly lower than the gas temperature, as the fuel vapor concentration decreases along the centerline due to the entrainment of ambient gas. A constant wet-bulb temperature, typical of "steady evaporation," however, is never reached in a spray, since the environment of each drop continuously changes.

Similar behavior of a LHF model was observed by Khalil and Whitelaw[31] for combusting sprays. Figure 8 is an illustration of the comparison for a pressure-atomized kerosene spray with a hollow cone pattern.

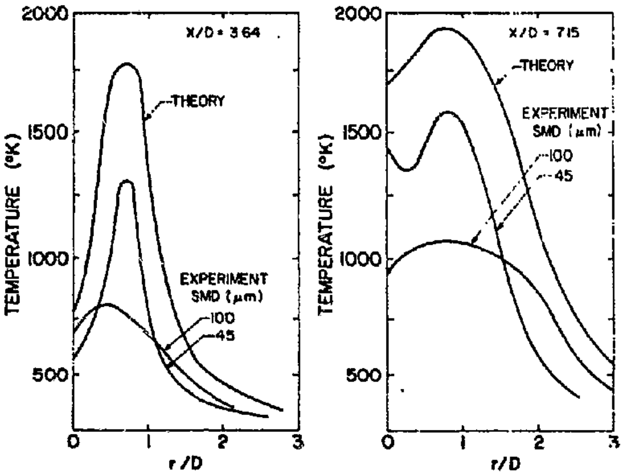

Fig. 8. Comparison between predictions of a LHF model and measurements in a swirling, hollow cone, spray flame.[31]

The parameter D=200 mm refers to the diameter of a disk surrounding the injector. The measurements tend to approach the theory as the SMD of the spray becomes smaller. However, the agreement is still relatively poor for a spray having an SMD of 45 μm.

In a later study, Khalil[32] was able to achieve a better prediction for a portion of the data illustrated in Fig. 8. This was accomplished by introducing an eddy break-up model of fuel consumption, as discussed earlier. Including a finite rate process allows the predicted rate of development to be slowed in the LHF model; however, slip effects cannot be adequately treated in this manner and the usefulness of the method is limited.

From these results, we conclude that LHF models provide a useful qualitative description of the flow. The models are relatively easy to use, since they require only moderate amounts of information concerning injector characteristics and they draw heavily on existing models of turbulent gaseous combustion processes. However, with the possible exception of liquid injected at conditions near their critical point,[21] LHF models generally overestimate the rate of development of the flow, even for high pressure sprays with an SMD as low as 30 μm. Thus, the main value of the LHF model lies in its ability to provide a preliminary assessment of the spray process, so that potential slip effects can be evaluated. For most practical spray processes, models which allow for slip and finite rate transport processes between the phases must be considered.

SINGLE DROP MODELS

Description of Model

Drop transport characteristics must be determined in order to assess the validity of LHF models and to undertake TPF models. The basis for this theory is consideration of an isolated drop in a specified ambient environment. Only a brief account of this methodology will be considered here; further details may be found in recent reviews and references cited therein.[3-12]

Typical assumptions used to analyze the transport properties of a multicomponent fuel droplet at moderate pressures are as follows:[3]

1. The drop is assumed to be spherical and well-mixed (i.e., temperature and composition do not vary with position in the liquid phase).
2. The gas phase is assumed to be quasisteady (i.e., it immediately adjusts to the <u>mean</u> boundary conditions at each instant of time). This implies that the effect of turbulent velocity and mixture fraction fluctuations is negligible. The radial velocity of the liquid surface is also assumed to be small.
3. The enhancement of heat and mass transfer rates by convection is obtained by an empirical convection correction (which may employ film theory).
4. Chemical reaction in the liquid phase is neglected. Equilibrium evaporation occurs at the liquid surface with negligible temperature jump. The liquid and gas phase compositions, and the surface temperature, are related by phase equilibrium criteria. The solubility of the ambient gases in the liquid phase is neglected. These assumptions are not valid at high pressures, but successful modifications are known.[3]
5. The pressure is equal to the ambient pressure everywhere.
6. Only concentration diffusion occurs, represented by an effective binary diffusion coefficient, and the Dufour effect is neglected in the heat flux.

7. Radiation is neglected.

8. If an envelope flame is present, fuel and oxidizer react in stoichiometric proportions within an infinitely thin flame zone.

9. For convenience in the following formulation, fluid properties are assumed to be constant, determined at an appropriate reference condition, and the Lewis number is taken to be unity. The constant property assumption can be removed, and recent models allow for the effect of property changes with both composition and temperature, at least in the absence of convection.[3]

Transport Equations

With the previous assumptions, the equations for conservation of mass, momentum and energy, for a drop containing N species, are as follows:[3]

$$\frac{dm_i}{dt} = -\varepsilon_i \dot{m}_t \ , \ i = 1,N \tag{14}$$

$$m \frac{d\vec{u}_p}{dt} = \frac{-\pi}{8} D^2 \rho C_D |\vec{u}_p - \vec{u}| (\vec{u}_p - \vec{u}) \tag{15}$$

$$mC_{pf} \frac{dT}{dt} = \pi D^2 h (T_F - T) - \dot{m}_t \sum_N \varepsilon_i h_{fgi} \tag{16}$$

Equations (14) - (16) have been simplified by neglecting body forces, Saffman lift, Magnus, Bassett, virtual mass terms, etc., in the momentum equation. The heat transfer coefficient is based on the flame temperature, if a flame is present. An equation of state is also needed in order to compute the drop size and specific heat from its composition and temperature. The drop position is obtained from

$$\vec{x}_p = \int_0^t \vec{u}_p dt \tag{17}$$

In order to fix ideas, the effect of convection will be treated using a multiplicative correction

$$h/h_{Re=0} \text{ or } \dot{m}_t/\dot{m}_{t_{Re=0}} = 1 + \frac{0.278Re^{1/2}Pr^{1/3}}{(1 + 1.232/(RePr^{4/3}))^{1/2}} \tag{18}$$

Equation (18) has good asymptotic properties at low Reynolds numbers and provides a reasonable fit of existing data for Re < 2000.[3,62,63] Kadota and Hiroyasu[64] describe the film theory treatment of convection for an evaporating drop. The following expression for drag coefficient is also effective for this range of Reynolds numbers[3,65]

$$C_D = \frac{24}{Re}\left(1 + \frac{Re^{2/3}}{6}\right) \tag{19}$$

where

$$Re = \rho D|\vec{u}_p - \vec{u}|/\mu \tag{20}$$

In order to complete the model, h, T_F, $\dot{m}_t$, and the ϵ_i must be determined for Re = 0. Following Law, et al.,[66] the overall reaction between fuel species and the oxidizing gas is taken to be

$$\sum_N \epsilon_i[F_i] + \sum_N(\epsilon_i/\nu_i^{o})[O] \rightarrow \text{Products} \tag{21}$$

Then the quasisteady transport equations, which have spherical symmetry for Re = 0, can be solved to yield[3]

$$\frac{\dot{m}_t C_p}{2\pi D\lambda} = \ell n[(1 + B_Y)(1 + B_o)] \tag{22}$$

where

$$\epsilon_i = Y_{is}(1 + B_Y)/B_Y \tag{23}$$

$$B_Y = (1 - Y_{as})/Y_{as} \tag{24}$$

$$B_o = Y_{o\infty} / (\sum_N \varepsilon_i / \nu_i^{\,o}) \tag{25}$$

The quality Y_{as} is the mass fraction of nonfuel species at the drop surface. This quality is obtained from the equation of state, knowing the liquid temperature and composition, and the pressure. The heat transfer coefficient is

$$hD/\lambda = 2\ell n[(1 + B_Y)(1 + B_o)]/B_Y \tag{26}$$

and the flame temperature, neglecting dissociation is

$$\frac{T_F - T_s}{T_\infty - T_s} = \left[\frac{Y_{o\infty} Q_r}{C_p(T - T_s)} + 1\right] \Bigg/ \left[1 + \frac{B_o}{B_Y}(B_Y + B_o)\right] \tag{27}$$

where Q_r is the heat released per unit mass of oxidizer consumed at the flame front.

$$Q_r = \sum_N \varepsilon_i Q_i / (\sum_N \varepsilon_i / \nu_i^{\,o}) \tag{28}$$

Given a knowledge of the ambient conditions of a drop, Eqs. (14) - (28) can be integrated to yield the temperature, diameter, composition, velocity and position of a drop as a function of time.

Steady Evaporation

At moderate pressures, single component drops in a constant ambient environment will tend to heat up to a constant wet-bulb temperature. At this condition, all the energy reaching the drop is utilized for the heat of vaporization of the fuel evaporating from the drop. A simple expression can be obtained for the rate of evaporation at this condition, as follows (Re = 0):[3]

$$\frac{\dot{m}_t C_p}{4\pi D\lambda} = \ell n[1 + (C_p(T_\infty - T_s)) + Q_r Y_{o\infty})/h_{fg}] \tag{29}$$

For a combusting drop, T_s can be taken to be the boiling temperature of the fuel with little error[3]. In the absence of combustion, the drop temperature has a stronger influence on the evaporation rate. In this case, T_s is found from the vapor pressure relationship for the fuel and the fixed relationship between the driving potentials for heat and mass transfer at the wet-bulb state.[3]

If the Lewis number is not unity, the wet-bulb temperature varies slightly with Reynolds number, even if ambient conditions are constant. Due to changes in liquid composition, multicomponent drops have no fixed wet-bulb state, even if ambient conditions are fixed. Similarly, no drop in a spray has a fixed wet-bulb temperature, since ambient conditions are continuously changing. The major value of equations simular to Eq. (29) is that the wet-bulb state is readily achieved in single drop experiments, and evaporation rate data can be readily correlated for this condition.

Model Validation

There have been numerous studies of the evaporation of combusting and non-combusting single drops, which have been discussed in earlier reviews.[3-12] In general, models similar to Eqs. (14) - (29) have been successful in correlating data for a wide range of conditions. This quantitative agreement arises since there are large property variations in the flow field around a drop, which provides significant latitude for adjusting "average" properties so that agreement with experiment is obtained. A unified method of selecting a model, convection corrections, and proper average properties, so that reliable a priori predictions can be obtained for a wide range of conditions, has not yet appeared.[3] Until this comes about, it is recommended that any model be calibrated with results from single drop experiments, prior to use in a spray model. Some data is available for drops in flames, when spray combustion is contemplated.[3,62,63] More data of this type is needed.

TWO-PHASE FLOW MODELS

Description of Model

All TPF models attempt to treat aspects of the interaction between phases; however, the models vary widely in regard to the thoroughness with which interactions are considered. A major distinguishing feature of current models involves a group which ignores the relative velocity difference (slip) between the phases,[67-70] as opposed to more complete models where slip is considered.[1,2,71-76] If slip is ignored, the models are similar to LHF models, except that finite rate heat and mass transfer rates are considered between the phases. Ignoring slip considerably simplifies the calculations; however, such models involve limitations in accuracy similar to LHF models.

It is generally assumed that the spray is dilute. This implies that single drop formulas can be used to describe drop transport rates, that the presence of the drops has a negligible effect on the constitutive equations describing the transport characteristics of the gas phase, and that drop collisions can be ignored.

The void fraction requirements of all these assumptions are not well-defined at this time. For monodisperse particles, however, it is recognized that single particle transport formulas apply reasonably well if the center-to-center distance between particles is greater than two particle diameters.[77] If the particles have equal spacing, this requirement implies a void fraction greater than 0.92.

A rough idea of the spatial regime of the spray where the high void fraction requirement is satisfied can be obtained if some simplifying assumptions are accepted. The worst situation involves a pressure atomized spray where the liquid leaves the injector with a zero void fraction. We assume that the liquid is distributed uniformly over the cross-section of the spray, the outer boundary of which is defined by the spray angle which implies a well-atomized spray. We also assume that the velocity of the liquid remains equal to the velocity at the exit of the injector throughout the high void fraction region. This yields the following expression for the axial distance required to attain a given void fraction.

$$x/d = [(1 - \alpha)^{-1/2} - 1]/2 \tan(\theta/2) \qquad (30)$$

Spray angles are narrowest for straight sided injector passages having large length-to-diameter ratios, with no liquid swirl. In this case, spray angles in the range 12-25° have been observed for injection into stagnant gases (the latter angle roughly corresponds to the natural angle of spread of a fully developed constant density jet).[30,78] Values of $\alpha = 0.92$ then yield x/d in the range 6-12. However, these values are quoted with some misgivings. Spray angles are largely based on measurements made much farther from the injector (x/d on the order of 100) and similar to a single-phase jet, the flow can be narrower near the injector. The uniform concentration and constant velocity assumptions also tend to underestimate the distance required to reach a given void fraction.

For combusting sprays in a stagnant environment, the region where drops are present typically extends to values of x/d on the order of 100, c.f. Fig. 2. If the previous estimates of the high void fraction region are reasonable, this suggests that the dilute spray assumption is adequate for the bulk of the two-phase portion of the flow. The near-injector region requires a different formulation, although this region has yet to be studied in any detail for combusting sprays.

The manner in which the initial conditions of the spray are specified has a strong bearing on the need to treat the high void fraction region. TPF models which consider slip require size and velocity component distributions as a function of position, at some point in the flow, as a boundary condition. In the few instances where detailed information of this type has been obtained,[79] the measurements were made at some distance from the injector, in cold flow. Due to current experimental limitations for completing measurements in low void fraction regions,[80] it appears that detailed validation efforts for TPF models will be limited to the high void fraction region, in any event.

When current models are used for design, crude measurements such as "spray angle" and SMD are frequently used.[1,2] In this case, Simmons[81] represents a useful relationship between SMD and the actual size distribution of the spray, which should be helpful in specifying initial conditions for TPF calculations.[13]

Liquid Phase Conservation Equations

Equations (14) - (29) are appropriate for a single drop in a non-turbulent flow. In spite of these limitations, current TPF models employ equations similar to these to compute liquid transport rates.[67-76] The limitations of this approach, as far as interparticle spacing is concerned, have already been treated. We now consider other aspects, including: the presence of envelope flames, turbulent diffusion of drops, the enhancement of drop transport rates by turbulence, and the use of mean ambient properties in the drop transport equation.

Whether envelope flames are present or not around individual drops within a combusting spray has generated some controversy.[3,10,18,19] Resolution of this question has implications both with respect to drop transport rates and the mechanism of fuel oxidation in a spray flame.

There are three basic drop states in a heated oxidizing atmosphere: (1) ignited with an envelope flame present, (2) ignited, but with the flame stabilized in the wake of the drop, and (3) not ignited. Past work has shown that in the latter two states, drop transport rates can be described by considering the process to be drop evaporation with no combustion.[82-85] In terms of the single drop formulation, this can be accomplished by setting $Y_{O\infty} = 0$ in Eqs, (14) - (29), even though oxygen is present in the ambience of the drop.

Figure 9 is an illustration of the effect of the presence of an envelope flame on the steady evaporation rate of an n-pentane drop. The evaporation rate is plotted as a function of gas phase equivalence ratio, taking the environment of the drop to correspond to the conditions of Fig. 1. This implies that the gas phase is in equilibrium, with negligible radiation losses, etc., and neglects forced convection effects. For gas phase equivalence ratios greater than 0.5, the difference approaches the uncertainty of evaporation rate predictions at either limit. At lower equivalence ratios, it becomes increasingly important to determine whether an envelope flame is present.

As far as the fuel oxidation mechanism is concerned, postulating that envelope flames are always present implies that only combustion products pass into the gas phase around each drop, as long as the ambient oxygen concentrations are never zero due to unmixedness. In this case, if mean properties are used to determine drop transport rates, consistent treatment implies that no fuel vapor is present in the gas phase. This does not correspond either to intuition or to existing observations (for example Ref. 18). Unmixedness, where drops evaporate as they pass through fuel-rich eddies as opposed to combusting, when they pass through oxygen-rich eddies, and the absence of envelope flames, even when oxygen is present, appear to be significant factors during spray combustion.

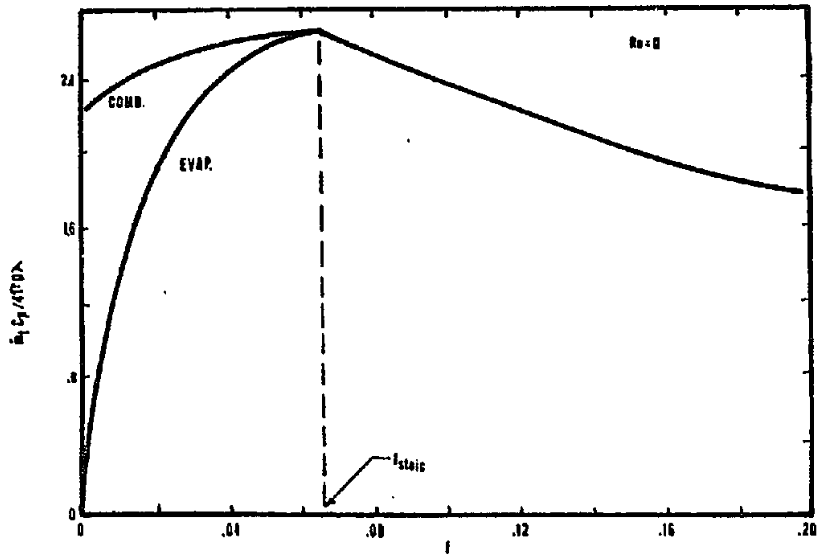

Fig. 9. Influence of the presence or absence of an envelope flame on the steady evaporation rate of an n-pentane drop in equilibrium gas (conditions same as Fig. 1).

Stability criteria for envelope flames provide a necessary condition for their existence around moving drops. Measurements yielding stability criteria have been completed for drops in air streams at various temperatures and pressures.[84-86] Based on these results, Komijama, et al.,[19] conclude that envelope flames are unlikely in spray combustion tests that they conducted (coaxial flow in a duct).[19] However, more information is needed, considering partly combusted ambient gases, before envelope flame assessments can be adequately made for the gas phase conditions encountered in sprays.[3,87] The stability of wake flames is also a factor, since their presence influences the oxidation mechanism of the fuel vapor, even when drop transport rates are not affected. Finally, ignition criteria must be specified for moving drops in order to obtain the more restrictive sufficient conditions for fuel oxidation in the vicinity of a drop. Although attempts have been made to provide models of drop ignition,[3,82,83,100-103] existing methods are not highly developed and are unwieldy; therefore, they have not been applied in current TPF models.

In view of these difficulties, most investigators have chosen to circumvent the envelope flame-fuel consumption difficulties by assuming that envelope flames are never present. In this case, drops act as a source of fuel for the gas phase and subsequent oxidation follows procedures developed for gas fueled flames. The model of Mongia and coworkers,[1,2] is an exception; drops are assumed to evaporate or combust, depending upon whether the mean gas phase mixture fraction is greater or less than stoichiometric. Definitive consideration of the adequacy of either of these methods is not yet available.

Another problem encountered with slip models involves consideration of the effect of turbulent diffusion on drop motion. Large drops don't respond significantly to the turbulence and follow trajectories which are only influenced by the mean motion (describable by Eqs. (14) - (28)). However, small particles track the turbulent motion similar to particles used for LDA measurements in a turbulent flow. Methods for estimating the drop size range, where turbulent diffusion is important, have been described in the literature.[3,88]

One method of treating turbulent drop diffusion is to estimate a diffusional drift velocity based on Fick's law of diffusion.[89,90] This requires the specification of a turbulent Prandtl/Schmidt number as a function of drop size and local flow properties. Some measurements are available to estimate this quantity.[25,77,91,92] The turbulent Prandtl/Schmidt number for particles is largely a function of an inertial parameter which can be taken as the ratio of a characteristic particle relaxation time (based on Stokes drag)

$$\tau_p = \rho_f D^2/18\mu \tag{31}$$

and the Lagrangian integral time scale of the turbulence.[91,92] When the inertial parameter is small, the Prandtl/Schmidt number equals the value for turbulent mass transfer of gases. Existing information indicates that the turbulent Prandtl/Schmidt number decreases for increasing values of the inertial parameter, at least over the range where measurements have been made.[91,92] This implies that turbulent diffusion increases with particle size. However, since large particles have greater slip velocities, turbulent diffusion is still most important for small particles.

Crowe and Pratt[93] suggest some alternative treatments of particle diffusion, based directly on local values of k and ε. However, these methods have not been developed to a significant degree as yet.

In TPF calculations conducted to date, drops respond relatively slowly to the mean motion and to a lesser degree to turbulent fluctuations, until nearly the end of their lifetime. Since the bulk of their mass has been transferred to the gas by this time, turbulent drop motion does not appear to be a primary means of transporting fuel within a spray. On this basis, most spray models which consider slip have ignored turbulent drop diffusion.[1,2,71-76]

If the largest drops in a spray are relatively uninfluenced by turbulent diffusion, the possibility remains that the turbulence will modify the transport rates from the values obtained from single drop correlations (which were generally obtained under conditions where ambient turbulence levels are negligible).[77] All current TPF models ignore this effect.[71-76] A justification for this approach can be obtained by comparing turbulent microscales, which may be considered as a measure of the average dimension of the smallest turbulent eddies[94,95] with the drop size. In cases where the drop sizes are smaller than the microscales, it can be concluded that the direct effect of turbulence on drop transport is negligible.

A variety of microscales can be defined for combustors fueled with sprays. Aside from droplet wakes, which should introduce only a small effect when the spray is dilute, the smallest scales are generated by the spray jet itself. Microscales have been measured in the fully developed portions of single-phase jets.[57,94,95] The transverse scales are smaller than the longitudinal scales, and these are smallest along the axis of the jet, yielding[57]

$$\lambda_g \approx 4 \times 10^{-3} x \tag{32}$$

Introducing drop diameter in Eq. (32), yields

$$\lambda_g/D \approx 4 \times 10^{-3} (x/d)(d/D) \tag{33}$$

For well atomized conditions, the ratio of d/D is smallest for constant area injectors with no swirl, falling in the range 10-100 for the largest drops in a spray. Under these conditions, λ_g/D is of order unity when x/d is in the range 2.5-25. This range corresponds to the low void fraction region of the flow where most of the other assumptions of current TPF models break down as well. The previous estimate is somewhat conservative, since the effect of ambient turbulence is less at low drop Reynolds numbers,[77] and the characteristic dimension of the flow field around a drop is smaller than the drop diameter at large Reynolds numbers. In view of the current state of TPF model development, neglecting turbulent enhancement of drop transport rates is reasonable.

A more significant effect of turbulence on drop transport rates involves fluctuations at each point in the flow, which influences the instantaneous ambient environment of a drop. Current TPF models neglect this effect and base drop transport characteristics on mean properties.[67-76] This is adequate if transport properties vary either linearly or slowly with the relevant fluctuating parameters, (e.g., velocity and mixture fraction, or if the intensity of the fluctuations is small). The results of Fig. 9 suggest that the former requirement is marginal, particularly if envelope flames are not present, (if we ignore convection and assume that the drop instantly reaches a steady evaporation condition for the current ambient state). Furthermore, turbulent fluctuations are certainly not small near the edge of a jet. A full treatment of the effect of fluctuations for a spray requires consideration of the transient response of the drops, and the turbulent structure of the flow. Although this is an interesting problem, the author is not aware of any definitive studies along these lines. In view of the uncertainties in drop transport characteristics discussed earlier and the fact that including the effect of fluctuations would significantly complicate the models, the current methods appear to be reasonable.

In addition to ignoring drop collisions via the dilute spray approximation, current TPF models also ignore drop shattering.[1,2,67-76] This effect has been treated in one-dimensional models of liquid rocket engine combustion, and including it presents only minor difficulties.[12,96] However, in view of the limited availability of data on injector characteristics, it seems premature to include the phenomena in current models.

With these assumptions, Eqs. (14) - (28) describe the transport characteristics of the liquid phase. Formal treatment involves solution of the spray equation.[97] This provides the spatial variation of the joint probability distribution function for droplet size, temperature, composition and velocity components, given appropriate initial and/or boundary conditions. In cases where a simplified analysis is conducted for the liquid phase (no slip or steady evaporation constant, etc.), the spray equation provides a convenient formulation. For more complex cases, this is frequently not done. Rather, the initial joint probability distribution is divided into a finite number of groups (by size, velocity components, initial position, etc.). Each group is then tracked through the flow field by solving their Lagrangian equations of motion. The numerical computations can be simplified by integrating the equations once, assuming fixed ambient conditions over a small spatial increment, prior to including them in the computer calculation.[73-75]

Gas Phase Conservation Equations

Most of the current TPF models employ the k-ε turbulence model, with Reynolds averaging, and ignore density fluctuation terms. The model of Jones and Pridden[70] is an exception. They consider density fluctuations through the use of Favre averages. As noted earlier, the equations to be solved are similar in both cases. The author is not aware of any studies indicating a clear advantage for either approach for spray calculations at this time.

Consistant with the dilute spray approximation, the presence of drops in the flow is assumed not to influence the properties of the turbulence, (i.e., turbulence production and dissipation by drops is ignored). Existing measurements in turbulent two-phase jets are limited to very high void fractions (greater than 99.9%) and under these conditions, no significant effects of particles have been found.[27,29] (The hot wire measurements of Hetsroni and Sokalov[59] are an apparent exception; however, these measurements appear to be erroneous due to drop impacts on the hot wire sensor.[27])

Under these assumptions, the conservation equations for the gas phase are similar to those described earlier for the LHF model, (e.g., Eqs. (1) - (10)) for an axisymmetric flow where the boundary layer assumptions apply. The major difference is the appearance of source terms, due to mass, momentum and energy transport between the phases. The source terms are generally obtained by summing over all drop groups. Original references should be consulted for details.[1,2,67-76]

If the effects of envelope and wake flames are neglected, treating the reaction process also parallels the methods developed for gas flames, as discussed for the LHF models. However, the use of the statistical probability density function procedure, coupled with an equilibrium gas phase approximation, implies assumptions in addition to those acquired for LHF (except in those cases where slip is ignored). In order for the gas phase to be fully specified by a single parameter (e.g., gas phase mixture fraction), only liquid can be injected and the sensible energy absorption by the drops must be small.

The treatment of radiation and pollutant production in TPF models also follows the procedures developed for gases, similar to LHF models. The effect of absorption and scattering by drops is ignored, and mean properties are used in the transport equations for radiation and the chemical reaction terms for pollutant production. The validity of these approximations is questionable in any flow, due to the highly nonlinear characteristics of the terms.

Solution

Crowe, et al,[73] describe a solution procedure (PSI-Cell) which is suitable for two-phase elliptic flows. An iterative method is used where the Eulerian equations are solved for the gas flow. These gas properties are then used to solve the Lagrangian equations of motion for the drops. Each class of drops is tracked through the flow field, allowing the source term in the gas conservation equations to be evaluated. The gas phase equations are then solved again, including these source terms, etc. The procedure continues until the solution closes with desired accuracy.

Spalding has also developed a general purpose program capable of solving the turbulent TPF equations.[98]

Model Validation

Table 3 is a summary of recent TPF models that have been reported. The list is limited to recent calculations for sprays, considering at least two-dimensional flow, and employing finite difference calculations of the flow field. In view of the complexity of the calculations, current activity in developing TPF models is surprisingly high. Undoubtedly, additional models will be reported in the near future.

Model development, however, has far outstripped systematic efforts at model validation. Where predictions have been compared with experiments, injector characteristics have not been defined adequately for a TPF model and measurements within the flow have been limited. The models are very complex, involving numerous assumptions and empirical parameters. Convincing validation will require careful testing of the component parts using the results of simpler, well-defined experiments prior to an overall test with a combusting spray. This type of validation is beginning to appear for the LHF models. The demands of the measurements are greater for TPF models, however, the technology for making these measurements is available, at least in the dilute spray regions of the flow.[10,13,80,88] With models and experimental techniques in hand, improved validation of TPF models should also appear in the near future.

Table 3

Summary of TPF Models of Spray Evaporation and Combustion[a]

Reference and Date	Dimensions	Turbulence Model[b]	Combustion Model[c]	Pollutant Prediction	Radiation[d]	Drop Model
No Slip Models:						
Elghobashi, et al. (1976)[67]	2D + t	k-ε	EBU	None	None	Steady drop evaporation or combustion
Swithenbank, and coworkers (1978)[68,69]	2D, 3D	k-ε	EBU	None	MF	Steady drop evaporation or combustions
Jones and Pridden (1978)[70]	3D	k-ε, Favre averaging	EQGP	CO, HC, NO	None	Steady drop evaporation
Slip Models:						
Anasoulis, et al. (1974)[71]	2D	algebraic	EQG	NO	MF	Steady evaporation corrected for convection
Gibeling, et al. (1975-76)[72]	3D	k-ε	EQG	NO	MF	Steady evaporation corrected for convection
Crowe and coworkers (1974-78)[73-75]	2D	k-ε	evaporation	None	None	Transient heat-up and evaporation with convection, treats drop diffusion
Abou Ellail and Khalil (1978)[76]	2D	$\underline{k-\varepsilon \text{ and}}$ $\rho' u'_i$	EB	None	MF	Transient heat-up (no evap.), evaporation with convection

Table 3 (Continued)

Summary of TPF Models of Spray Evaporation and Combustion[a]

Reference and Date	Dimensions	Turbulent Model[b]	Combustion Model[c]	Pollutant Prediction	Radiation[d]	Drop Model
Mongia and co-	3D	k-ε	MEBU	CO, HC, NO_X	MF	Transient heat-up and evaporation with convection

[a] Finite difference calculations assuming a dilute spray.

[b] Reynolds averaging unless noted otherwise, no direct effect of drops on turbulence.

[c] EBU denotes eddy break-up model of Spalding[23,24,40,41]; EQGP denotes equilibrium gas phase and use of probability distribution function; EQG denotes equilibrium gas phase with drop evaporation; EB denotes drop evaporation with reaction expression following Borghi[103]; MEBU denotes eddy break-up model, but drops evaporate or combust depending on whether mean mixture ratio is greater or less than stoichiometric.

[d] MF denotes multiflux radiation model following Patankar and Spalding[47].

Keeping the above limitations in mind, several of the models have been compared with experiments.[1,2,71,72,76] Mellor[13] discusses the results for the models of Anasoulis, et al.[71] and Gibeling, et al.[72] In both cases, the complex flow within a gas turbine was considered. Predictions of mean temperature distributions and NO were very poor.

Abou Ellail and Khalil[76] consider the cylindrical oil-fired furnace experiments of Khalil, et al.[99] The experiment involves a kerosene spray (maximum drop number density 40-50 μm, 1.1 mm nozzle diameter) in a swirling air flow. For the case illustrated, the swirl number was 0.721, yielding a recirculation flow. The comparison between predicted and measured profiles of axial and tangential velocities is reasonably good. Maximum discrepancies of mean temperature are less than 150 K.

Mongia and coworkers[1,2] have only considered limited comparisons between predictions and measurements. This work has been confined to complex gas turbine geometries and are good examples of the potential of TPF calculations. It was found that model parameters could be adjusted to give reasonable predictions of CO, HC and combustion efficiency. While the authors consider their model to be a useful design tool, they don't characterize it as an accurate, a priori, predictive method.[1,2] The state of development of the other models listed in Table 3 is certainly no better.

CONCLUSIONS

1. Several studies have been completed to evaluate the LHF approximation for modeling sprays. The advantages of this method are that predictions are qualitatively correct, necessary injector specifications are minimal and the computations are no more difficult than those required for a gaseous combustion process. However, it appears that slip is important for most practical combusting sprays, and the LHF models generally overestimate the rate of development of the flow.

2. Methods are available for predicting heat-up, evaporation or combustion, and trajectories of multicomponent drops. For best results, calculations should be calibrated with single drop experimental results, since property selection is uncertain. The need for calibration could be reduced if a comprehensive method for predicting drop heat and mass transfer rates and drag (including property selection rules) were developed. Several aspects of treating drop transport in turbulent combusting flows are in need of further investigation. This includes: the effect of turbulent fluctuations on transport rates, (i.e., the appropriateness of the use of mean ambient properties; the enhancement of transport rates by small scale turbulence; improved criteria for ignition, envelope flames and wake flames; and methods for treating turbulent drop diffusion. The experimental apparatus developed by Sangiovanni and coworkers,[100-102] where drops are propelled through a combusting gas field, could provide one approach for examining these questions.

3. The general framework for practical TPF models of three-dimensional spray combustion processes now exists. Several models of this type have already been reported, including instances where they have aided the development of gas turbine combustors. Systematic validation of these

models, however, is still needed. Current models are more correlation schemes rather than reliable prediction tools. The technology for completing the necessary measurements is currently available, at least for dilute sprays. Many of the weaknesses in current models will benefit from ongoing work in turbulent gas flames. However, special problems due to the presence of drops must also be considered, including: dense spray effects; turbulence generation and dissipation by drops; convenient methods for measuring injector characteristics; and a comprehensive method for injector specification matched to the needs of TPF models which consider slip.

REFERENCES

1. Reynolds, R. S., Kuhn, T. E., and Mongia, H. C., *An Advanced Combustor Analytical Design Procedure and its Application in the Design and Development Testing of a Premix/Prevaporized Combustion System,* 1977 Spring Technical Meeting, Central States Section, The Combustion Institute, March, 1977.

2. Mongia, H. C., and Smith, K., *An Empirical/Analytical Design Methodology for Gas Turbine Combustors,* AIAA Paper No. 78-998, July, 1978.

3. Faeth, G. M., *Current Status of Droplet and Liquid Combustion,* Prog. Energy Combust. Sci., Vol. 3, 1977, pp. 191-224.

4. Williams, A., *Combustion of Sprays of Liquid Fuels,* Elek Science, London, 1976.

5. Williams, A., *Fundamentals of Oil Combustion,* Prog. Energy Combust. Sci., Vol. 2, 1976, pp. 167-179.

6. Williams, A., *Combustion of Droplets of Liquid Fuels: A Review,* Combustion and Flame, Vol. 21, 1973, pp. 1-31

7. Williams, A., *The Mechanism of Combustion of Droplets and Sprays of Liquid Fuels,* Oxidation and Combustion Reviews, Vol. 1, 1968, pp. 1-45.

8. Krier, H., and Foo, C. L., *A Review and Detailed Derivation of Basic Relations Describing the Burning of Droplets,* Oxidation and Combustion Reviews, Vol. 6, 1973, pp. 111-143.

9. Kanury, A. M., *Introduction to Combustion Phenomena,* Gordon and Breach, New York, 1975, pp. 142-194.

10. Chigier, N. A., *The Atomization and Burning of Liquid Fuel Sprays,* Prog. Energy Combust. Sci., Vol. 2, 1977, pp. 97-114.

11. Hedley, A. B., Nuruzzaman, A. S. M., and Martin, G. F., *Combustion of Single Droplets and Simplified Spray Systems,* J. Inst. Fuel, Vol. 44, 1971, pp. 38-54.

12. Harrje, D. T., and Reardon, F. H. (ed.), *Liquid Propellant Rocket Combustion Instability,* NASA SP-194, National Aeronautics and Space Administration, Washington, DC, 1972, pp. 37-102.

13. Mellor, A. M., *Turbulent-Combustion Interaction Models for Practical High Intensity Combustors,* Seventeenth Symposium (International) on Combustion, The Combustion Institute, Pittsburgh, in press.

14. Mellor, A. M., *Gas Turbine Engine Pollution,* Prog. Energy Combust. Sci., Vol. 1, 1976, pp. 111-133.

15. Collier, J. G., *Convective Boiling and Condensation,* McGraw-Hill, London, 1973, pp. 7-32.

16. Weimer, J. C., Faeth, G. M., and Olson, D. R., *Penetration of Vapor Jets Submerged in Subcooled Liquids,* AIChE J., Vol. 19, 1973, pp. 552-558.

17. Avery, J. F., and Faeth, G. M., *Combustion of a Submerged Gaseous Oxidizer Jet in a Liquid Metal,* Fifteenth Symposium (International) on Combustion, The Combustion Institute, Pittsburgh, 1975, pp. 419-428.

18. Onuma, Y., and Ogasawara, M., *Studies on the Structure of a Spray Combustion Flame,* Fifteenth Symposium (International) on Combustion, The Combustion Institute, Pittsburgh, 1975, pp. 453-465.

19. Komiyama, K., Flagan, R. C., and Heywood, J. B., *The Influence of Droplet Evaporation on Fuel-Air Mixing Rate in a Burner,* Sixteenth Symposium (International) on Combustion, The Combustion Institute, Pittsburgh, 1976, pp. 549-560.

20. Tuttle, J. H., Colket, M. B., Bilger, R. W., and Mellor, A. M., *Characteristic Times for Combustion and Pollutant Formation in Spray Combustion,* Sixteenth Symposium (International) on Combustion, The Combustion Institute, Pittsburgh, 1976, pp. 209-219.

21. Lockwood, F. C., and Naguib, A. S., *The Prediction of the Fluctuations in the Properties of Free, Round-Jet, Turbulent Diffusion Flames,* Combustion and Flame, Vol. 24, 1975, pp. 109-124.

22. Gosman, A. D., Lockwood, F. C., and Syed, S. A., *Prediction of a Horizontal Free Turbulent Diffusion Flame,* Sixteenth Symposium (International) on Combustion, The Combustion Institute, Pittsburgh, 1976, pp. 1543-1555.

23. Spalding, D. B., *Concentration Fluctuations in a Round Turbulent Free Jet,* Chemical Engineering Science, Vol. 26, 1971, pp. 95-107.

24. Spalding, D. B., *Mathematical Models of Turbulent Flames: A Review,* Combustion Science and Technology, Vol. 13, 1976, pp. 3-25.

25. Davies, C. N., *Aerosol Science,* Academic Press, New York, 1976, pp. 393-468.

26. Gordon, S., and McBride, B. J., *Computer Program for Calculation of Complex Equilibrium Compositions, Rocket Performance, Incident and Reflected Shocks, and Chapman-Jouguet Detonations*, NASA SP-273, 1971.

27. Shearer, A. J., Tamura, H., and Faeth, G. M., *Evaluation of a Locally Homogeneous Model of Spray Evaporation*, AIAA Paper 78-1042, 1978.

28. Thring, M. W., and Newby, M. P., *Combustion Length of Enclosed Turbulent Jet Flames*, Fourth Symposium (International) on Combustion, Williams and Wilkins, Baltimore, 1953, pp. 789-796.

29. Newman, J. A., and Brzustowski, T. A., *Behavior of a Liquid Jet Near the Thermodynamic Critical Region*, AIAAJ, Vol. 9, August, 1971, pp. 1595-1602.

30. Shearer, A. J., and Faeth, G. M., *Combustion of Liquid Sprays at High Pressures*, NASA CR-135210, March, 1977.

31. Khalil, E. E., and Whitelaw, J. H., *Aerodynamic and Thermodynamic Characteristics of Kerosene Spray Flames*, Sixteenth Symposium (International) on Combustion, The Combustion Institute, Pittsburgh, 1976, pp. 569-576.

32. Khalil, E. E., *A Simplified Approach for the Calculation of Free and Confined Spray Flames*, AIAA Paper No. 78-29, 1978.

33. Launder, B. E., and Spalding, D. B., *Mathematical Models of Turbulence*, Academic Press, London, 1972.

34. Bilger, R. W., *Turbulent Jet Diffusion Flames*, Prog. Energy Combust. Sci., Vol. 1, 1976, pp. 87-109.

35. Kent, J. H., and Bilger, R. W., *The Prediction of Turbulent Diffusion Flame Fields and Nitric Oxide Formation*, Sixteenth Symposium (International) on Combustion, The Combustion Institute, Pittsburgh, 1977, pp. 1643-1656.

36. Parker, S. F., and Sirignano, W. A., *A Numerical Study of Planar, Turbulent, Reacting Mixing Layers*, Paper No. 70, 1978 Fall Technical Meeting, Eastern Section of The Combustion Institute, Miami Beach, Florida, November, 1978.

37. Kennedy, I. M., and Kent, J. H., *Measurements of a Conserved Scalar in Turbulent Jet Diffusion Flames*, Seventeenth Symposium (International) on Combustion, The Combustion Institute, in press.

38. Pope, S. B., *The Implications of the Probability Equations for Turbulent Combustion Models*, Combustion and Flame, Vol. 29, 1977, pp. 235-246; also, *The Probability Approach to Modeling of Turbulent Reacting Flows*, Combustion and Flame, Vol. 27, 1976, pp. 299-312.

39. Lockwood, F. C., *The Modeling of Turbulent Premixed and Diffusion Combustion in the Computation of Engineering Flows*, Combustion and Flame, Vol. 29, 1977, pp. 111-122.

40. Spalding, D. B., *Mixing and Chemical Reaction in Steady Confined Turbulent Flames*, Thirteenth Symposium (International) on Combustion, The Combustion Institute, Pittsburgh, 1971, pp. 649-657.

41. Mason, H. B., and Spalding, D. B., *Prediction of Reaction Rates in Turbulent Premixed Boundary Layer Flows*, Combustion Institute European Symposium, Academic Press, New York, 1973, pp. 601-606.

42. Khalil, E. E., Spalding, D. B., and Whitelaw, J. H., *The Calculation of Local Flow Properties in Two-Dimensional Furnaces*, Int. J. Heat Mass Transfer, Vol. 18, 1975, pp. 775-791.

43. Spalding, D. B., *Development of Eddy Break-Up Model of Turbulent Combustion*, Sixteenth Symposium (International) on Combustion, The Combustion Institute, Pittsburgh, 1976, pp. 1657-1663.

44. Patankar, S. V., and Spalding, D. B., *Heat and Mass Transfer in Boundary Layers*, 2nd Ed., Intertext Books, London, 1970; also, *A Calculation Procedure for Heat, Mass and Momentum Transfer in Three-Dimensional Parabolic Flows*, Int. J. Heat Mass Transfer, Vol. 15, 1972, pp. 1787-1806.

45. Gosman, A. D., Lockwood, F. C., and Salooja, A. P., *The Prediction of Cylindrical Furnaces Gaseous Fired with Premixed or Diffusion Flames*, Seventeenth Symposium (International) on Combustion, The Combustion Institute, Pittsburgh, in press.

46. Gossman, A. D., and Pun, W. M., *Calculation of Recirculating Flows*, Lecture Notes, Imperial College of Science and Technology, London, December, 1973.

47. Patankar, S. V., and Spalding, D. B., *Computer Model for Three-Dimensional Flow in Furnaces*, Fourteenth Symposium (International) on Combustion, The Combustion Institute, Pittsburgh, 1973, pp. 605-614.

48. Kamimoto, T., and Matsuoka, S., *Prediction of Spray Evaporation in Reciprocating Engines*, SAE Paper 770413, 1977.

49. Hiroyasu, H., and Kadota, T., *Models for Combustion and Formation of Nitric Oxide and Soot in Direct Injection Diesel Engines*, SAE Paper 760129, 1976.

50. Shahed, S. M., Chiu, W. S., and Yumlu, V. S., *A Preliminary Model for the Formation of Nitric Oxide in Direct Injection Diesel Engines and Its Application in Parametric Studies*, SAE Paper 730083, 1973.

51. Khan, I. M., Greeves, G., and Wang, C. H. T., *Factors Affecting Smoke and Gaseous Emissions from Direct Injection Engines and a Method of Calculation,* SAE Paper 730169, 1973.

52. Khan, I. M., Greeves, G., and Probert, D. M., *Prediction of Soot and Nitric Oxide Concentrations in Diesel Engine Exhaust,* Proc. Inst. Mech. Engrs., Vol. C142, 1971, pp. 205-217.

53. Kerney, P. J., Faeth, G. M., and Olson, D. R., *Penetration Characteristics of a Submerged Steam Jet,* AIChEJ, Vol. 18, 1972, pp. 548-553.

54. Hawthorne, W. R., Weddell, D. S., and Hottel, H. C., *Mixing and Combustion in Turbulent Gas Jets,* Third Symposium on Combustion, Flame and Explosion Phenomena, Williams and Wilkins, Baltimore, 1949, pp. 266-288.

55. Wohl, K., Gazley, C., and Kapp, N., *Diffusion Flames,* Third Symposium on Combustion, Flame and Explosion Phenomena, Williams and Wilkins, Baltimore, 1949, pp. 288-300.

56. Shearer, A. J., *Evaluation of a Locally Homogeneous Flow Model of Spray Evaporation,* Ph.D. Thesis, The Pennsylvania State University, June, 1978.

57. Wygnanski, I., and Fiedler, H. E., *Some Measurements in the Self-Preserving Jet,* J. Fluid Mech., Vol. 38, 1969, pp. 577-612.

58. Becker, H. A., Hottel, H. C., and Williams, G. C., *The Nozzle-Fluid Concentration Field of the Round, Turbulent, Free Jet,* J. Fluid Mech., Vol. 30, 1967, pp. 285-303.

59. Hetsroni, G., and Sokolov, M., *Distribution of Mass, Velocity and Intensity of Turbulence in a Two-Phase Turbulent Jet,* Trans. ASME, J. Appl. Mech., Vol. 38, 1971, pp. 315-327.

60. Corrsin, S., and Uberoi, M. S., *Further Experiments on the Flow and Heat Transfer in a Heated Turbulent Air Jet,* NACA Report No. 998, 1950.

61. Tross, S. R., *Characteristics of a Turbulent, Two-Phase, Submerged, Free Jet,* M. S. Thesis, The Pennsylvania State University, August, 1974.

62. Faeth, G. M., and Lazar, R. S., *Fuel Droplet Burning Rates in a Combustion Gas Environment,* AIAAJ, Vol. 9, November, 1971, pp. 2165-2171.

63. Canada, G. S., and Faeth, G. M., *Combustion of Liquid Fuels in a Flowing Combustion Gas Environment at High Pressures,* Fifteenth Symposium (International) on Combustion, The Combustion Institute, Pittsburgh, 1974, pp. 419-428.

64. Kadota, T., and Hiroyasu, H., *Evaporation of a Single Droplet at Elevated Pressures and Temperatures,* Trans. Japan Soc. Mech. Engrs., Vol. 42, 1976, pp. 1216-1222.

65. Putnam, A., *Integrable Form of Droplet Drag Coefficient,* ARS J, Vol. 31, 1961, pp. 1467-1468.

66. Law, C. K., Prakash, S., and Sirignano, W. A., *Theory of Convective, Transient, Multicomponent Droplet Diffusion,* Sixteenth Symposium (International) on Combustion, The Combustion Institute, Pittsburgh, 1976, pp. 605-617.

67. Elghobashi, S., Pratt, D. T., Spalding, D. B., and Srivatsa, S. K., *Unsteady Combustion of Fuel Spray in Jet-Engine After-Burners,* Third International Symposium on Air-Breathing Engines, 1976.

68. Swithenbank, J., Turan, A., and Felton, P. G., *Three-Dimensional, Two-Phase Mathematical Modeling of Gas Turbine Combustors,* Project Squid (ONR) Workshop on Gas Turbine Combustor Design Problems, Purdue University, May, 1978.

69. Boyson, F., and Swithenbank, J., *Spray Evaporation in Recirculating Flow,* Seventeenth Symposium (International) on Combustion, The Combustion Institute, Pittsburgh, in press.

70. Jones, W. P., and Pridden, C. H., *Predictions of the Flow Field and Local Gas Composition in Gas Turbine Combustors,* Seventeenth Symposium (International) on Combustion, The Combustion Institute, Pittsburgh, in press.

71. Anasoulis, R. F., McDonald, H., and Buggelin, R. C., *Development of a Combustor Flow Analysys. Part I: Theoretical Studies,* AFAPL-TR-73-98, 1974.

72. Gibeling, H. J., McDonald, H., and Briley, W. R., *Development of a Three-Dimensional Combustor Flow Analysis,* AFAPL-TR-75-59, Vol. I, 1975, Vol. III, 1976.

73. Crowe, C. T., Sharma, M. P., and Stock, D. E., *The Particle-Source-in-Cell (PSI-Cell) Model for Gas-Droplet Flows,* Trans. ASME, J. Fluids Engr., Vol. 99, 1977, pp. 325-332.

74. Crowe, C. T., *A Computational Model for the Gas Droplet Flow in the Vicinity of an Atomizer,* Paper 74-23, Western States Section, The Combustion Institute, 1974.

75. Crowe, C. T., *A Numerical Model for the Gas Droplet Flow Field Near an Atomizer,* First International Conference on Liquid Atomization and Spray Systems, Tokyo, August, 1978.

76. Abou Ellail, M. M. M., and Khalil, E. E., *A Prediction Procedure of the Aerodynamic and Thermodynamic Characteristics of Axisymetric Confined Spray Flames,* Seventeenth Symposium (International) on Combustion, The University of Leeds, Leeds, August, 1978.

77. Soo, S. L., *Fluid Dynamics of Multiphase Systems,* Blaisdell Publishing Co., Waltham, MA, 1976, pp. 51-60 and 185-218.

78. Vara Prasad, C. M., and Kar, S., *An Investigation on the Diffusion of Momentum and Mass of Fuel in a Diesel Fuel Spray,* Trans, ASME, J. Engr. for Power, Vol. 99, 1977, pp. 225-236.

79. Mellow, R., Chigier, N. A., and Beer, J. M., *Pressure Jet Spray in an Air Stream,* ASME Paper No. 70-GT-101, 1970.

80. Jones, A. R., *A Review of Drop Size Measurement--The Application of Techniques to Dense Fuel Sprays,* Prog. Energy Combust. Sci., Vol. 3, 1977, pp. 225-234.

81. Simmons, H. C., *The Correlation of Drop Size Distributions in Fuel Nozzle Sprays,* Engr. for Power, Vol. 99, July, 1977, pp. 309-319.

82. Faeth, G. M., and Olson, D. R., *The Ignition of Hydrocarbon Fuel Droplets in Air,* SAE Paper 680465, 1978.

83. Kadota, T., Hiroyasu, H., and Oya, H., *Spontaneous Ignition Delay of a Fuel Droplet in High Pressure and High Temperature Gaseous Environments,* Japan Soc. Mech. Engrs., Vol. 41, 1975, pp. 2475-2483.

84. Spalding, D. B., *The Combustion of Liquid Fuels,* Fourth Symposium (International) on Combustion, Williams and Wilkins, Baltimore, 1953, pp. 847-864.

85. Gollahalli, S. R., and Brzustowski, T. A., *Environmental Studies on the Flame Structure in the Wake of a Burning Droplet,* Fourteenth Symposium (International) on Combustion, The Combustion Institute, Pittsburgh, 1973, pp. 1333-1344.

86. Ogasawara, M., and Sami, H., *Study on the Burning of a Fuel Drop in Heated and Pressurized Air Stream,* Japan Soc. Mech. Engr. Bull., Vol. 13, 1970, pp. 395-426.

87. Chigier, N. A., and McCreath, C. G., *Combustion of Droplets in Sprays,* Acta Astronautica, Vol. 1, 1974, pp. 687-710.

88. Durst, F., Melling, A., and Whitelaw, J. H., *Principles and Practice of Laser-Doppler Anemometry,* Academic Press, London, 1976.

89. Jurewicz, J. T., Stock, D. E., and Crowe, C. T., *The Effect of Turbulent Diffusion on Gas Particle Flow in an Electric Field,* Symposium on Turbulent Shear Flows, The Pennsylvania State University, April, 1977.

90. Jurewicz, J. T., and Stock, D. E., *A Numerical Model for Turbulent Diffusion in Gas-Particle Flows,* ASME Paper 76-WA/FE-33, 1976.

91. Goldschmidt, V. W., Householder, M. K., Ahmadi, G., and Chuang, S. C., *Turbulent Diffusion of Small Particles Suspended in Turbulent Jets,* Progress in Heat and Mass Transfer, Vol. 6, 1972, pp. 487-508.

92. Lilly, G. P., *Effect of Particle Size on Particle Eddy Diffusivity*, Ind. Eng. Chem. Fundam., Vol. 12, 1973, pp. 268-275.

93. Crowe, C. T., and Pratt, D. T., *Finite-Difference Methods for Calculation of Heterogeneous Combustion*, Spring Meeting, Central States Section, The Combustion Institute, April, 1978.

94. Hinze, J. O., *Turbulence*, McGraw-Hill, New York, 1976, pp. 1-82.

95. Lumley, J. L., and Tennekes, H., *A First Course in Turbulence*, The MIT Press, Cambridge, MA, 1972, pp. 19-24.

96. Lambiris, S., Combs, L. P., and Levine, R. S., *Stable Combustion Processes in Liquid Propellant Rocket Engines*, Combustion and Propulsion, Fifth AGARD Colloquium; High Temperature Phenomona, Macmillan, New York, 1963, pp. 596-634.

97. Williams, F. A., *Combustion Theory*, Addison-Wesley, Reading, MA, 1965, pp. 250-287.

98. Spalding, D. B., *The Calculation of Free-Convention Phenomena in Gas-Liquid Mixtures*, Mech. Engr. Dept. Report No. HTS/76/11, Imperial College, London, 1976.

99. Khalil, K. H., El-Mahallawy, F. M., and Moneib, H. S., *Effect of Combustion Air Swirl on the Flow Pattern in a Cylindrical Oil Fired Furnace*, Sixteenth Symposium (International) on Combustion, The Combustion Institute, Pittsburgh, 1976, pp. 135-143.

100. Sangiovanni, J. J., and Kesten, A. S., *Effect of Droplet Interaction on Ignition in Monodispersed Droplet Streams*, Sixteenth Symposium (International) on Combustion, The Combustion Institute, 1976, pp. 577-592.

101. Sangiovanni, J. J., and Kesten, A. S., *A Theoretical and Experimental Investigation of the Ignition of Fuel Droplets*, Comb. Sci. and Tech., Vol. 16, 1977, pp. 59-70.

102. Sangiovanni, J. J., and Dodge, L. G., *Observations of Flame Structure in the Combustion of Monodispersed Streams*, Seventeenth Symposium (International) on Combustion, The Combustion Institute, Pittsburgh, in press.

103. Borghi, R., *Chemical Reaction Calculations in Turbulent Flows Applicable to Co-containing Turbojet Plume*, Advances in Geophysics, Vol. 18B, 1974, pp. 349-365.

Comments and Replies on

"Spray Evaporation and Combustion Models: A Review"

by G. Faeth

A. Varma: Are the equations used the constant density equations? If that is the case, I don't understand why these equations should work for variable density flows.

G. Faeth: Density is treated as a variable in Eqs. (1) - (8), however, many of the density fluctuation terms in the transport equations have been dropped, similar to the single phase flow model of Lockwood and coworkers (See refs. 21, 22). Similar to Refs. 21 and 22, modeling variable density flows in this manner was reasonably successful, although the values for the "Universal" constants were different for constant and variable density flows. This is not very desirable. The use of Favre averaging in an alternative procedure that might eliminate this difficulty, but this remains to be shown.

P. Sforza: What do you use for the initial conditions in the calculations illustrated in Figures 3-6?

G. Faeth: Measurements of initial conditions across the exit plane of the jet are not available for any of the flows illustrated. We assume that the flow is equivalent to fully developed pipe flow at the jet exit.

X. Reed: Could you clarify the computation of drop life histories? Since drops will certainly be fluctuating along their trajectories, they don't see the mean field. Do you average the drop trajectories as well as the flow field through which they pass? I don't understand quite how that is supposed to represent the proper average heat and mass transfer of a drop in the flow.

G. Faeth: The calculations illustrated in Fig. 7 involve the determination of ballistic trajectory of a drop, ignoring turbulent diffusion. The local environment of a drop is specified by mean properties. Therefore, the calculations ignore effect of turbulent fluctuations on transport rates. This approach is typical of spray models in use at this time, c.f. Table 3. The effects you mention are discussed in the paper. The present approach appears to be a reasonable first approximation, capable of yielding agreement with experiment in view of uncertainties in physical and flow properties. Further study of the effects of diffusion and turbulent fluctuations on drop life history calculations would be desirable, however.

A. Varma: The relaxation time for a ten micron drop comes out to be a very small number. Why does it take so long for the ten micron drop to follow the gas in Fig. 7?

G. Faeth: For single phase jets, the rate of change of gas velocity with axial distance is proportional to u_o/d. Sprays at least qualitatively follow this behavior, c.f. Fig. 5. For a spray injector, however, d is relatively small (1.19 mm for the results shown in Fig. 7), yielding high rates of deceleration. In this environment, the small relaxation time of a ten micron drop is simply not small enough. From this observation, one is led to the general conclusion that practical sprays are almost always influenced by slip effects, due to their relatively small injector diameters.

M. Finson: Isn't the scaling parameter for this behavior $\rho_f D/\rho d$? If this number is greater than a number on the order of unity, then you know you're going to have an important slip effect, and the same essential result applies to heat transfer, too. You have to do the same thing in reverse to design tracer particles for the LDA.

G. Faeth: The parameter you suggest does provide a rough guide to slip effects for relatively simple flow configurations. As an example, consider the case illustrated in Fig. 7. Appropriate data involves $\rho_f = 1500$ kg/m^3, $\rho = 1$ kg/m^3, d = 1190 μm, yielding a value of the parameter on the order of unity for a 1 μm drop, and a proportionally higher value for larger drops. From Fig. 7, it is evident that drops smaller than 1 μm have little slip, while 10 μm drops clearly do slip, in accord with the criteria that you mention. This rule would be less effective for the spray data in Fig. 2, however, where the parameter is much less than unity at high pressures for the SMD drop size, and yet the LHF model is still not satisfactory. While this particular criteria does not provide an effective measure of heat and mass transfer effects, similar, relatively simple rules can be found, as discussed in the paper. The difficulty with simple measures of this type is that properties vary widely in sprays, introducing uncertainty in the application of a rule. A particular relaxation time or length also only has relevance in comparison to the length of the spray process itself. In view of this, a more reliable approach for estimating the need for a slip model is the one illustrated in the paper. Namely, to compute a first estimate of the flow using the locally homogeneous flow approximation, and then compute drop life histories in the flow in order to determine the importance of slip and loss of thermodynamic equilibrium.

P. Sforza: Since you've done such a nice job of drawing together all the different problems which exist with models, perhaps you could mention, briefly, what problems you see in terms of experiments and what experiments should be done.

G. Faeth: I think the technology exists for doing the experiments needed to evaluate the models, except in the low void fraction region (void fractions less than 90-95%) near the injector. The LDA provides capabilities for measuring gas velocities and turbulence quantities; there are a number of optical techniques available for sizing drops and measuring their velocities. Sampling and probes are usually required for composition and temperature measurements in a spray, which presents difficulties, but these problems have been solved in the past.

I would advocate well-defined, two-dimensional configurations for model evaluation, as opposed to the complex flow fields of typical combustion chambers. In this way, both the measurements and calculations can be simplified, providing a more convincing comparison.

P. Sforza: Has there been any application of Raman spectroscopy of concentration measurements in sprays?

G. Faeth: I am not aware of any studies using Raman spectroscopy in sprays.

P. Ponzi: Is drop coalescence of any concern?

G. Faeth: It undoubtedly is an important factor in the low void fraction, dense spray region. There has been little work in this area, and I am not aware of any quantitative information on the effect for sprays. A major problem is the difficulty of making measurements in the dense spray region.

CARBON FORMATION IN FLAMES: AN OVERVIEW

Howard B. Palmer

This discussion includes a brief summary of some experimental facts about soot and about sooting in combustion systems; comments on mechanisms of carbon formation; and a review of some experiments that seem especially interesting. For a more extensive background than that provided here, I recommend the chapter on carbon in the book by Gaydon and Wolfhard (1) and the reviews by Palmer and Cullis (2), Homann (3), Lahaye and Prado (4) and Wagner (5). The last two are very recent, are quite different, and are excellent. The tables and figures in these reviews and in that of Homann are especially valuable.

Characteristics of Soot

In fuel-rich flames, *i.e.* when oxygen is deficient, the burning of hydrocarbons becomes very complicated. Because of the huge number of possible species, there may even be a problem in deciding what the final equilibrium products should be, quite apart from questions of intermediates and the details of the combustion mechanism. Concentrations of hydrocarbon radicals, H atoms, and H_2 all become significant. Broadly speaking, one can say that thermal cracking reactions play an important role, modified by the presence of oxygen, O and H atoms, and OH radicals. Radical combination and addition reactions lead to formation of higher hydrocarbons. Attainment of chemical equilibrium becomes very sluggish. If there is a sufficiently great excess of fuel, very large polymeric molecules may be formed, which in the extreme range of molecular weights may (with some liberty) be called carbon. The carbon, or soot, will not be expected to be entirely free of oxygen or hydrogen. Its chemical composition will be a function of parameters such as the fuel type, the composition and temperature history of the combusting mixture, and the residence time of the soot at high temperature, before cooling.

"Mature" soot or carbon black usually contains roughly 99 per cent C and 1 per cent H by weight, with very little oxygen. Thus its atomic composition is on the order of C_8H or $C_{10}H$. If one thinks of a soot "molecule" as a system of fused 6-membered rings with H atoms around the periphery, then it requires of the order of 200 fused rings to make a soot molecule. However, this model of soot is probably useful only in a very crude way.

Soot typically contains spherical particles that may be arranged in clumps or strings. Their diameters are 100 to 500 Angstroms, normally. In heavily sooting flames, particle diameters may range up to 2000 A or more. One can easily calculate that soot particles contain from about 10^5 to 10^7 carbon atoms. Electron microscopy shows (6) that within the particles, these atoms are contained within graphite-like layer planes, but they are not stacked in an orderly array. Rather, they are concentric, like the structure of an onion, and the layer planes are replete with breaks and non-parallel alignments. The particles have low porosity.

The small particle size of soot guarantees that in virtually all soot-containing systems the particle temperature will be very close to the gas temperature.

Hot particles in flames will radiate energy (and also absorb it and scatter it). Radiation from sooting flames has been studied somewhat, but it is difficult to generalize the results. In principle, the optical properties of a dispersion of particles can be calculated from the theory of light scattering. Foster (7) has carried out some calculations by making use of the fact that soot particles are normally much smaller than the wave length of visible or infrared light.

The emissivity of a cloud of particles is approximately given by:

$$\varepsilon_\lambda = 1 - \exp(-K_\lambda cL)$$

where ε_λ = emissivity at wave length

K_λ = attenuation coefficient of soot

c = concentration of soot

L = thickness of cloud

The attenuation coefficient, K_λ, is a function of particle size (and of λ). To calculate it, one must know the complex refractive index of the particles. Dalzell and Sarofim (8) found that a value of the refractive index, $n = 1.57-0.56i$, held adequately for soot. However, the value is dependent upon the C/H ratio of the soot. For practical purposes an empirical correlation with the soot C/H ratio may be possible. Studies at the International Flame Research Foundation suggest that it may in turn be possible to empirically connect the C/H ratio with combustion conditions. Work on practical flames directed to this end seems to be needed.

In the work of Foster, limited data available from the literature were used to calculate K_λ as a function of particle size and wave length. Only a single experimental point was available for comparison, referring to a soot having particle size $\simeq$ 500 A, $\lambda \simeq 6500$ A. The point agreed well with the calculations. For some rough calculations, K_λ is sometimes approximated by $K_\lambda = B/\lambda^n$, where B and n are constants. The work of Foster shows that this approximation should be used with caution. More recent work on calculating K_λ has been carried out by Keeton (9).

Parameters Affecting Sooting

(a) Composition of the combusting mixture.

In hydrocarbon-air (or oxygen) flames, solid carbon can exist at equilibrium when O/C atomic ratio in the mixture is equal to or less than approximately 1.0. However, carbon formation usually occurs well to the fuel-lean side of O/C = 1.0. Because, once formed, carbon is removed only slowly by oxidation or gasification, the system may not equilibrate and soot may escape. For example, in a very rich, sooting premixed flame of C_2H_4 and air, the flame remains sooty as air is added, all the way up to O/C = 1.45. With CH_4-air, the critical O/C ratio is a surprising 2.16. These numbers imply that a lot of the oxygen is tied up in CO_2 and H_2O at the sooting limit and the system composition is far from equilibrium. Experiments confirm this condition. Thus we see immediately that soot formation must be controlled by kinetic features, not by equilibrium considerations.

(b) Molecular Structure. There are some differences in the effects of molecular structure of the fuel, depending upon whether the flame is premixed or is of the diffusional type.

(i) Diffusion flames. Measurements of heights-to-soot in laminar diffusion flames give an order of increasing tendency to soot as follows: paraffins < diolefins < benzenes < naphthalenes. Increasing paraffinic content tends to decrease the soot-forming tendency. In general, the C/H ratio of the fuel seems to control matters. Flame luminosity can also be used as a measure of sooting tendency, but it is complicated by the effects of temperature and the competition between oxidation and carbon formation.

(ii) Premixed flames. We have noted that carbon formation can be understood only as a kinetic problem, and not as an equilibrium one. There is some evidence that it boils down to a competition between the kinds of reactions that lead to carbon in purely pyrolytic (no oxygen) systems and the oxidation (mainly by OH radicals) of the intermediates that otherwise tend to form carbon. It follows as a truism that in any combustion system that is not premixed, flow and mixing patterns will be crucial in determining the sooting tendency. Interestingly, it has also been found that in premixed systems, backmixing can appreciably influence soot formation, as noted by Wright (10) and Blazowski (11). The effect is to somewhat reduce the sooting tendency. These studies are very important for high-intensity combustors.

There are some correlations between carbon-forming tendencies and fuel structure in laminar premixed flames, as shown by Street and Thomas (12). Straight-chain paraffins have a slightly greater carbon-formation tendency than do branched-chain paraffins of the same molecular weight. A surprise is to find that olefins and acetylene apparently have less tendency to form soot than do the paraffins. Aromatics are stongly sooting, especially those of large molecular weight.

P. H. Daniels (13) showed that it is possible to find some quite systematic relations among different types of fuels, if the data of Street and Thomas are treated suitably. For example, for the data it is possible to calculate the number of oxygen atoms per molecule of hydrocarbon in a barely non-sooting gaseous fuel-air mixture. Daniels called this the "OASC" (oxygen atoms to suppress carbon). The OASC behaves systematically. It is a linear function of the number of carbon atoms in the molecule. One can convert the OASC to a critical ratio of carbon atoms to oxygen atoms. This (C/O_{crit}) is approximately constant for a particular homologous series; *e.g.* for the paraffin hydrocarbons from ethane to cetane, $(C/O)_{crit} \approx 0.46$.

Correlations of this sort are interesting and useful but rarely provide insight into fundamental chemical phenomena. Looking for conditions in the burning gases at a critical sooting limit might be more revealing. Fenimore, Jones, and Moore (14) examined the stable products withdrawn from flames of a wide variety of hydrocarbons with oxygen. At the sooting limit, they found a correlation among the concentrations of four simple molecules, expressed as (pressure in cm. Hg):

$$R \fallingdotseq 0.6 = (2p_{C_2H_2} + p_{CH_4})(p_{H_2})^{1/2}/p_{H_2O}$$

They further noted that if, as expected, equilibria are attained among the species H, H_2, OH, and H_2O, (*i.e.* $H + H_2O \rightleftarrows H_2 + OH$) the correlation implies:

$$R = 0.6 = (2p_{C_2H_2} + p_{CH_4})/p_{OH}$$

which is of interest as perhaps expressing a competitive relationship between the carbon-forming species, CH_4 and C_2H_2, and the oxidizing species, OH. This begins to approach the fundamental chemistry of sooting (rather than simple correlations), and is a subject to which we return later.

(c) Influence of pressure. Qualitatively, changes in pressure have the same effects upon carbon formation in both diffusion flames and premixed flames. Lowering of pressure decreases sooting and raising of pressure increases it. This is shown clearly in the experiments of Macfarlane, Holderness, and Whitcher (15). The study of Fenimore, Jones, and Moore (14) further showed that as pressure rises, one needs a greater oxygen/carbon ratio to suppress sooting. These features are not well understood, nor are the effects of combustion system pressure upon characteristics of soot.

In diffusion flames one can imagine that an increase in pressure enhances the rates of cracking or polymerization reactions and slows interdiffusion of fuel and oxidant. The situation in premixed flames is more subtle. Homann (3) suggests that at higher pressures, species such as H, OH, and O recombine into relatively inactive molecules more rapidly, and present less competition to carbon-forming reactions.

(d) Influence of temperature. The effect of temperature depends upon the mixture composition. Near the sooting limit, an increase in temperature reduces the tendency to soot, as Millikan (16) has shown. He has further shown that (for ethylene-air flames) there is a linear relationship between burned gas temperature and the critical (C/O) ratio in the reactant mixture. The ratio goes up as the temperature increases.

On the other hand, when the system is very fuel-rich, an increase in temperature may dramatically increase the extent of carbon formation. This was shown by Macfarlane *et al* (15), who substituted "argon-air" for normal air in fuel-air mixtures, thus increasing the flame temperature substantially, without changing the input fuel-oxygen ratio. The qualitative explanation of this observation is undoubtedly the influence of temperature on the rates of cracking and polymerization-type reactions, occurring with little competition from oxidation or gasification reactions. The explanation of Milliken's observation is more subtle. He offered an interpretation based upon the hypothesis (mentioned previously) of competition between soot-producing pyrolytic reactions and soot-preventing reactions, particularly oxidation by OH radicals. More recent studies (17-19) have lent support to the importance of OH in soot consumption or in the prevention of soot formation.

(e) Influence of diluents and additives. Here there are some similarities and also some differences between diffusion flames and premixed flames of hydrocarbons such as CH_4. However, in general one can say that relatively few non-metallic additives seem to have prounounced effects on sooting. A few observations reported in the literature are summarized below:

Diluent or additive	Effect	
	Diffusion flame	Premixed flame
H_2O vapor	....	decrease
SO_2	decrease	slight decrease
SO_3	decrease	strong increase
H_2	decrease	slight decrease
Halogens	increase	increase
Organic halides	increase	increase
NO, NO_2	....	slight decrease
H_2S	....	slight decrease
Amyl nitrate	....	increase

The most striking feature of this tabulation is the extraordinary effect of SO_3 in premixed flames. The effect presumably has its root in some enhancement by SO_3 of chain reaction steps that are of importance in carbon formation, or else in inhibition of oxidation. SO_3 does possess the capability of reacting with H· and O·, but the former would produce OH· and the latter O_2, so the inhibition should not be strong. It is more probable that the effect of SO_3 at high temperatures is analogous to the accelerating effect of small amounts of O· in low-temperature cracking of hydrocarbons; *i.e.,* SO_3 may help to start chains by reactions such as $SO_3 + RH \rightarrow R\cdot + OH + SO_2$.

Metallic additives have received much more attention, especially within the past decase, and a large number of metals have been examined. Recent research includes the excellent work of Cotton *et al* (20), in which 40 metals were studied, the work of Addecott and Nutt [as discussed by Miller (21)], and the very interesting work of Feugier (17) on alkali and alkaline-earth metals. Many metals are found to be effective, but the order in which they are ranked differs in the first two studies cited. A detailed mechanism for the function of alkaline earths (Ba, Sr, Ca) and molybdenum based on catalysis of radical production is proposed by Cotton *et al.* Addecott and Nutt offer a possible alternative based on charge exchange between flame ions and metal atoms. The potential for productive work on this subject seems very large, and although a fair amount of research has been done [for a brief review see Salooja (22)], it is somewhat surprising that there has not been more. One of the most useful studies has been reported by Friswell (22a). He studied the soot reduction in a kerosene-fired simulated gas turbine combustor using the additives barium, manganese, and iron. Barium and manganese were studied as a function of concentration for three air-fuel ratios. Further support for the radical-production mechanism for soot suppression by Ba was found in the observation that Ba addition increases the rate of formation of NO at the same time that it inhibits sooting. Manganese and iron, in contrast appear to operate by being incorporated into soot particles (Fenimore and Jones (23)) and catalyzing soot burnout. Friswell found that the efficiency of Ba is approximately independent of the overall air-fuel ratio in his simulated gas turbine, whereas Mn and Fe function better as the exhaust temperature rises (*i.e.,* as the air-fuel ratio moves toward stoichiometric).

(f) Effects of electric fields. It is possible to control sooting in flames to an extraordinary degree - either enhancing it or suppressing it - by suitable application of electric fields. Payne and Weinberg (24) first showed that electric fields could have a pronounced effect on carbon formation with respect to its onset, the rate of growth and the character of the carbon formed. [In fact electric fields can be used to control a whole suite of combustion phenomena from burning of sprays and particles to growth of inorganic oxides (25, 26)]. Place and Weinberg (27) established beyond reasonable doubt that positive ions in flames can act as nuclei for carbon formation. The ions do not even have to be organic in nature (*e.g.* Cs ions also cause nucleation). Their findings are supported by experiments of W. J. Miller (28).

The effects of electric fields imposed on counterflow diffusion flames (29) indicate that all carbon particles are charged and that each carries only a single charge. The study also shows that carbon growth occurs both on neutral and on charged species, *i.e.* some particles acquire a charge after substantial growth has occurred. In new work on rich premixed flames, Wersborg, *et al*(30) report that 13 to 40% of the soot particles are charged and that the charged particles carry one or two charges in most cases. These results and those of Weinberg seem to be in essential agreement.

Although the ability to control soot growth by manipulation of fields has been demonstrated, there seems not to have been a practical application yet in the control of soot in high-output combustors such as engines or furnaces. Perhaps there are proprietary developments in this area of which I am not aware.

The Mechanism of Soot Formation

Many diagrams have appeared from time to time in the literature, showing ideas about the chemical transformations that occur during the course of converting a hydrocarbon into more or less pure carbon. For purposes of the present discussion, it is useful to employ a scheme that is broadly divided into stages in time, rather than into stages in chemical characteristics. The objective of such a presentation is to underscore the importance of kinetics as well as mechanism. There are no rigorous boundaries between the regions of time in the diagram; rather, it should be construed as somewhat analogous to a collection of elementary reaction steps that, taken together, constitute the kinetic description of a complex reaction. The extent to which the various steps may be separated depends strongly upon the conditions of the reaction. To illustrate the point, we might recall that for some purposes it is convenient and not totally unrealistic to think of a premixed flame of a hydrocarbon with oxygen as consisting of three stages: in the first stage, hydrocarbon is oxidized to a mixture of carbon monoxide and water, and with some hydrogen and free radicals remaining; in the second stage, carbon monoxide and the residual hydrogen are oxidized to carbon dioxide and water; and finally, in the third stage, the excess concentrations of free radicals are reduced to their equilibrium values by recombination reactions. One knows that these are not sharply defined stages, and one also knows that by modifying the conditions--concentrations, pressures, and temperatures--the boundaries among the stages can be modified or perhaps even completely obliterated. One also knows that all of the processes are occurring all of the time; thus, even in the earliest stages of the flame, some radical recombination is occurring.

With these reservations and clarifications in mind, let us examine a possible time sequence for the formation of carbon from a combusting hydrocarbon. It might be divided into four stages as follows:

Stage I.	Gaseous decomposition Condensation reactions Polymerization	oxidation → wall →	Removal Deposition
Stage II.	Formation of polynuclear aromatics, polyacetylenes and related species Nucleation Ionization	oxidation → wall →	Removal Deposition
Stage III.	Growth of nuclei Decomposition of gases on particle surfaces Ionization Charge exchange	oxidation → wall →	Removal Deposition
Stage IV.	Agglomeration Curing of particles Casting-off of residual species	oxidation → wall →	Removal Deposition

The scheme indicates the possibility that deposits on surfaces may be formed at any stage of the process. The character of the surface deposit will depend upon the competition between the diffusion of the various species to the wall and the kinetics of processes that lead ultimately to a well-cured soot. The scheme also includes the possibility of interruption or cessation by oxidation processes, *e.g.* by OH attack.

The several stages in soot formation are discussed in the reviews cited earlier and, because of their complexities, will not be outlined here in any detail. The review of Lahaye and Prado (4) gives particularly thorough consideration to the stages in soot formation. Here I offer only some general remarks.

Stage I. The kinetics of decomposition of many small gaseous molecules are reasonably well understood. However, hydrocarbons have been rather difficult to study becasue of the complexities of their decomposition mechanisms. Aromatic molecules are, unfortunately, in especially poor shape. The general features are known for aliphatics and aromatics: aliphatics tend to crack to smaller, unsaturated species that can then undergo polymerization; aromatics tend to condense to multi-ring systems unless the temperature is very high, in which case they undergo ring rupture and form smaller molecules such as acetylene.

Stage II. Condensation reactions of aromatics are in general faster than cracking and polymerization. Thus formation of nuclei from aromatics is fast and they tend to be heavy soot-formers; aliphatics are slower. The brilliant researches of Homann, Wagner, and others at Göttingen (31) have shown that aliphatics form polyacetylenic species in the early stages of soot formation and that these undergo further addition and condensation reactions that produce nuclei having a free radical character. These can then grow by addition reactions.

It is known that ions also can act as nuclei, and that ions are created very early in flames. Recent studies of this route to carbon formation have been most actively pursued by J. B. Howard's group at M.I.T. (32).

Lahaye and Prado (33) support the view that nucleation generally occurs by vapor condensation of large hydrocarbon molecules to form droplets, which then grow by both chemical and physical processes. They eventually carbonize to form solid spherical particles.

The problem of identifying the nuclei and the nucleation process is important because if it can be dramatically influenced, the whole pattern of sooting behavior can be altered.

Stages III and IV. The early particle growth to diameters of the order of 100 Angstroms seems to be rapid. This growth apparently occurs largely by addition reactions similar to those in earlier stages. Beyond that point, however, the addition reactions play a lesser role and the bulk of the later growth takes place by particle-particle collisions. There is some decrease in the number of density (concentration) of particles as this occurs.

The growing particles exhibit a normal distribution of sizes about the mean. Above 100 Angstroms, the enlargement in average size occurs increasingly slowly. It is well known that soot from flames rarely has an average particle size in excess of 500 Angstroms. However, in pyrolyzing systems where residence times may be very much longer, the slow growth process may continue to sizes well in excess of 1000 Angstroms.

Kunugi and Jinno (34) have used the light-scattering technique pioneered by Erickson, Williams, and Hottel (35) to follow the growth of carbon particles in sooting flames of paraffinic hydrocarbons. Their method was restricted to rather large particles (over 1000 Angstroms), but they were able to obtain some very interesting results on growth and on the number densities in various regions of a diffusion flame.

Soot growth is so complex a process that in practice one may have to seek a correlation relating soot growth to temperature, pressure, and fuel concentration, probably with the inclusion of a fuel/oxygen ratio. A significant first step in this direction was taken by Datschefski (36), using a "controlled mixing history" furnace to study the rate of soot formation in very rich propane-air flames and in propane pyrolysis. A semiempirical rate expression was found to describe the data adequately.

The technique was extended to soot formation from methane by Narasimhan & Foster (37) who derived a form for the expected rate based upon a model in which growth occurred by direct decomposition on particle surfaces. The expression was

$$dC/dt = \text{const}\ (N_s)^{1/3}(C)^{2/3}(x/T^{0.5})\exp(-E/RT)$$

Where C = soot mass concentration in mg/cm^3, N_s = soot particle concentration in cm^{-3}, and x = mole fraction of CH_4.

Their data fit the expression well when $E = 57.6$ kcal. More work along these lines would undoubtedly be useful, because of the need for global kinetic expressions for soot-formation rates, for use in reactor modeling.

A paper by Fenimore and Jones (38) provides virtually all that is known about the kinetics or mechanism of soot agglomeration in the absence of electric fields. Fenimore and Jones argued that if particles can be prevented from growing beyond a diameter of about 100 Å and can be prevented from coagulating, they should ultimately be consumed and not escape as smoke. Their reasoning was based on the assumption, supported by previous work (23), that soot is oxidized mainly by OH. Its burnout rate could then be compared to the rate of oxidation of CO by OH. Information on coagulation rates was obtained by observing the conditions under which soot coagulated to sufficiently large sizes that it escaped from the flame. The well-known effect of increasing the pressure (*i.e.* an increase in smoke) was also accounted for by the associated increase in coagulation rates.

The curing or aging process is a deactivation that is responsible for the ultimate cessation of particle growth. It is known that electron spin resonance signals of particles decrease in the later portions of sooting flames. Clearly, the free radical properties of the particles are disappearing. Little can be said about the mechanistic details or the kinetics. Interestingly, the fraction of charged particles increases in the later stages (30), perhaps because larger particles have a lower work function.

One of the small puzzles that exists in the phenomenology of sooting is why there are residual hydrocarbons that manage to survive the rigors of the conditions that produce carbon particles. Some of the species than can be extracted from commercial carbon blacks (39), for example, are relatively small molecules that may even be aliphatic in nature. One can only assume that in the curing of particles, such species are formed and, when an exit route is available, thrown off. Some of them stick to the particles long enough to survive when the particles are finally cooled and collected.

Other species associated with the particles are more clearly molcules that are intimately involved in the carbon formation process, being in all probability formed in competition with some of the species that go on to become soot. The species that survive in this way are very stable and unreactive aromatics such as pyrene (39).

Soot Burnout

Efforts to understand and predict the rates of soot burnout are increasingly successful. The basic point of reference is the work of Lee *et al.*(40) on the rate of soot combustion in a sooting laminar flame. Magnussen (41) has extended the experiments to a turbulent flame and has presented a theoretical analysis that bears some resemblance to the qualitative model offered by Dalzell *et al.* (42). It suggests that the kinetic correlation of Lee *et al.* cannot be directly applied to turbulent flames. Kito *et al.* (43) find that the burnout of residual carbon particles generated from heavy fuel oil is kinetically different from soot burnout, mainly because the residual particles are orders of magnitude larger than soot and the rate is controlled by boundary layer diffusion rather than surface chemistry. Rosner and Allendorf (44) have reported experimental rates of attack of graphite surfaces by O, O_2, OH, and H at a wide range of temperatures.

An attempt to model the consumption of soot in gas turbines has been presented by Radcliffe and Appleton (45). One interesting conclusion in their work is that, contrary to the hypothesis of Fenimore and Jones (23), OH is probably not the main oxidant of soot. The very high efficiency of reaction of O atoms with graphite found by Rosner and Allendorf suggests that O atoms may be more significant oxidizers of soot than had previously been thought. However, recent work by Page and Ates (46) lends strong support to OH as the principal oxidizer of soot in flames.

Exciting work on soot oxidation has been published by Park and Appleton (47), who have succeeded in studying the process in shock waves, using two types of carbon black. They have covered the temperature and pressure (O_2) ranges, 1700-4000°K and 0.05-13 atm, and have found that a semiempirical kinetic expression for the oxidation of pyrographite (48) correlates the soot data suprisingly well. This is consistent with the observation noted earlier that graphite layer planes in a soot particle are oriented roughly parallel to the particle surface. The data were also compared with the results of Lee *et al.* (40), Fenimore and Jones (23), and Tesner and Tsibulevsky (49). The study of Park and Appleton offers real hope for an understanding of soot burnout of sufficient quality to permit kinetic modeling in practical situations.

References

1. A. G. Gaydon and H. G. Wolhard, Flames, Chapman and Hall, London (1970).
2. H. B. Palmer and C. F. Cullis, Chapter 5 in Chemistry and Physics of Carbon, Vol. 1, Ed. P. L. Walker, Jr., Marcel Dekker, Inc., New York (1965).
3. K. H. Homann, Combust. Flame 11, 265 (1967).
4. J. Lahaye and G. Prado, Chapter 3 in Chemistry and Physics of Carbon, Vol. 14, ed. P. L. Walker, Jr. and P. A. Thrower, Marcel Dekker, Inc., New York (1978).
5. H. Gg. Wagner, 17th Internat. Sym. Combust., Combustion Institute, Pittsburgh (1979).
6. L. L. Ban and W. M. Hess, private comm. from Columbian Carbon Co., Princeton, NJ. See also Ref. 4.
7. P. S. Foster, Combust. Flame 7, 277 (1963).
8. W. H. Dalzell and A. F. Sarofim, J. Heat Transfer (Trans. ASME Ser. C) 91, 100 (1969).
9. S. C. Keeton, Report SAND 79-8210, Sandia Laboratories, Albuquerque, NM (1979).
10. F. J. Wright, 12th Internat. Sym. Combust., Combustion Institute, Pittsburgh, PA (1969), p. 867.
11. W. S. Blazowski, Combust. Sci. Tech. (in press, 1979).
12. J. C. Street and A. Thomas, Fuel, 34, 4 (1955).
13. P. H. Daniels, Combust. Flame 4, 45 (1960).
14. C. P. Fenimore, C. W. Jones, and G. E. Moore, 6th Internat. Sym. Combust., Reinhold Pub. Corp., New York (1957), p. 242.
15. J. J. Macfarlane, F. H. Holderness, and F. S. E. Whitcher, Combust. Flame 8, 215 (1964).
16. R. C. Millikan, J. Phys. Chem. 66, 794 (1962).
17. A. Feugier, in Evaporation-Combustion of Fuels, ed. J. T. Zung, Am. Chem. Soc., Washington (1978), p. 178.
18. F. M. Page and F. Ates, *ibid*, p. 190.
19. K. Müller-Dethlefs and A. F. Schlader, Combust. Flame 27, 205 (1976).

20. D. H. Cotton, N. J. Friswell, and D. R. Jenkins, Combust. Flame 17, 87 (1971).

21. W. J. Miller, 14th Internat. Sym. Combust., Combustion Institute Pittsburgh (1973), p. 307.

22. K. C. Salooja, J. Inst. Fuel 45, 37 (1972).

22a. N. J. Friswell, in Emissions from Continuous Combustion Systems, ed. by W. Cornelius and W. G. Agnew, Plenum, New York (1972), p. 161.

23. C. P. Fenimore and G. W. Jones, J. Phys. Chem. 71, 593 (1967).

24. K. G. Payne and F. J. Weinberg, Proc. Roy. Soc. (London), A250, 316 (1959).

25. K. C. Thong and F. J. Weinberg, Proc. Roy. Soc. (London), A324, 201 (1971).

26. D. R. Hardesty and F. J. Weinberg, 14th Internat. Sym. Combust., Combustion Institute, Pittsburgh (1973), p. 907.

27. E. R. Place and F. J. Weinberg, 11th Internat. Sym. Combust., Combustion Institute, Pittsburgh (1967), p. 245.

28. W. J. Miller, *ibid*, p. 252.

29. P. J. Mayo and F. J. Weinberg, Proc. Roy. Soc. (London) A319, 351 (1970).

30. B. L. Wersborg, J. B. Howard, and G. C. Williams, 14th Internat. Sym. Combust., Combustion Institute, Pittsburgh (1973), p. 929.

31. See Refs. 3 and 6.

32. G. Prado and J. B. Howard, in Evaporation-Combustion of Fuels, ed. J. T. Zung, Am. Chem. Soc., Washington (1978), p. 153, and references therein.

33. See Ref. 4.

34. M. Kunugi and H. Jinno, 11th Internat. Sym. Combust., Combustion Institute, Pittsburgh (1967), p. 257.

35. W. D. Erickson, G. C. Williams, and H. C. Hottel, Combust. Flame 8, 127 (1964).

36. G. Datschefski, Dissertation, Univ. of Sheffield (1962).

37. K. S. Narasimhan and P. J. Foster, 10th Internat. Sym. Combust., Combustion Institute, Pittsburgh (1965), p. 253.

38. C. P. Fenimore and G. W. Jones, Combust. Flame 13, 303 (1969).

39. H. B. Palmer, A. Voet, and J. Lahaye, Carbon 6, 65 (1968).

40. K. B. Lee, M. W. Thring, and J. B. Beer, Combust. Flame 6, 137 (1962).

41. B. F. Magnusson, 13th Internat. Sym. Combust., Combustion Institute, Pittsburgh (1971), p. 869.

42. W. H. Dalzell, G. Williams, and H. C. Hottel, Combust. Flame 14, 161 (1970).

43. M. Kito, M. Ishimaru, S. Kawahara, T. Sakai, and S. Sugiyama, Combust. Flame 17, 391 (1971).

44. D. E. Rosner and H. D. Allendorf, AIAAJ 6, 650 (1968); see also Heterogeneous Kinetics at Elevated Temperatures, ed. G. R. Belton and W. L. Worrell, Plenum Press, New York (1970), p. 231.

45. S. W. Radcliffe and J. P. Appleton, Comb. Sci. Tech. 4, 171 (1971).

46. F. M. Page and F. Ates, in Evaporation-Combustion of Fuels, ed. J. T. Zung, Am. Chem. Soc., Washington (1978), p. 190.

47. C. Park and J. P. Appleton, Combust. Flame 20, 369 (1973).

48. J. Nagle and R. F. Strickland-Constable, Proc. 5th Carbon Conf., Pergamon Press, London (1962), Vol. 1, p. 154.

49. P. A. Tesner and A. M. Tsybulevskii, Combust. Explos. Shock Waves 3, 163 (1969).

MODELING PARTICULATE FORMATION FOR THE ANALYSIS OF FUEL RICH OPERATION IN PRACTICAL SYSTEMS

Presented by Raymond B. Edelman, Science Applications, Inc.

The development of any new reacting flow system or modifications of existing systems seems to be plagued by the discovery that a sufficient understanding of the relationship between the process and the controllable design variables is not in hand. Current design practice is typically built upon experience coupled with a degree of empiricism. Until recently, this approach could not be faulted because of its success in dealing with the complex mechanisms embodied and coupled within the typical multiphase, turbulent reacting flow. Now the requirements have become more exacting and the development of new energy conversion processes cannot await nor afford the cost of trial and error procedures. What is evident, however, is that in the treatment of complex processes, there is the practical need to recognize the important parameters and design according to their control of the process. The problem is that a particular design procedure will be constrained to limited application because it implicitly neglects mechanisms that become important when changes in configuration and operating conditions are required.

Reacting flows involve the mechanisms of convection, conduction, turbulent transport in the gas phase, ballistic and turbulent transport of particulate matter, interphase transport, radiation and chemical kinetics including pyrolysis, particulate formation and oxidation of the gaseous and particulate components. It is clear, without displaying the full contingent of describing equations, that the number of parameters, whether expressed in terms of characteristic times or dimensionless groups, is large. The significance of this is that extrapolation, or scaling, will generally not result in preserving exact similarity. This is the source of problems encountered in current design practice. Predictive tools, if available, would provide the means to "scale", and if these predictive methods contain the correct description of each potentially important mechanism, then any change in relative importance of each mechanism would be properly taken into account under changes in configuration and operating conditions. Achieving this as a goal is dependent upon several factors. The main factor is that of having an "adequate" description of each mechanism. The next factor is based upon the obvious need for engineering models. Consequently, the development of an "adequate" representation of a given process by characterizing the major observables rather than every detail of the process becomes a matter of practicality and is necessary in providing near term engineering models.

This presentation represents a summary of the evidence that engineering models for particulate formation can be developed that are both meaningful for design purposes, while also helping to guide detailed, fundamental studies as well. Emphasis is on development of models capable of providing insights into the behavior and control of particulate formation in practical systems.

The types of problems that are encountered as a result of particulate formation are shown in Fig. 1.

•Experience on Particulte Formation in Combustion Systems
  ••Fuel Management and Delivery Systems
    •••Fuel/Oil Heat Exchanger
    •••Fuel Metering Control
    •••Fuel Injection Nozzles
  ••Combustion Chamber Walls, Liners, Etc.
    Fuel Rich Regimes
    Droplet Impingement

•Problems
  ••Clogging
  ••Fouling of Cataltic Surfaces
  ••Heat Transfer Characteristics
  ••Erosion
  ••Environment
  ••Visibility

<u>General Observations</u>

High Pressures, Elevated Temperatures, and Long Residence Times Correlate Directly with Increased Particulate Formation

Fig. 1. Problems in particulate formation.

The term "particulates", as used here, represents a variety of possible types of condensed materials formed out of the reacting environment generated by the interaction of fuel and oxidizer. The spray process of interest here is perhaps one of the most general sources of particulate emissions. This is summarized in Fig. 2, where liquid is included in the list of particulate emissions. The variety of particulates formed out of gaseous and liquid fuels is discussed in several places (Williams, 1976; Hottel, et al., 1955; Gaydon and Wolfhard, 1960). The composition of particulates including soot and coke (both hard and soft) is not pure carbon. Soot has a nominal C_8H makeup, while the cokes range form 80 to 90+ percent carbon with the remainder comprised of H_2, O_2, S and ash (NACA TR 1300, 1957). Some general observations on particulate formation are given in Fig. 3. More has been done on identifying the atom makeup rather than the structures of the compounds contained in the particulate matter, but in some limited cases, aromatic ring structures have been identified. While it has been proposed that these compounds can suggest the origin of the particulate matter, there is, in fact, no way of delineating which of the species may have become part of the already formed particulate through physical or chemical absorption (Jensen, 1974). The complexity of particulate formation in terms of the possible paths and intermediates that may be involved is illustrated in Fig. 4 (Bankston, et al., 1978). This path diagram incorporates the suggestions of Street and Thomas, 1955, and Bonne, et al., 1965. Although the structure of the initial fuel plays an important role in the particulate formation process, high molecular weight cyclic compounds are formed out of low molecular weight straight chain paraffins (Homann and Wagner, 1967).

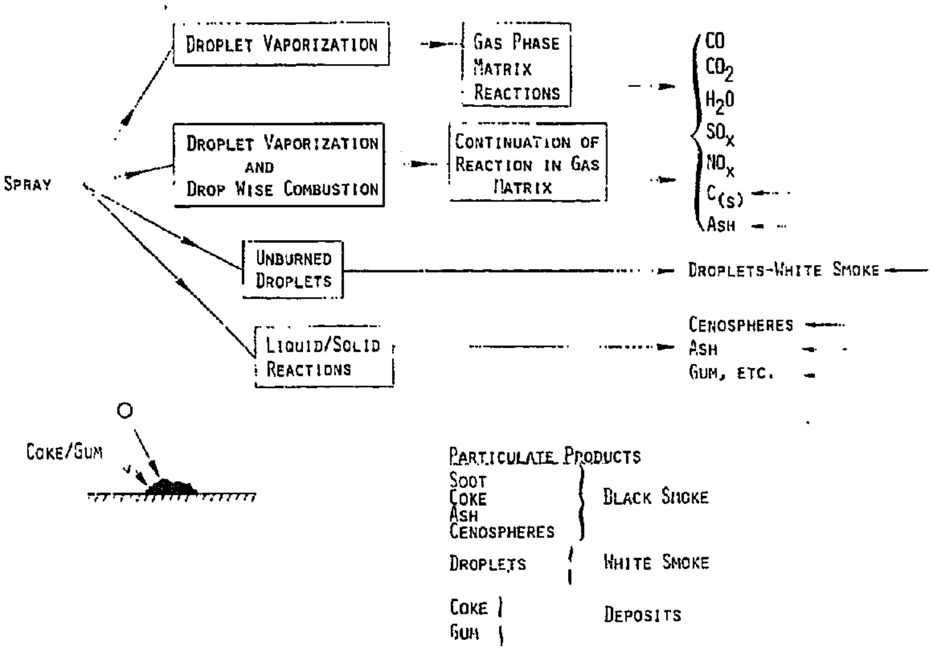

Fig. 2. Spray combustion and particulate formation.

- PARTICULATES ARE FORMED AS A RESULT OF THE CARBON BUT THEIR COMPOSITION IS NOT PURE CARBON
  - SOOT: NOMINAL C_8H, MEASUREMENTS INDICATE: 95% C, 1% H_2 AND 4% O_2
  - SOFT COKE: 80% C, 2% H_2, REMAINDER: O_2 AND S
  - HARD COKE: 92% C, 1.6% H_2, REMAINDER: O_2 AND S
  - FUEL NOZZLE DEPOSIT: C 60%, REMAINDER: O_2, N_2, S, H_2, ASH
- FUEL RICH REGIONS MUST BE PRESENT
- AROMATIC RING STRUCTURES ARE FOUND IN COKE
- PARTICULATE LEVELS INCREASE WITH INCREASING C/H RATIO
- PARTICULATE LEVELS DEPEND ON FUEL STRUCTURE
- PARTICULATE LEVELS INCREASE WITH INCREASING TEMPERATURE, PRESSURE AND RESIDENCE TIME
- PARTICULATE LAGS THE FORMATION OF $C_xH_yO_z$ SPECIES

Fig. 3. Some observations on particulate formation--general.

The difficulty is in the sorting out of the actual role that the many intermediates play in the process. The identification of species is crutial in this determination, but what is not fully understood is whether an observed specie is a precursor, is consequential, or is a passive intermediate in the particulate formation process. It is difficult to independently control the history of a particular specie in order to make this determination.

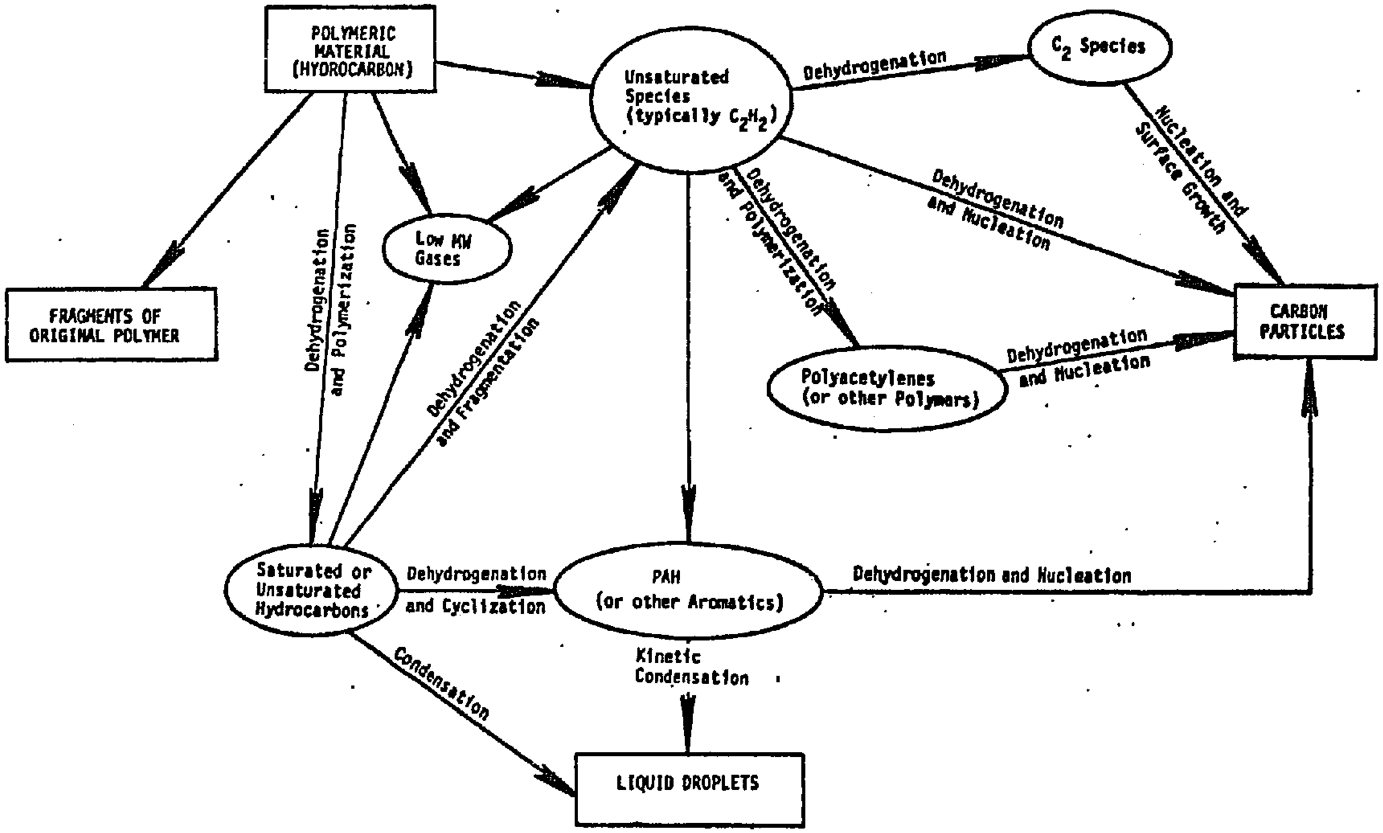

Fig. 4. Postulated mechanisms for smoke particulate formation.

There are several theories for the formation of particulates (Fig. 5).

- Non-Equilibrium Process – Particulates Such as Soot Form at Signicantly Lower Equivalence ratios than are Predicted on the Basis of Thermodynamics (Equilibrium)
- Overall Process Takes Place in Three Steps
    1. Nucleation
    2. Growth
    3. Agglomeration
- Most Popular Approaches to the Detailed Steps
    - Free Radical
    - Ionic
    - C_2 Condensation, C and C_2 Form Particulates through polymerization
    - H/C Polymerization-Condensation, H attack on C_NH_M Forming Higher Radicals
    - Acetylene, Polymerization and Dehydrogenation,

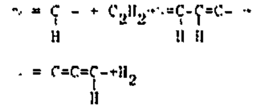

$$\sim = \underset{H}{C} - + C_2H_2 \rightarrow \sim = \underset{H}{C} - \underset{H}{C} = C - \rightarrow$$

$$\cdot = C = C = \underset{H}{C} - + H_2$$

Fig. 5. Mechanisms of particulate formation.

The two broad categories upon which the various theories can be delineated are the neutral species mechanisms and the ionic mechanisms. The evidence available to date suggests that both mechanisms are relevant to the formation of particulates, and that there are operating regimes where one or the other dominates. Presumably, the ionic mechanism plays a negligible role at low temperatures where the formation of particulates in very fuel rich operation is important. In the temperature range between 1500 and 2000K, the situation is different, yet unclear, as to the role of the ionic mechanisms. Calcote, 1978, presents results which suggest that ions can act as nuclei in the particulate formation process, and he is in the process of postulating reaction steps in order to interpret charged species histories observed in sooting flames. Farmer and Matula, 1978, in their work on aromatics, suggest a neutral radical chain reaction as the precursor mechanism for soot formation. Using toluene as the fuel, they postulate phenyl as the key radical in their proposed chain mechanism. Graham, et al., (1975 - 1978) propose that the parent aromatic hydrocarbon can produce soot either by ring condensation or by fragmentation followed by polymerization. Their shock tube studies show that the preferred path is temperature dependent (Fig. 6). Jensen, 1974, postulates a C_2 mechanism for nucleation followed by growth via coagulation and absorption through chemical processes. All proposals are plausible in terms of available data.

Clearly, the process of particulate formation is not well understood. There are, however, some global observations that support the notion of global modeling as a mean of characterizing the particulate formation process. Classification according to fuel structure is well established (Fig. 7.)

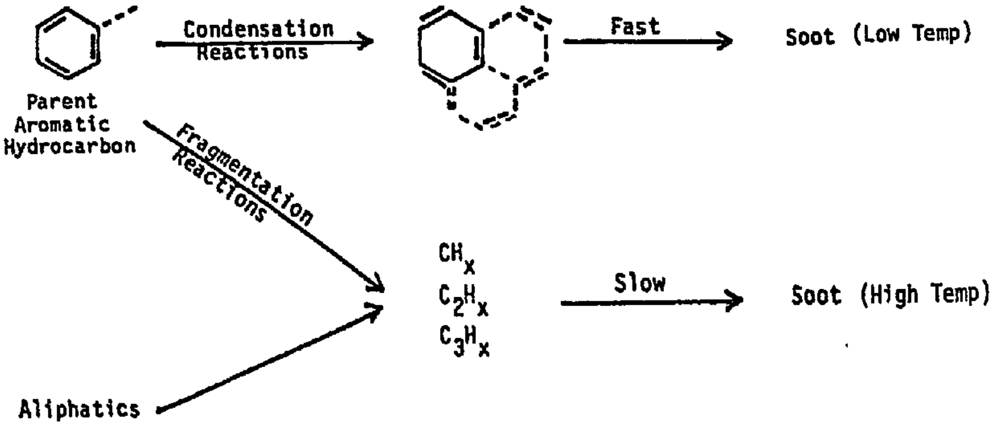

Fig. 6. Formation of soot form aromatics, Graham, et al., 1975.

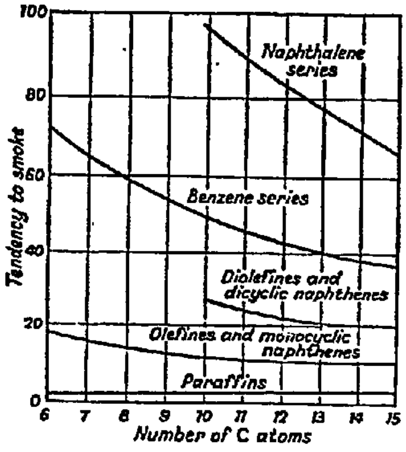

Tendency of various fuels to smoke.
[*After Clarke, Hunter and Garner* (1946)]

NACA TR 1300, 1957

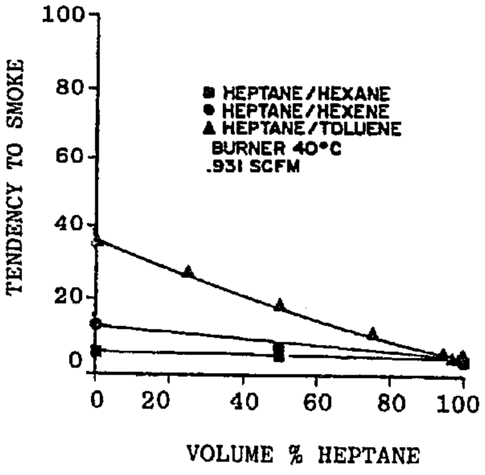

Glassman, et al. 1978

Fig. 7. Smoke tendency for various fuels.

In terms of the tendency to smoke, this can be expressed as follows:

Aromatics > Alkynes > Monolefins > n-paraffins

Furthermore, particulate formation follows initial fuel decomposition or fragmentation. Thus, a pyrolysis-like step is suggested and represents a convenient way to characterize the initial generation of precursors for each fuel type. In general, the rate of decomposition for paraffins and for many cyclic hydrocarbons can be represented as first-order in the fuel concentration (Fig. 8).

- First Order in Fuel Concentration

$$\frac{dC_F}{dT} = -kC_F$$

k = First Order Rate Constant, 1/time

- • Paraffins
- • Naphthenes (and other saturated cyclic hydrocarbons)

Note: Acetylene Pyrolysis is Second Order in $C_{C_2H_2}$

$$-\frac{dC_{C_2H_2}}{dT} = -kC^2_{C_2H_2}$$

Fig. 8. Pyrolysis.

Furthermore, significant data exists for these fuels which substantiates simple subglobal reactions for the initial decomposition of the fuel (Laidler, 1965; Skinner, et al., 1959, 1960; Nixon, 1964, 1965; Gordon, 1963; Glassman, et al., 1978; and others, (Fig. 9)). Similar observations have been made on cyclic hydrocarbons (Figs. 10 and 11). Recently, Blaxowski, Edelman, and Harsha (1978) reported upon the initial results of a combined experimental and analytical program designed to provide engineering predictions for the combustion characteristics of alternative fuels. The results of the experiments have already shown that incipient soot formation and the amount of soot formed can be correlated with the total unburned hydrocarbon in the system (Figs. 12 and 13). This observation is consistent with other work in which global modeling is employed and the rate of production of soot could be correlated with the concentration of the hydrocarbon in the system (Magnussen, 1976). The recent work of Farmer and Matula, 1978, may provide information allowing a generalization of the Magnussen model by eliminating the totally empirical specification of "constants" appearing in the model. The soot "delay" time correlation being developed by Farmer and Matula (Figs. 14 and 15) appears to be related to the soot "formation" time in the Magnussen expression for formation of soot particles through the growth of nuclei.

p

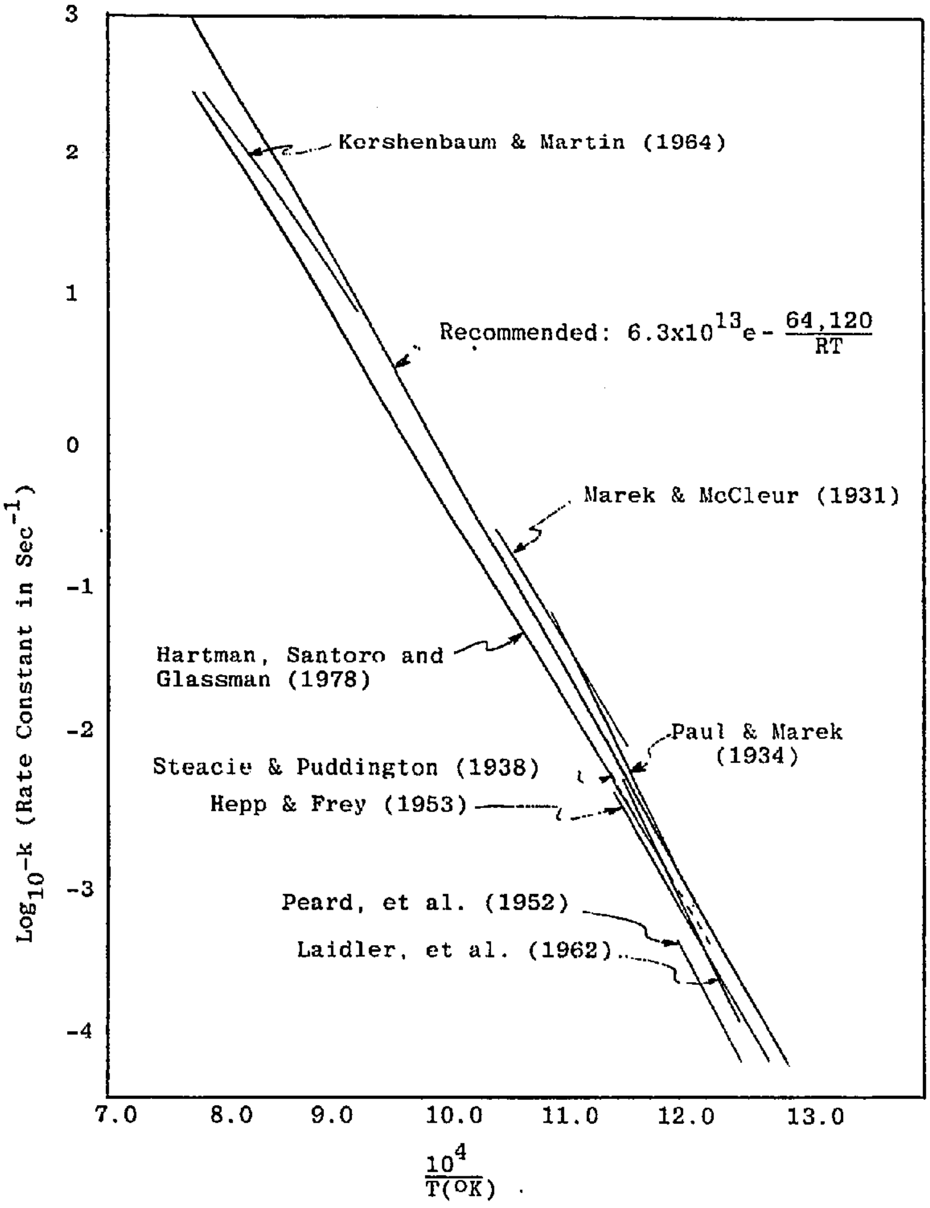

Fig. 9. The first order rate constant for the pyrolysis of propane.

- $\frac{DC_{C_NH_{2N}}}{DT} = K\,C_{C_NH_{2N}}$

  $K = K_0 + \text{CONST.}\ X$, X : PERCENT CONVERSION

  $K_0 = A + BN + CN^2$ AT $T = T_0$

  N IS A CHARACTERIZATION NUMBER DEFINED BY THE NUMBER OF C-H BONDS AND CORRECTED, AS APPROPRIATE, FOR SIDE CHAINS AND SEPARATED POLYCYCLICS

- PARTICLE FORMATION - INDUCTION TIME

  $\tau_{pcd} \approx (aK)^{-1}$ at 50% conversion

- IN GENERAL:

  $K = K(P,T)$

Fig. 10. Estimation of the rate of decomposition--napthenes.

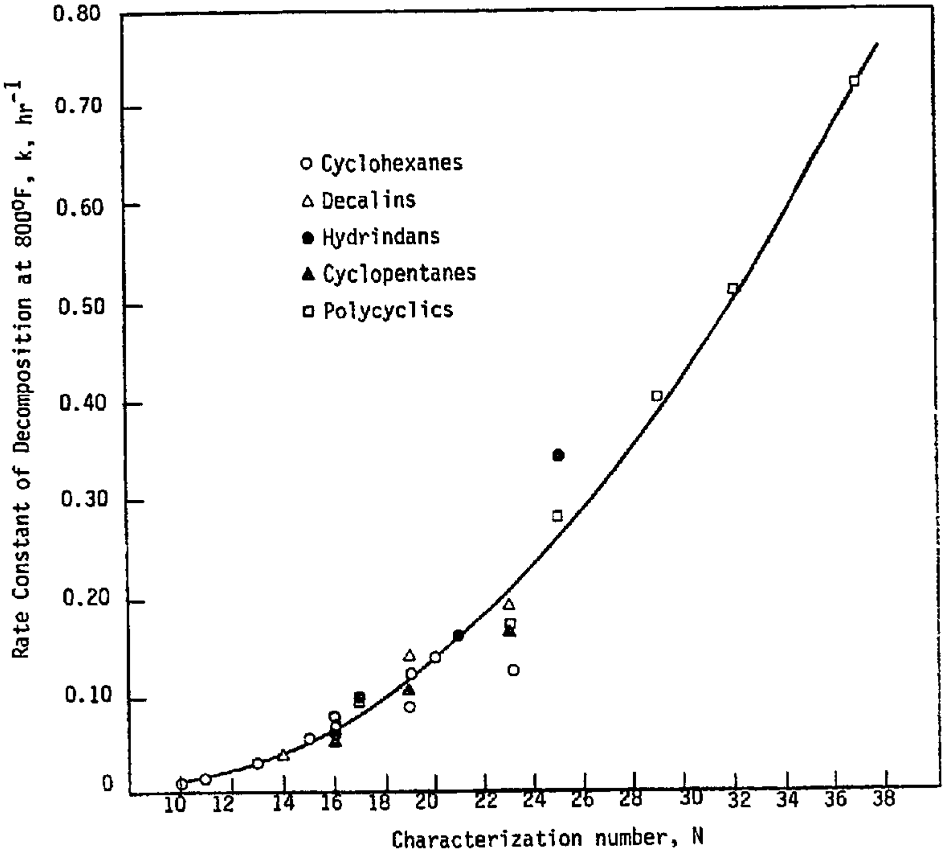

Fig. 11. Rates of decomposition of naphthenic hydrocarbons at 800°F.

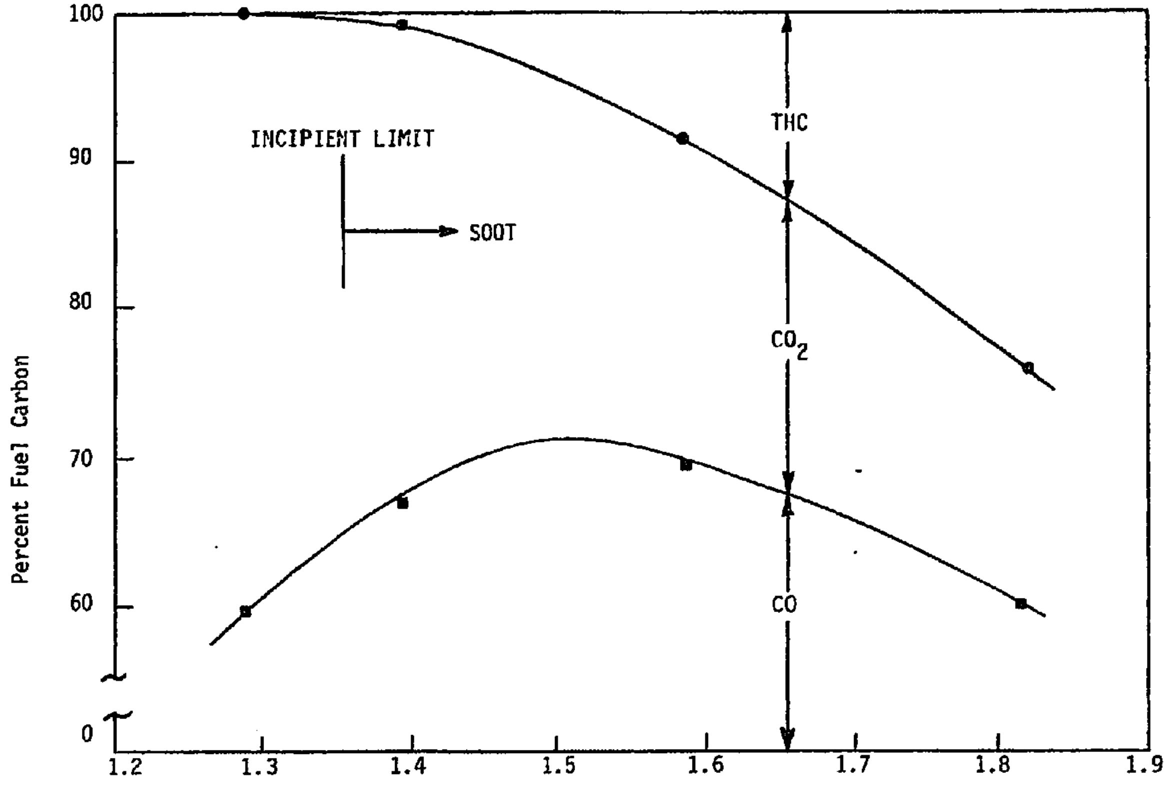

Fig. 12. Fraction of fuel carbon converted to each exhaust product for toluene-air combustion (air mass flow = 112.5 gm/min, inlet temperature = 3000°C).

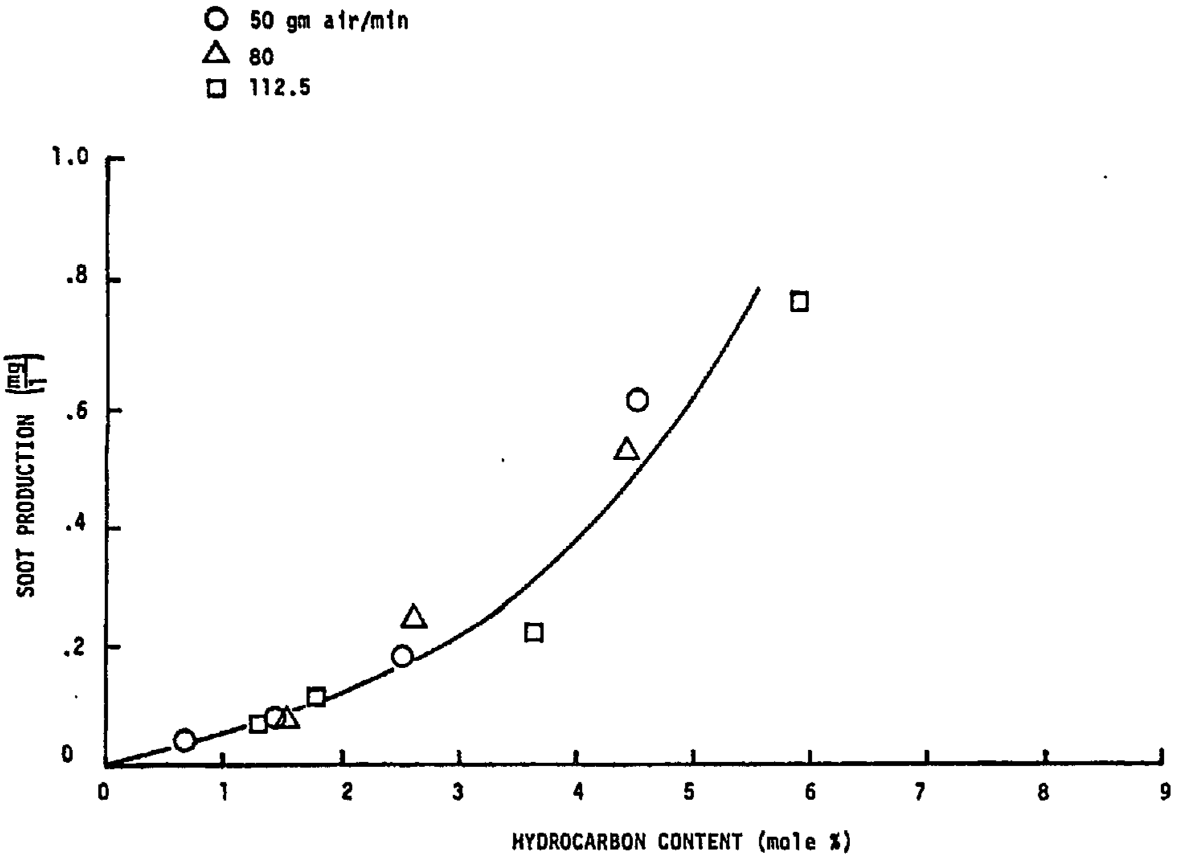

Fig. 13. Correlation of soot production data with hydrocarbon concentration.

FUEL: TOLUENE

$\phi = 1.2$ and 2.0

$\tau = A\ e\ (\frac{E}{RT})\ (C_F)^a\ (O_2)^b\ A_r^c$,

FARMER AND MATULA, 1978

Fig. 14. Soot formation--delay time.

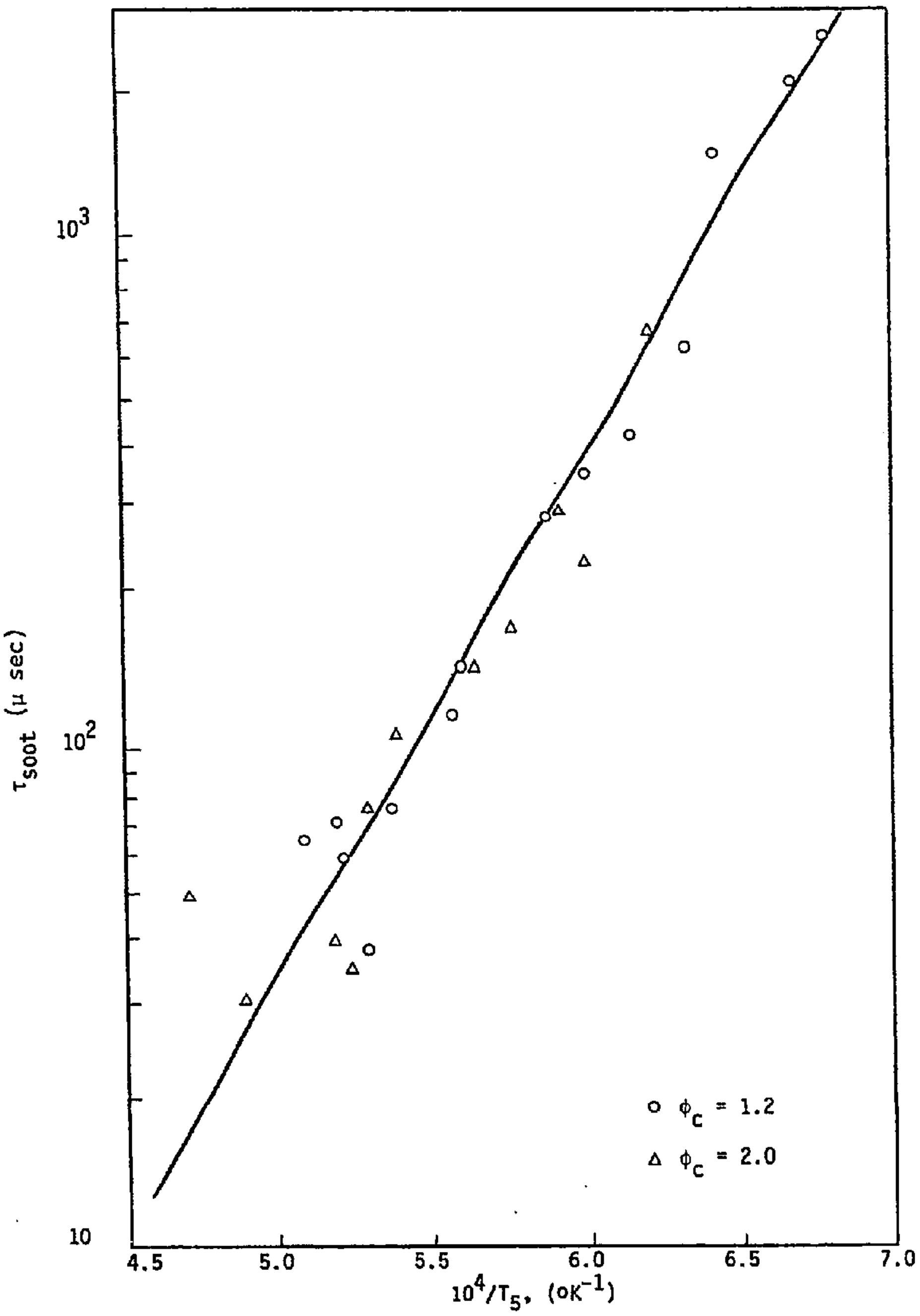

Fig. 15. Soot formation delay times for toluene/oxygen/argon mixtures at a pressure of 5 (atm).

Thus, while the particulate formation process is extremely complex, when analyzed in detail it appears that meaningful modeling can be accomplished by accounting for the appearance of the appropriate major product species during the particulate formation process. For example, based upon the Exxon

(ER&E) data for temperature and hydrocarbon levels, soot concentrations were calculated and compared with the measured soot levels (Fig. 16).

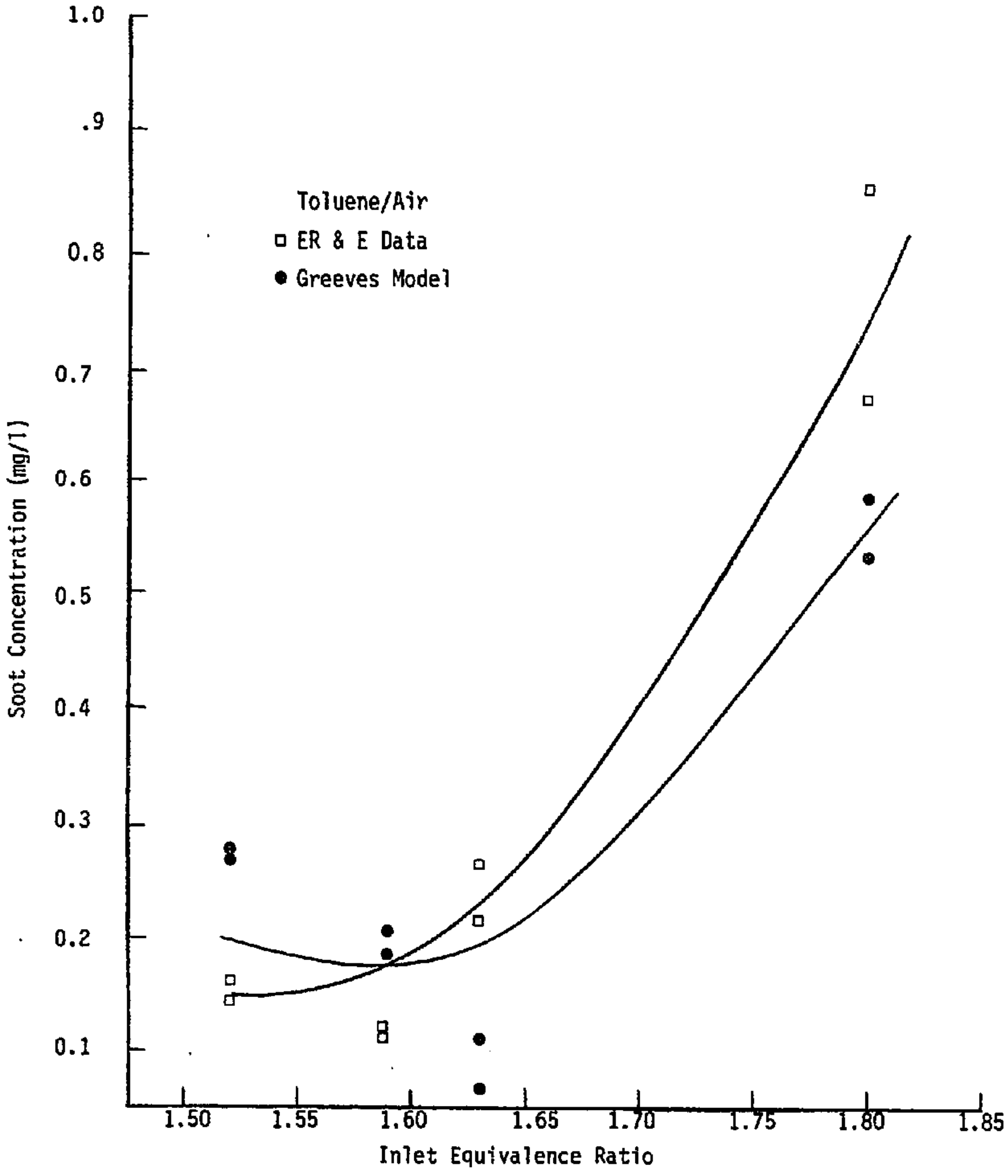

Fig. 16. Comparison of measured and calculated soot formation.

This comparison was made using a one step global reaction based upon the work of Greeves (see Magnussen, 1976). This result is significant showing that simple modeling is a viable approach to the description of the effect of operating conditions on particulate formation. A complete model requires the prediction of temperature and hydrocarbon concentration (recall that these variables were taken equal to their measured values in the comparison given in Fig. 16). Figure 17 illustrates the approach to the complete description of the chemical process including pyrolysis, soot formation, gas phase oxidation and soot oxidation. We include fuel bound nitrogen in terms of the NX

QUASIGLOBAL REACTIONS	REACTION RATES	INFORMATION NEEDED
Fuel Pyrolysis and Soot Formation		
$F_1 + M \rightarrow F_2 + M + \alpha (F_1, F_2) H_2 + NX_1$	$\frac{dC_{F_1}}{dt} = -A_1 C_{F_1} \exp(-E/RT)$	F_2 A_1, A_2, E_1, E_2
$F_2 + M \rightarrow C_s + H$	$\frac{dC_{F_2}}{dt} = -A_2 C_{F_2} \exp(-E_2/RT)$	
Fuel Oxidation		
$F_1 + O_2 \rightarrow CO + H_2 + NX_2$	$\frac{dC_{F_1}}{dt} = -A_3 T^{b_1} p^{c_1} C_{O_2}^{\alpha_1} C_{F_1}^{\beta_1}$ $\exp(-E_3/RT)$	$A_3, A_4, E_3, E_4,$ $b_1, b_2, c_1, c_2,$ $\alpha_1, \alpha_2, \beta_1, \beta_2$
$F_2 + O_2 \rightarrow CO + H_2 + NX_3$	$\frac{dC_{F_2}}{dt} = -A_4 T^{b_1} p^{c_1} C_{O_2}^{\alpha_1} C_{F_1}^{\beta_2}$ $\exp(-E_4/RT)$	
Soot Oxidation $C_s + O_2 \rightarrow CO_2$	• Nagle and Strickland - Constable • Park and Appleton	Initially none
Detailed Mechanism • "Wet" CO • HO_2 and H_2O_2 NX_1, NX_2, NX_3	Literature	

Fig. 17. Multistep quasiglobal kinetics.

type species which are of interest in other applications. We term this type of modeling "quasiglobal", since it incorporates detailed steps (wet CO mechanism to account for the CO-H_2 oxidation through propagation, branching and recombination reactions) as well as subglobal steps. The information already discussed for pyrolysis and soot formation are examples of the type of information applicable to the various subglobal steps. The model includes the effects of C/O ratio, water vapor (steam)/fuel ratio and other operating conditions including the pressure and temperature of the reactants.

The approach outlined here provides a direction and some recommendations for an interrelated modeling and experimental program. The chemical kinetics should be emphasized initially and should include consideration of liquid phase chemistry. Fluid dynamics should be considered and should include spray dynamics as appropriate to the mixing process. Figure 18 summarizes the topics that need to be considered.

Quasiglobal Model Development

- Soot Formation
- Pyrolysis
- Soot Oxidation
- Liquid Phase Chemistry

Fluid Dynamics

- Turbulence/Unmixedness
- Spray Dynamics and Thermodynamics

Modular Model Development (Coupled Kinetics/Fluid Dynamics)

- Development
- Verification
- Utilization

Fig. 18. Overall modeling approach.

Experiments should be performed under controlled conditions which isolate each of the broad areas (chemistry and fluid dynamics). The type of experiments should be related to the operating conditions anticipated in practice, but should be developed in complexity to provide the data needed for kinetics model development (see last column in Fig. 17), fluid dynamics model development, and finally, models involving the coupling of these processes.

FLUID MECHANICAL ASPECTS OF TURBULENT MIXING

Michael L. Finson, Physical Sciences, Inc.

I. INTRODUCTION

This section is concerned with the state-of-the-art of turbulent mixing, with emphasis on the more fluid mechanical aspects of the subject. This can include the rate of spreading of the turbulent zone and the decay of both mean and fluctuating properties. Species concentrations and temperatures, as well as velocities, will be considered. The one issue that will specifically not be discussed here is that of mixing on a molecular basis, also called "mixedness". That issue is discussed at some length by Prof. Patterson and Dr. Varma in other sections of these proceedings. Furthermore, the emphasis of this section will be primarily on assessing the computational techniques that are available for making predictions or for developing sound scaling laws.

The nature of the problem of turbulent mixing in fuel processors is complicated by a number of factors. First of all, most seriously, the flow is turbulent. It is also a reacting flow, but that is the subject of other sections. The mixing geometries can be fairly complicated.

Swirl is often introduced to increase the rate of mixing. At high swirl levels, one can encounter the further complication of recirculation or zones of reversed flow. The flows are compressible or, at least, highly variable in density. Energy release due to the chemical reactions is also usually significant. Furthermore, the mixing regions rarely have a chance to settle down to the asymptotic self-similar flow behaviors. Finally, large-scale structures may be present within the flows and could play an important role in determining the nature of the chemical reactions.

II. TYPES OF MODELS

There are a number of levels at which predictive techniques may be performed. The lowest level is simply to scale the answer from available data. For example, one could use the observed spreading rate to estimate the decay of species concentrations. However, this simple method yields little understanding and requires data under well-matched conditions.

The next level of sophistication is to perform turbulent calculations with what could be called first-order closure methods or methods based on the eddy viscosity. This classic approach has been widely used by turbulence investigators for many years. It has the advantage of being quite tractable in that the resulting equations are essentially no more complex than the laminar flow equations. The important point of eddy viscosity methods is that the effective turbulent viscosity must be specified. Generally, this is done empirically, deriving the viscosity from observations. Of course, the eddy viscosity methods are only as good as the specification of the viscosity.

The somewhat higher level of sophistication, and what might properly be called the current state-of-the-art, involves second-order closure methods. These are also called turbulent energy or Reynolds stress models. In these approaches, one solves additional equations for the various fluctuating turbulent quantities. If done properly, the empiricism that is introduced to these additional equations can be introduced in a geometry-independent manner and, hopefully, results in a formulation that will be valid for all geometries. Of course, these techniques require somewhat more effort, in that additional equations have to be solved.

Finally, there are higher methods that are being investigated at the present time. These go under names such as sub-grid closure, Fourier methods, etc. Generally, they are in the realm of what would be called computational fluid dynamics. To date, these methods have only been applied to extremely simple situations and I think it is clear at this time that they are not yet ready for engineering applications.

In eddy viscosity models, one relates the turbulent shear stress to the mean shear through the eddy viscosity coefficient:

$$\tau = \overline{-\rho u v} = \rho \varepsilon \frac{\partial u}{\partial y} \qquad (1)$$

To specify the eddy viscosity, the mixing length expression introduced originally by Prandtl is often used:

$$\text{Mixing length:} \quad \varepsilon = \ell^2 \frac{\partial u}{\partial y} \qquad (2)$$

In this expression, the mixing length is generally taken to be proportional to the width of the mixing zone and this is the point at which empiricism enters. An alternate expression to Eq. (2) for the eddy viscosity would have the viscosity be proportional to the velocity difference across the mixing zone and to the width of the zone. The latter approach may be more valid for free shear flows. For the transport of species or energy, one generally specifies a turbulent Prandtl or Lewis number, often taken to be unity or a number very close to unity. The net result, as already mentioned, is that one obtains a set of equations that are essentially no more complex than those describing laminar flows. On the other hand, the eddy viscosity approach is relatively empirical, and this empiricism is dependent upon the geometry of the situation. Furthermore, the eddy viscosity method is essentially applicable only to two dimensional flows. For more complicated three-dimensional flows, one then has not one shear stress, but a number of shear stresses and the eddy viscosity coefficient would really become a tensor. Very little work has been done along these lines.

With second order closure methods, one solves additional equations for the fluctuating quantities. There have been various choices regarding what this set of equations is. The simplest choice is to solve an additional equation for the kinetic energy of the turbulence (q^2) as done by Bradshaw.[1]

or equations for the kinetic energy and a length scale ℓ (e.g. Spalding,[2] and Saffman and Wilcox[3]). Others have used Reynold stress models which describe the various components of the Reynolds stress. For a two-dimensional flow in which the boundary layer approximation applies, there are four components of the Reynolds stress: $\overline{u'^2}$, $\overline{v'^2}$, $\overline{w'^2}$, and $\overline{u'v'}$. When one adds a length related variable ℓ, this then results in five equations. These methods originated with Rotta[4] and have been used by Launder and coworkers[5], Donaldson, et al.,[6] and the present author.[7] In these methods, one attempts to invoke closure from basic laboratory data. With the Reynolds stress models, formulation is made in a general tensor form and can then potentially be applied to any geometry, thus the empirical approximations that have to be made are not specifically to any given problem. The typical equation that is solved is that for the kinetic energy:

$$\rho \frac{Dq^2}{Dt} = -\rho\overline{uv}\,\frac{\partial u}{\partial y} - \rho\,\Phi + \frac{\partial}{\partial y}\left(\rho\varepsilon\,\frac{\partial q^2}{\partial y}\right) \qquad (3)$$

where

$$\Phi \sim q^3/\ell,\ \varepsilon \sim q\ell$$

The left side of this equation is, of course, the convective operator which one desires to compute. The first term on the right is the production of kinetic energy by the action of the Reynolds stress on the mean shear. The second term is the rate of dissipation which converts turbulent energy into thermal energy and is always negative. The final term describes the diffusion of turbulent energy by the turbulent motion. When writing equations for the individual Reynolds stresses, additional terms will enter which will describe the exchange of energy between the different Reynolds stress components. Comparable equations may, also, be written for passive scalar quantities such as temperature and species concentrations.

The choice between an eddy viscosity method and a second order closure method depends very much on the specific problem. If one is dealing with a fairly familiar flow geometry where eddy viscosity approximations have been well developed, the eddy viscosity method may be an obvious choice. On the other hand, for unfamiliar geometries, or flows where the turbulence may not be able to approach similarity, then the second order methods may be superior. Also, of course, if details of the fluctuating quantities are needed, then second order closure models are clearly indicated. On the other hand, for a type of flow where the eddy viscosity method is well developed, one generally finds that the eddy viscosity will give somewhat superior results compared to Reynolds stress methods. This is to be expected simply because the eddy viscosity methods are already finely tuned to such a problem.

A good example of the level of accuracy given by Reynolds stress models is shown in Figure 1, which was computed by the present author using a Reynolds stress model comparable to that of Launder et al.[5] This calculation is for a low-speed mixing layer between two parallel flows of different velocities. In the upper plot, the mean velocity as a function of distance across the zone is

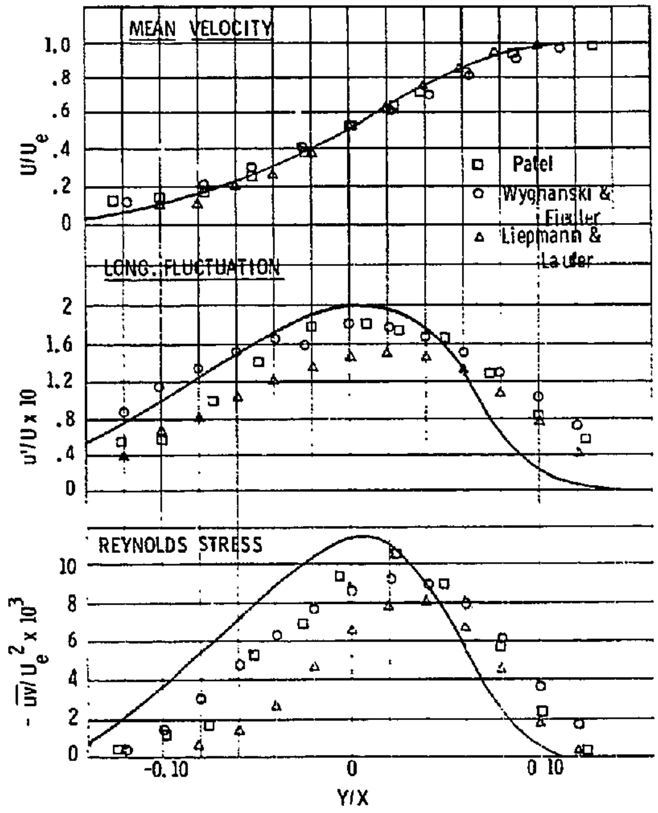

Fig. 1. Comparison of calculations based on a Reynolds stress model with data for constant density plane mixing layers.

seen to be reproduced relatively well. However, the rms fluctuations in the middle curve and the Reynolds stress in the bottom curve are clearly not the optimum agreement with data. With each of these quantities, the low-speed tail of the calculation is somewhat long and the fluctuations are definitely chopped off on the high-speed side of the flow. Undoubtedly, this level of disagreement reflects inadequacy in the closure approximations. Another example where some inaccuracies can result from second order closure models is the case of the round jet. Calculations by Launder[8] have shown a spreading rate which is approximately 50% greater than observed, whereas eddy viscosity solutions can yield good agreement with data.

III. SWIRL

Swirl is often of interest in combustion applications in that it can increase the rate of mixing. For a round jet, the effective swirl is measured by the swirl number which is the ratio of tangential momentum to the axial momentum:

$$S = \frac{\int \rho u w r^2 dr}{R \int \rho u^2 r dr} \tag{4}$$

This number is generally evaluated at the jet exit. Figure 2 is an example of how swirl can increase the mixing rate. This figure shows estimated flame fronts taken from the location of maximum temperature for round jets as a function of increasing swirl number. The data were obtained from the experiments of Chigier and Chervinsky[9] and the lines indicate the calculations of Lilley.[10]

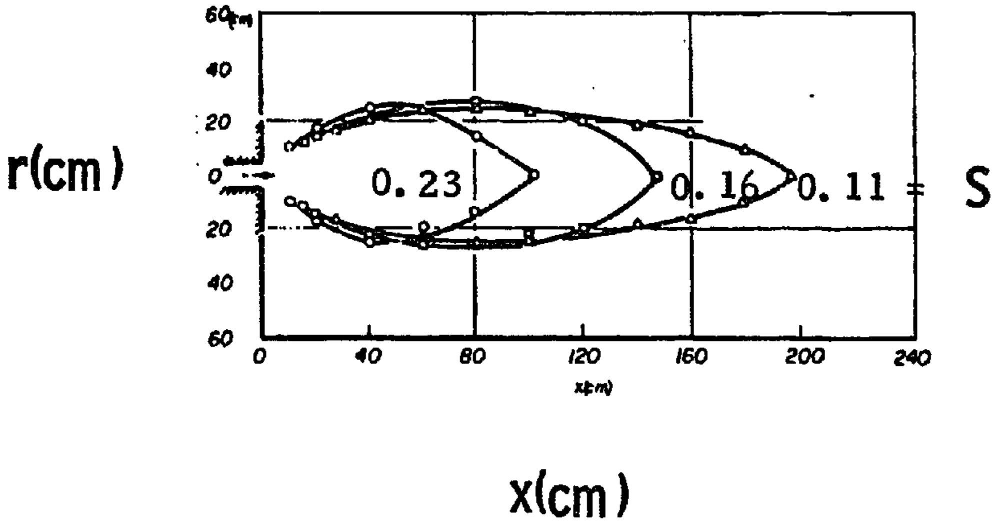

Fig. 2. Effect of increasing swirl on jet mixing (data of Ref. 9, theory of Ref. 10).

Clearly, for swirl increasing from 0.11 to 0.23, the flame length is reduced by, at least, a factor of 2, directly related to the increase in mixing rate. Furthermore, the levels of swirl indicated in Figure 2 are relatively low. Strong swirl, corresponding to swirl number greater than about 0.6, will cause recirculation or zones or reverse flow. This results directly from the fact that there must be an adverse pressure gradient upon leaving a jet.

While an important problem, the prediction of recirculating flows will not be discussed in any detail here. Recirculation, of course, involves flow of an elliptic nature, in contrast to the more familiar parabolic flows, and requires much greater numerical effort. Great advances have been made in recent years in developing more efficient methods for solving recirculating flows. Furthermore, some approximate techniques may be available based on considerations of essentially uniform pressure over the reverse flow zone and separation and reattachment criteria.

Lilley was the first to seriously develop models for swirl flows.[10]

With an eddy viscosity approach, he found that it was necessary to make the closure approximations be an empirical function of the local swirl. This includes the mixing length as well as additional eddy diffusivity for shear in the r θ direction:

$$\ell \sim 1 + 0.6\, S_x \qquad (5)$$
$$\varepsilon_{r\theta} \sim 1 + 5\, S_x^{1/3}$$

Lilley also investigated kinetic energy methods using a two-equation model. Again, it was necessary to introduce empirical approximations for closure involving a centrifugal force term in the kinetic energy equations and, again, the eddy viscosity or shear stress in the r θ direction.

No new closure approximations are required for treating swirl flows with Reynolds stress methods. However, all components of the stress tensor are now important, including the correlations $\overline{u'w'}$ and $\overline{v'w'}$. Launder and Morse[8] have published calculations for comparison with swirling jet data at relatively low swirl numbers. These comparisons are shown in Figure 3. They found their computed results to be relatively sensitive to their basic closure parameters and found, as indicated in the figure, that some adjustments were required to obtain adequate agreement. It is somewhat bothersome that they found it necessary to make these adjustments in that the types of closure approximations that were involved were ones that had presumably already been established rather soundly. In principal, however, the Reynolds stress methods are well suited to handling swirling flows with no additional empirical inputs.

IV. VARIABLE DENSITY EFFECTS

Density variations can arise due to mixing of dissimilar gases, heat release, or high flow velocities. Generally speaking, variations in mean density can be handled without difficulty, at least with finite different solutions. The effects of fluctuating densities on turbulence is far more controversial. For example, a reduced spreading rate is often observed in mixing layers at supersonic velocities. The mechanisms responsible for this behavior have not been demonstrated. From a modeling point of view, the governing equations contain numerous terms involving fluctuating density. Many investigators have realized that one can formally transform much of the dependence away by introducing "Favre" or "mass" averaging:

$$\bar{u} \longrightarrow \overline{\rho u}/\bar{\rho} \qquad (6)$$
$$\overline{u'u'} \longrightarrow \overline{\rho u_i' u_j'}/\bar{\rho}$$

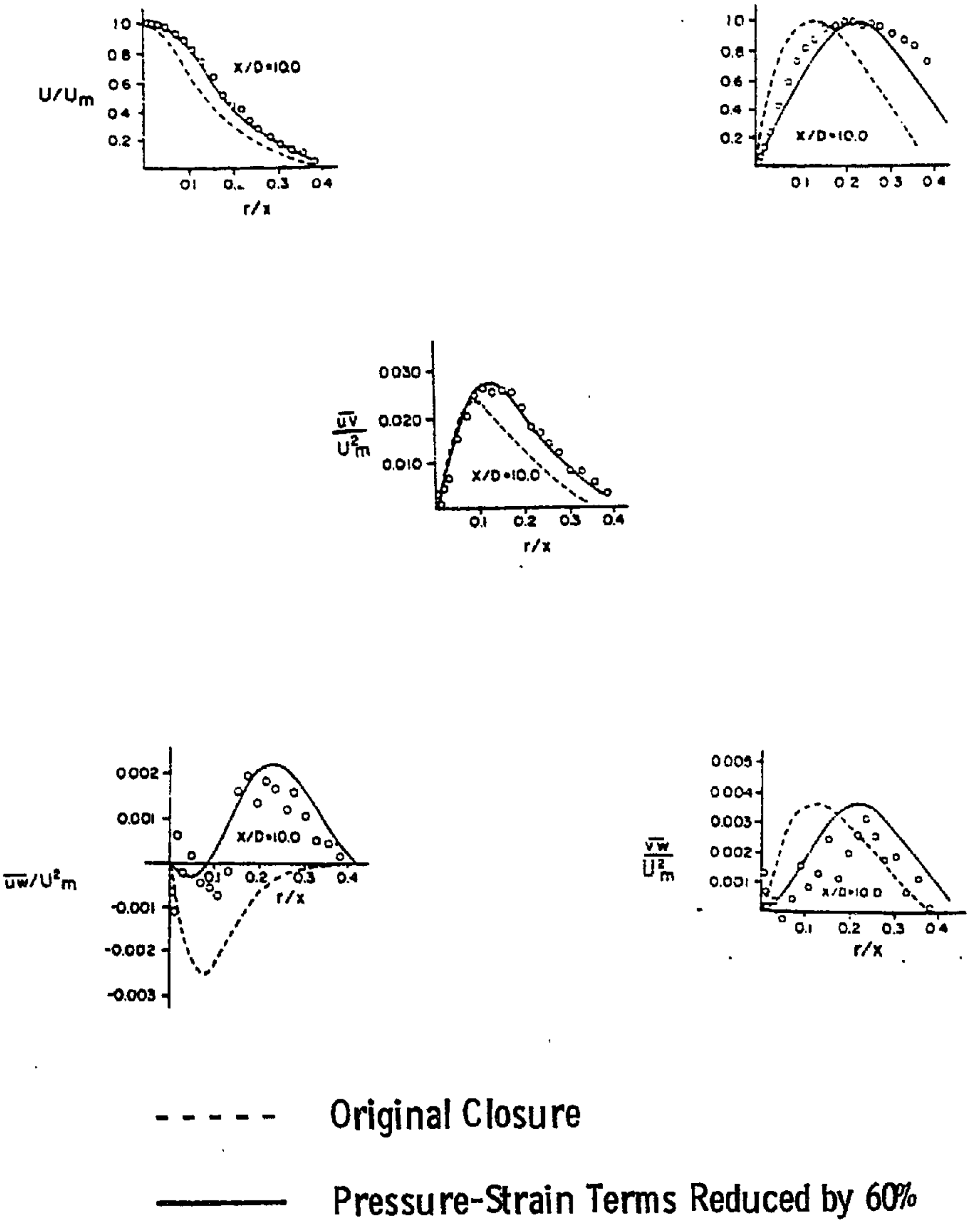

Fig. 3. Calculations of Launder and Morse[8] for a jet with swirl.

With these transformations, the various governing equations take forms which are essentially identical to the forms applying in the constant density case. Of course, this is only a formalism; one makes the fundamental assumption that the incompressible closure approximations still apply in the compressible case. It is also necessary to neglect a term involving correlations between pressure fluctuations and the dilatation. The adequacy of these approximations is unknown. In our work we have achieved satisfactory results for various compressible flow situations using only Favre averaging. We have obtained good results for low speed flows with variable densities, an example of which is given in Figure 4. This figure plots the mixing between two parallel flows of different gases with a density ratio of 7 (data of Brown and Roshko[11]).

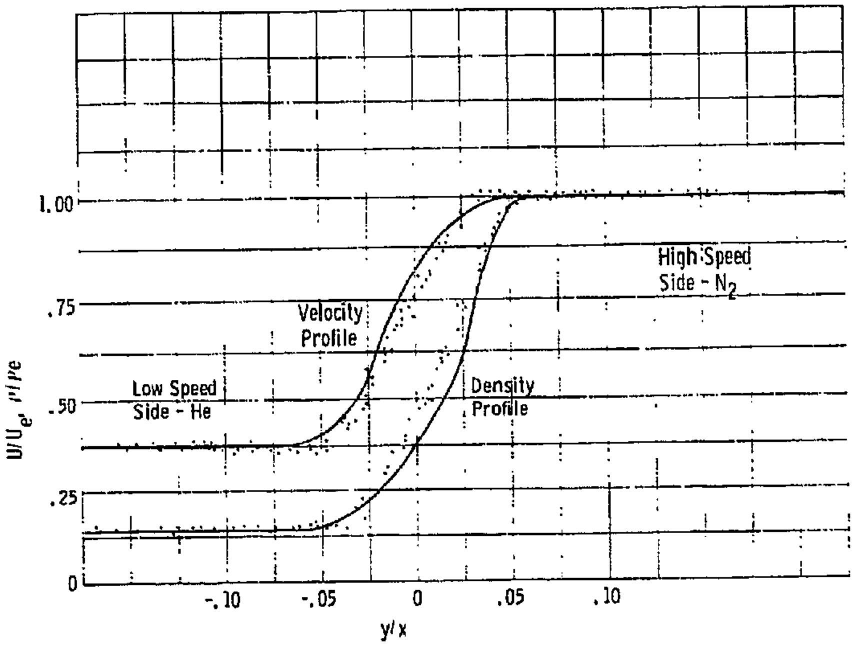

Fig. 4. **Comparison of Reynolds stress model results with data of Brown and Roshko[11] for mixing between helium and nitrogen streams.**

It can be seen that both the mean velocity and density profiles are reproduced very well. Another example, for a supersonic case, is shown in Figure 5. Here we show the comparison with the measured velocity profile for a boundary layer at an edge Mach number of 7.[12] The computed boundary layer thickness and various other parameters including the turbulent intensity were in good agreement with measurements. This good agreement is not to say that all high Mach number turbulent flows are well understood. However, for fuel processors, we are invariably talking much lower Mach numbers and I think it is a safe conclusion that the various effects of variable density are not difficult to predict.

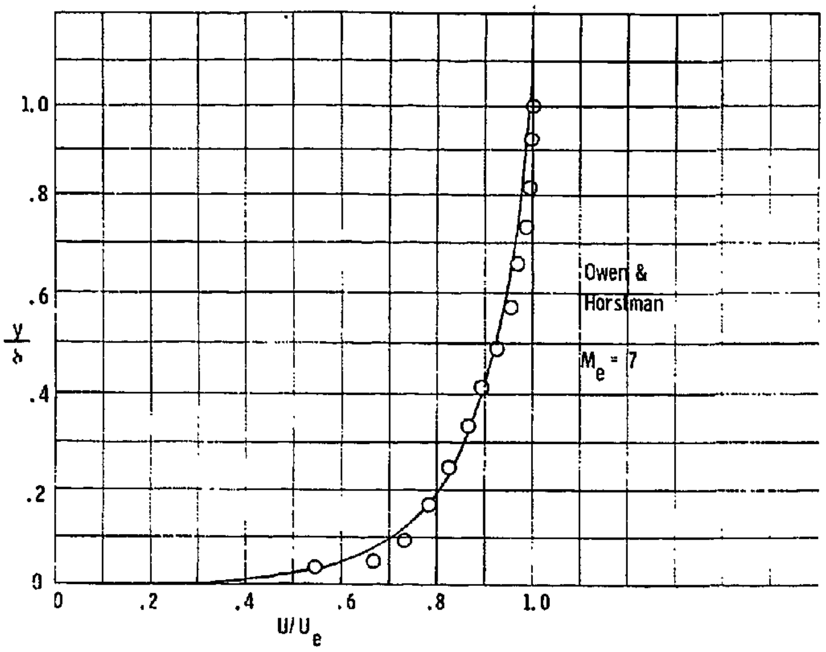

Fig. 5. Example of the success of a Reynolds stress model for a hypersonic boundary layer flow

V. NONSIMILARITY

It may be expected that many cases will involve initial conditions or boundary conditions which are arranged in a manner that the flow will not approach similarity within the apparatus. Pressure gradients, for example, can cause a variation in the edge conditions which will make it difficult for the turbulence to catch up with the edge velocity. Alternatively, initial conditions could be far out of similarity. Perhaps the most significant example of this situation has to do with free shear flows that begin with a turbulent boundary layer. For example, a plane mixing layer between parallel flows that originates from a turbulent boundary layer on the splitter plate can be very slow in approaching fully turbulent mixing layer behavior. Another example is the wake that originates from a body with a turbulent boundary layer. In such cases, one needs to perform a detailed calculation of the development of turbulence in the mixing zone and this generally requires a second-order closure model.

Figure 6, taken from the work of Bradshaw[13], illustrates this point. Here we plot the Reynolds stress in a low speed mixing layer as a function of distance from splitter plate. Bradshaw investigated the mixing layer behavior at a variety of Reynolds numbers. At low Reynolds numbers, where the boundary layer on the splitter plate was laminar, transition was observed to occur shortly downstream of the splitter plate. When this occurred, the Reynolds stress went through a local overshoot above the fully turbulent value, eventually settling down to the latter value. On the other hand, when the separating boundary layer was turbulent, no such transition occurred.

Instead, the mixing rate recovered slowly from the lower turbulent boundary layer level to the eventual asymptotic value for the mixing layer. Bradshaw concluded that a fully turbulent mixing layer would not be established downstream of a turbulent boundary level for distances less than about 10^3 times the momentum thickness of the separating boundary layer.

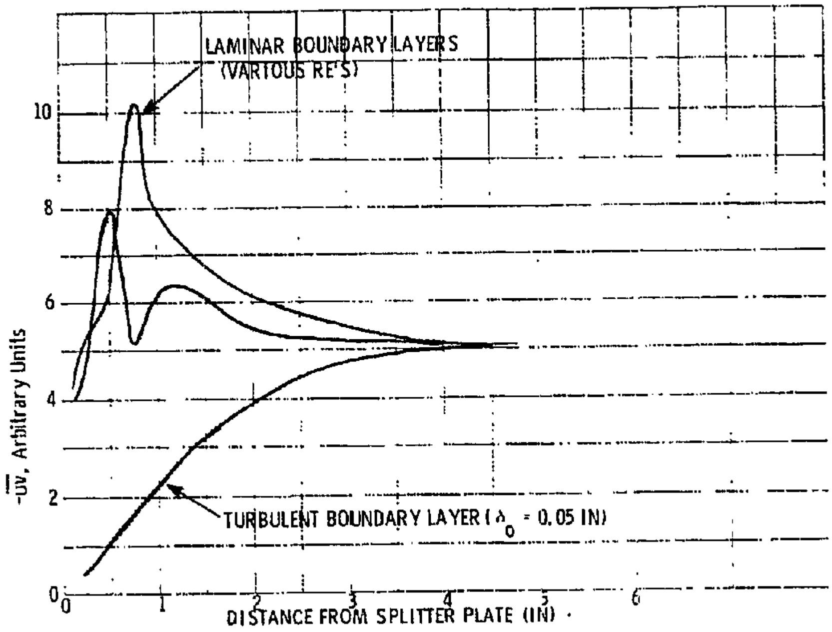

Fig. 6. Schematic of the effect of initial conditions on the development of the mixing rate (from Bradshaw[13]).

Figure 7 shows a calculation that we performed using the Reynolds stress model similar to the one of Launder et al. The case is here for the two-dimensional mixing layer investigated by Ikawa and Kubota[14] at Mach 2.5. In the figure, the high velocity flow is on top from left to right. The first profile at x = 0 is that of the separating boundary layer, which was turbulent. Our calculation agreed very well with the measured boundary layer profile. The succeeding profiles then show the spread of the mixing zone at selected downstream distances. Generally, agreement between the theory and the measurements can be seen to be quite satisfactory, at least as good as it is in the fully developed case shown in Figure 1. At the last downstream station, the dashed line shows the similarity profile, which would be about twice as wide as the actual profile at this distance. Thus, at least in this one case, it is possible to explain the reduced spreading rate in terms of initial condition effects rather than in terms of compressible effects. Whether this conclusion would stand up for a wider range of compressible flows remains to be seen. In general, mixing layer flows which have evidenced reduced spreading rates have been initiated from turbulent boundary layers and none of them have been carried sufficiently far downstream that recovery to similarity could be guaranteed.

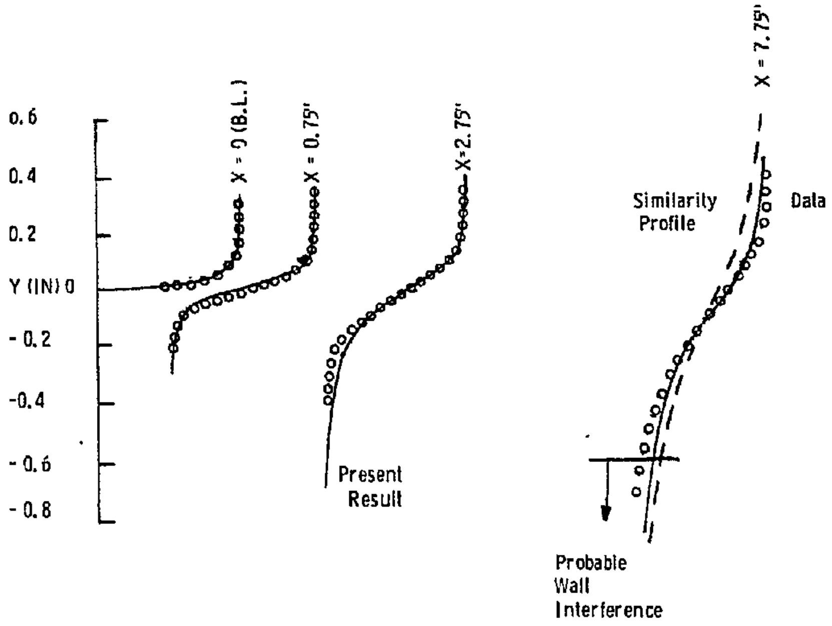

Fig. 7. Nonsimilar computations of a supersonic plane mixing layer (data of Ikawa and Kubota[14]).

VI. LARGE SCALE STRUCTURES

In recent years, there have been interesting observations of large scale, discrete, essentially two-dimensional structures in turbulent flows. Such structures have a fairly obvious importance in combusting flows, in that they may define the effective flame front across which mixing at the molecular level proceeds and across which reactions occur. Figure 8 shows the well-known shadowgraphs of Brown and Roshko[11]. The five shadowgraphs in this figure are for indicated variations in the Reynolds number. At the highest Reynolds number, one sees the large-scale structures persisting with the finer scale background turbulence superimposed. The actual behavior of these large-scale structures is not well understood at this time. Some numerical simulations have been attempted, for example, the calculations performed at Sandia by Ashurst (Figure 9)[15]. This numerical simulation consists of following a very large number of individual line vortices. If perturbed slightly, these vortices rotate about each other in the combined velocity field of all the others. These calculations indicate that the individual line vortices which make up the plane mixing layer indeed tend to roll up into the type of vortices observed by Brown and Roshko. However, these types of calculations have yet to reach a stage where they could be used for the prediction of a reacting flow. Furthermore, the conditions for the practical occurrence of the large-scale structure are not well understood. Recent studies by Bradshaw and coworkers have indicated that large-scale two-dimensional structures may occur primarily only for rather idealized situations[16]. In particular, they may occur only for two-dimensional geometries, primarily only at low Reynolds numbers and low levels of free-stream turbulence. However, the jury is still out on this issue. The potential implications for combustion applications are sufficiently great that future work in this area should be followed with great interest.

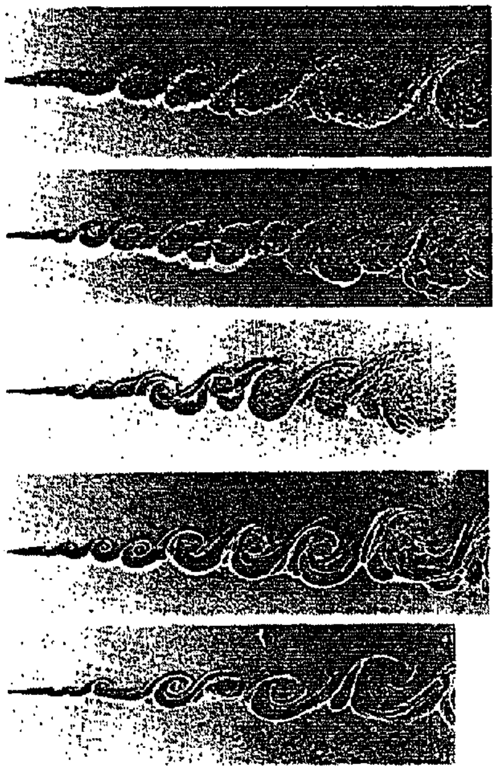

Fig. 8. Large-scale structure of the plane mixing layer - shadowgraphs of Brown and Roshko.[11] The Reynolds number decreases by a factor of four from top to bottom.

VII. OUTSTANDING ISSUES

In this brief presentation, we have attempted to discuss some of the most important issues involved in the prediction of turbulent mixing as it would occur in fuel processors. The state-of-the-art techniques should be useful for many engineering applications. However, there are clearly a number of ways in which these techniques can be improved. For example, as indicated above, Reynolds stress closure methods have not been perfected for free-shear flows. Also, swirl effects have not been studied in sufficient detail. Effects of compressibility, energy release, and acoustic radiation are still being argued in the turbulence community. The importance of large-scale structures is only now being investigated; whether these structures will prove to dominate chemical reaction rates remains to be seen. Finally, the most difficult and least solved aspect of the problem is the one not discussed here, the problem of mixedness.

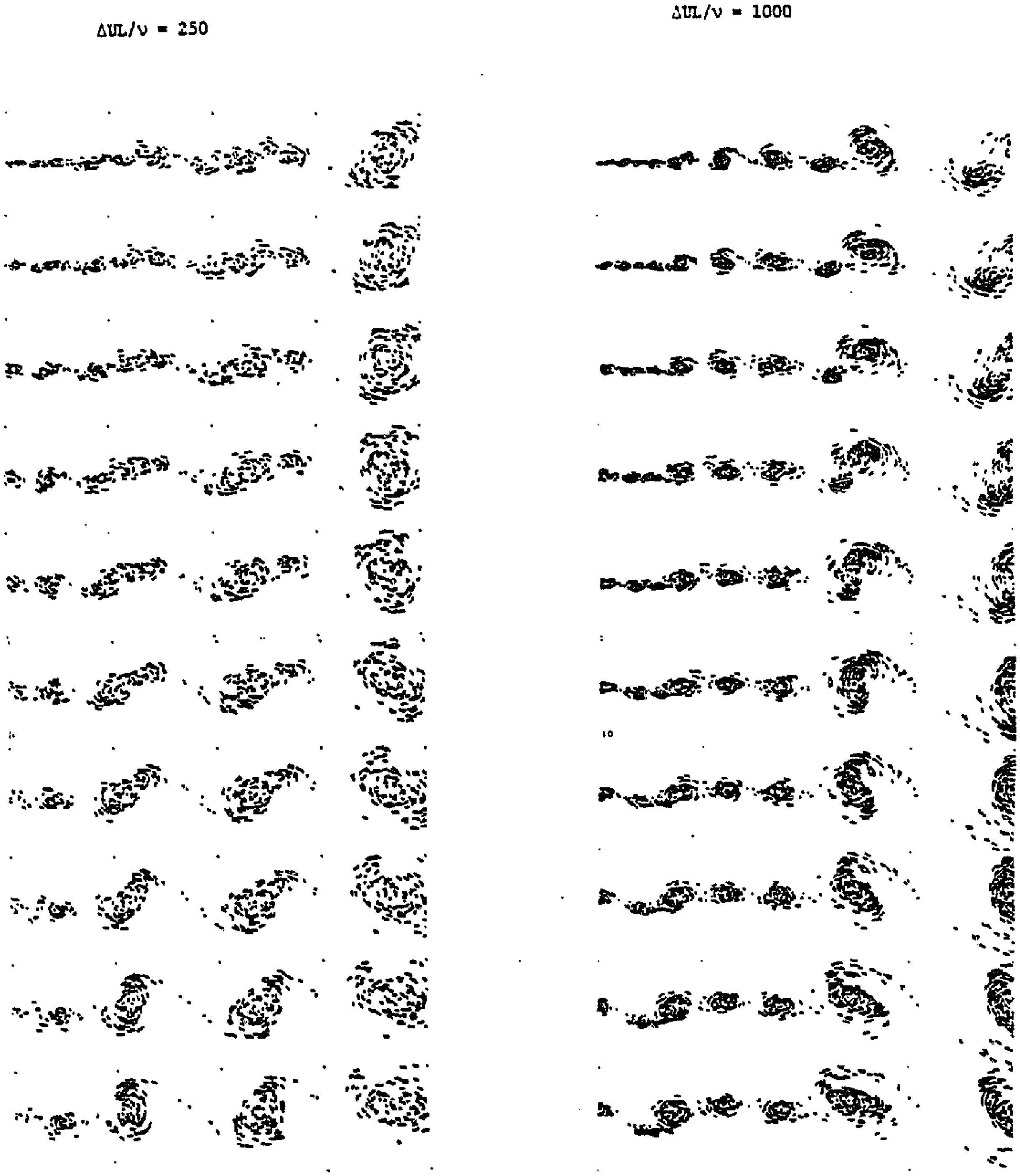

Fig. 9. Discrete line votrex simulation of large scale structures by Ashurst.[15]

REFERENCES

1. Bradshaw, P., Ferriss, D.H., and Atwell, N.P., J. Fluid Mech., 67, 593 (1967).

2. Spalding, D.B., Thirteenth Symposium on Combustion, 649 (1970).

3. Saffman, P.G. and Wilcox, D.C., AIEE J., 12, 541 (1974).

4. Rotta, J., Zeitschrift fur Physik, 129, 547 - 572 (1951) and 131, 51-77 (1951).

5. Hanjalic, K. and Launder, B.E., J. Fluid Mech., 52, 609 (1972).

6. Donaldson, C. DuP., AIAA J., 10, 4 (1972).

7. Finson, M.L. and Wu, P.K.S., AIAA P 79 - 0008 (1979).

8. Launder, B.E. and Morse, A., in Symposium on Turbulent Shear Flows, Penn. State Univ. (1977).

9. Chigier, N.A. and Chervinsky, A., Eleventh Symposium on Combustion, 487 (1967). Also AIAA J., 7, 1877 (1969).

10. Lilley, D.G., AIAA J., 15, 1063 (1977). Also AIAA J., 12, 219 (1974).

11. Brown, G.L. and Roshko, A., J. Fluid Mech., 64, 775 (1974).

12. Horstman, C.C. and Owen, F.K., AIAA J., 10, 1418 (1972). Also Mikulla, V. and Horstman, C.C., AIAA Paper No. 75 - 119 (1975).

13. Bradshaw, P., J. Fluid Mech. 26, 221 (1966).

14. Ikawa, H. and Kubota, T., AIAA J., 13, 566 (1975).

15. Ashurst, W.T., in Symposium on Turbulent Shear Flows, Penn State Univ. (1977).

16. Chandrsuda, C., Mehta, R.D., Weir, A.D., and Bradshaw, P., J. Fluid Mech., 85, 693 (1978).

Comments and Replies on

"Fluid Mechanical Aspects of Turbulent Mixing"

by M. L. Finson

P. Ponzi: You were discussing methods that just start from the Navier-Stokes equations and go from there? There would be no time averaging?

M. Finson: Some time averaging would probably be involved. In the most promising approaches, large eddies would be computed directly whereas closure (on a time averaged basis) would be invoked for the smaller eddies. The advantage stems from the fact that these smaller eddies are nearly isotropic and dissipative in character; the required closure approximations can be specified with some confidence. On the other hand, the larger eddies that are dominated by nonlinear inertial effects would be computed without approximation. However, we are many years from the time where this can be done for realistic problems.

R. Edelman: Higher order methods introduce differential equations. They require initial and boundary conditions. The choice of these conditions can affect comparisons with data.

M. Finson: Very difinitely. In general, the influence of initial conditions will die out after some distance. However, as I emphasized, there are numerous cases where this influence covers the range of practical interest. In terms of the data comparisons shown above, particularly those of Launder and Morse in Fig. 3, data from the first measured station were used as initial conditions.

P. Sforza: It seems to me that most experimentalists now are becoming "eddy hunters", and that they are deviating from doing the kind of experiments that are useful to people who are building complicated models such as you have discussed.

M. Finson: It is undoubtedly true that theoreticians and experimentalists tend to go separate ways in the study of turbulence. This is particularly so with respect to turbulent combustion, since it is extremely difficult to measure fluctuating reactant species. In many ways, our ability to predict turbulent combustion is limited by the availability of data against which to develop and validate our models.

T. Blake: I would like to follow up this response with two comments. If we are going to use models like these for chemical reactions, we must also have a program to obtain detailed measurements of the reactants and products. These are needs that I hope the people who are developing fuel processors will bear in mind. Secondly, as the geometries become more complex, the cost effectiveness of doing calculations versus experiments becomes a real consideration. Somewhere along the line, we need a better definition of the kinds of geometries that we will be facing in these simulations.